ISSN 2220-3176 (online)

World Journal of

Clinical Infectious Diseases

World J Clin Infect Dis 2022 April 26; 12(1): 1-49

Published by Baishideng Publishing Group Inc

WJCID

World Journal of Clinical Infectious Diseases

Contents

Continuous Publication Volume 12 Number 1 April 26, 2022

MINIREVIEWS

ORIGINAL ARTICLE

Basic Study

CASE REPORT

LETTER TO THE EDITOR

World Journal of Clinical Infectious Diseases

Continuous Publication Volume 12 Number 1 April 26, 2022

Contents

ABOUT COVER

Peer Reviewer of *World Journal of Clinical Infectious Diseases*, Sitanshu Barik, MBBS, DNB, MNAMS, MCh, FAGE, Assistant Professor, Department of Orthopedics, All India Institute of Medical Sciences, Deoghar 814142, India. sitanshubarik@gmail.com

AIMS AND SCOPE

The primary aim of *World Journal of Clinical Infectious Diseases* (*WJCID*, *World J Clin Infect Dis*) is to provide scholars and readers from various fields of infectious diseases with a platform to publish high-quality basic and clinical research articles and communicate their research findings online.

WJCID mainly publishes articles reporting research results and findings obtained in the field of infectious diseases and covering a wide range of topics including community-acquired infections, cross infection, eye infections, focal infection, infectious gingivitis, intraabdominal infections, laboratory infection, Ludwig's angina, necrotizing ulcerative periodontitis, opportunistic infections, pelvic infection, pregnancy complications, *etc*.

INDEXING/ABSTRACTING

The *WJCID* is now indexed in Reference Citation Analysis, China National Knowledge Infrastructure, China Science and Technology Journal Database, and Superstar Journals Database.

RESPONSIBLE EDITORS FOR THIS ISSUE

NAME OF JOURNAL
World Journal of Clinical Infectious Diseases

ISSN
ISSN 2220-3176 (online)

LAUNCH DATE
December 30, 2011

FREQUENCY
Continuous Publication

EDITORS-IN-CHIEF
Joao Mesquita, Caterina Sagnelli, Wei Wang, Haroon Ahmed

EDITORIAL BOARD MEMBERS
https://www.wjgnet.com/2220-3176/editorialboard.htm

PUBLICATION DATE
April 26, 2022

INSTRUCTIONS TO AUTHORS
https://www.wjgnet.com/bpg/gerinfo/204

GUIDELINES FOR ETHICS DOCUMENTS
https://www.wjgnet.com/bpg/GerInfo/287

GUIDELINES FOR NON-NATIVE SPEAKERS OF ENGLISH
https://www.wjgnet.com/bpg/gerinfo/240

PUBLICATION ETHICS
https://www.wjgnet.com/bpg/GerInfo/288

PUBLICATION MISCONDUCT
https://www.wjgnet.com/bpg/gerinfo/208

ARTICLE PROCESSING CHARGE
https://www.wjgnet.com/bpg/gerinfo/242

STEPS FOR SUBMITTING MANUSCRIPTS
https://www.wjgnet.com/bpg/GerInfo/239

ONLINE SUBMISSION
https://www.f6publishing.com

World Journal of Clinical Infectious Diseases

Submit a Manuscript: https://www.f6publishing.com

World J Clin Infect Dis 2022 April 26; 12(1): 1-19

DOI: 10.5495/wjcid.v12.i1.1

ISSN 2220-3176 (online)

MINIREVIEWS

Imaging related to underlying immunological and pathological processes in COVID-19

Elena Ilieva, Alexandra Boyapati, Lyubomir Chervenkov, Milena Gulinac, Jordan Borisov, Kamelia Genova, Tsvetelina Velikova

Specialty type: Infectious diseases

Provenance and peer review: Unsolicited article; externally peer reviewed.

Peer-review model: Single blind

Peer-review report's scientific quality classification

Grade A (Excellent): A
Grade B (Very good): B
Grade C (Good): 0
Grade D (Fair): 0
Grade E (Poor): 0

P-Reviewer: Bhatt KP, Omar BJ

Received: June 7, 2021
Peer-review started: June 7, 2021
First decision: October 18, 2021
Revised: November 9, 2021
Accepted: March 4, 2022
Article in press: March 4, 2022
Published online: April 26, 2022

Elena Ilieva, Alexandra Boyapati, Kamelia Genova, Department of Diagnostic Imaging, University Emergency Hospital (UMHATEM) "N. I. Pirogov", Sofia 1606, Bulgaria

Lyubomir Chervenkov, Department of Diagnostic Imaging, Medical University, Plovdiv, University Hospital "St George", Plovdiv 4000, Bulgaria

Milena Gulinac, Department of General and Clinical Pathology, Medical University, Plovdiv, University Hospital "St George", Plovdiv 4000, Bulgaria

Jordan Borisov, Department of Diagnostic Imaging, MBAL-Dobrich" AD, Dobrich 9300, Bulgaria

Tsvetelina Velikova, Department of Clinical Immunology, University Hospital "Lozenetz", Sofia 1407, Bulgaria

Tsvetelina Velikova, Medical Faculty, Sofia University "St. Kliment Ohridski", Sofia 1407, Bulgaria

Corresponding author: Tsvetelina Velikova, MD, PhD, Assistant Professor, Department of Clinical Immunology, University Hospital "Lozenetz", Kozyak 1 str., Sofia University "St. Kliment Ohridski", Sofia 1407, Bulgaria. tsvelikova@medfac.mu-sofia.bg

Abstract

The introduction of coronavirus disease-2019 (COVID-19) as a global pandemic has contributed to overall morbidity and mortality. With a focus on understanding the immunology and pathophysiology of the disease, these features can be linked with the respective findings of imaging studies. Thus, the constellation between clinical presentation, histological, laboratory, immunological, and imaging results is crucial for the proper management of patients. The purpose of this article is to examine the role of imaging during the particular stages of severe acute respiratory syndrome coronavirus 2 infection – asymptomatic stage, typical and atypical COVID-19 pneumonia, acute respiratory distress syndrome, multiorgan failure, and thrombosis. The use of imaging methods to assess the severity and duration of changes is crucial in patients with COVID-19. Radiography and computed tomography are among the methods that allow accurate characterization of changes.

Key Words: Coronavirus disease-2019; Ultrasound; Computed tomography; Magnetic resonance imaging; Ground-glass opacity; Acute respiratory distress syndrome; Cytokine storm; COVID-19 reporting and data system; High-resolution computed tomography; Severe acute respiratory syndrome coronavirus 2

Core Tip: The novel Coronavirus disease-2019 (COVID-19) infection may present as a multiorgan disease, with the lung being the most commonly affected target organ. The clinical presentation, course, and outcome of COVID-19 are heterogeneous. Various imaging modalities can be employed to evaluate different disease stages depending on the affected organ or system, with X-ray, computed tomography, and ultrasound being the most commonly used. Imaging plays an essential role in the primary diagnosis of all manifestations of the disease and its related complications, evaluating disease severity and follow-up. Proper utilization of different imaging modalities and interpretation of the key imaging findings are essential for effective patient management and treatment.

Citation: Ilieva E, Boyapati A, Chervenkov L, Gulinac M, Borisov J, Genova K, Velikova T. Imaging related to underlying immunological and pathological processes in COVID-19. *World J Clin Infect Dis* 2022; 12(1): 1-19
URL: https://www.wjgnet.com/2220-3176/full/v12/i1/1.htm
DOI: https://dx.doi.org/10.5495/wjcid.v12.i1.1

INTRODUCTION

Severe acute respiratory syndrome coronavirus 2 (SARS-CoV-2), the etiologic agent of coronavirus disease-2019 (COVID-19), caused a global pandemic dominated by acute respiratory failure mortality. COVID-19 manifestations are heterogeneous and overlapping. Therefore many challenges in the diagnostics and management of COVID-19 are still present[1]. In addition, typical symptoms without positive proof of infection (PCR/antigen tests) make the diagnosis inconclusive. However, a variety of imaging methods and techniques can be used for this purpose. Furthermore, imaging is also essential for classifying and managing patients during the infection.

Typically, imaging studies are carried out to determine the disease stage and estimate the organ involvement and severity. However, the features, such as ground-glass opacities (GGO), consolidations, interstitial fluid shifts, *etc.*, seen on imaging are not unique to COVID-19. Therefore, a combination of the clinical picture and laboratory assessment is necessary to fully evaluate the patient's state[2].

In the era of COVID-19, radiology plays a crucial role in the disease work-up and follow-up. Initially considered a purely pulmonary process, COVID-19 turned out to be a multisystemic disease that requires a comprehensive imaging approach, involving all techniques and studying all anatomical areas. As the primary manifestation of COVID-19 is a pneumonia-like respiratory process, the radiology modalities most involved in its diagnosis and follow-up are chest imaging, mainly chest X-ray (CXR) and chest computed tomography (CT). Diagnostic imaging capabilities show that CT is more sensitive than the gold standard RT-PCR for diagnosing COVID-19[2,3]. At the same time, it is cheaper and can be performed faster. The CT examination can give a quick, accurate diagnosis of patients, as the PCR test requires hours, even days, to complete as the number of COVID-19 infection cases grow. However, this comes with a large radiation dose, where the capacity is still lacking in many countries[4]. CXR is ubiquitous worldwide, with a 30–70-fold lower amount of radiation. Despite its low sensitivity and specificity, it is commonly performed as an initial investigation in COVID-19[4,5]. It is the modality of choice in the intensive care unit to detect disease progression and assess the position of the individual resuscitation means.

The imaging findings both on CXR and CT can be invaluable, especially for an atypical or organizing pneumonia with bilateral, multifocal randomly scattered GGO, in subpleural, mainly peripheral distribution with thickened pulmonary interstitium giving a reticular pattern, broncho-vascular prominence, and consolidation with increasing severity in the more seriously ill patients[6]. High-resolution CT (HRCT) with its modern available software techniques is the method of choice for an initial examination, staging, and follow-up of patients with suspected COVID infection. CT has higher sensitivity and specificity than radiography. On CT, the main changes are GGO, which tend to be more in the periphery, crazy paving changes are seen in later stages of the disease, thickening of the interstitium is also seen as well as dilation of the terminal lung vessels[7]. For staging of the changes seen on CT, we use the COVID-19 reporting and data system (CO-RADS) classification. It is a standardized classification proposed by the Dutch Radiological Society. It has 6 levels of suspicion from CO-RADS 1 to CO-RADS 6. In CO-RADS 1 patients, the exam is normal or has non-infectious changes.

CO-RADS 2 patients have low levels of suspicion, and the visualized changes are consistent with infections other than COVID. CO-RADS 3 patients are those in which the changes are unclear, and there is an indeterminate level of suspicion. CO-RADS 4 and 5 staged patients have high and very high levels of suspicion for COVID- 19 infection, respectively. CO-RADS 6 patients are those who have typical changes and are PCR positive[8].

Chest ultrasound (US) plays a role in emergency settings as a COVID-19 screening technique. However, it is often of limited use as a highly operator-dependent method for lung disease. In addition, point of care echocardiography might have utility in hemodynamically unstable patients.

As stated above, various extrapulmonary manifestations have been reported, including in the gastrointestinal tract, brain, heart, kidneys, or muscles. The identification of most of these pathologies needs imaging, including abdominal CT, US, and magnetic resonance imaging (MRI). Imaging helps detect, diagnose, and assess the virus-induced injury and associated complications of the organs and systems affected by COVID-19. In suspected pulmonary thromboembolism (PTE) cases, CT pulmonary angiography (CTPA) may help correct the diagnosis. PTE is frequently observed in patients with more severe COVID-19 pneumonia involving mainly the segmental (90.2%) and subsegmental arteries (61.0%) of pulmonary segments affected by a consolidation pattern (67.6%)[9].

Furthermore, CXR, chest CT, and echocardiography can readily evaluate the signs of cardiac failure. However, myocardial injury can be best assessed using cardiac MRI. Potential neurovascular complications such as stroke, hemorrhage, or venous sinus thrombosis can be identified by non-enhanced head CT, and in the setting of a suspected infarct, a non-enhanced MRI of the brain can be performed for definitive assessment[10].

The disease may present as a multisystem hyperinflammatory syndrome in pediatric patients, currently termed pediatric multisystem inflammatory syndrome (PMIS). In children with PMIS, a broad spectrum of abdominal abnormalities can be detected by

both abdominal US and CT, with periportal and pericholecystic edema, gallbladder wall, and bowel wall thickening and dilatation, splenic infarcts, hepatosplenomegaly, right lower quadrant mesenteric lymphadenopathy, and free fluid in the pelvis being among the most commonly encountered abnormalities[10,11].

The COVID-19 pandemic has facilitated research on the implementation of artificial intelligence (AI), machine learning, and its subfield deep learning into imaging, which can be used as an essential adjunct or alternative to the diagnosis and follow-up assessment of progression and therapeutic development of the disease[12]. Deep learning is the most successful machine learning technique, which provides helpful analysis to study a large number of chest images that can critically impact the screening of COVID-19. AI algorithms have been developed to help with the early detection of COVID-19 both on CXR and CT. A deep learning model was also trained to discriminate between COVID and non-COVID pneumonia[13]. In line with this, CT pneumonia analysis (developed by Siemens Healthineers and partners) is another algorithm designed to automatically identify and quantify abnormal patterns in the lungs, enabling simple-to-use analysis of non-contrast chest CT scans for research purposes. The results could be used to analyze the severity and progression of abnormalities in patients exhibiting COVID-19 symptoms.

ASYMPTOMATIC DISEASE

A person infected with SARS-CoV-2 who has not developed any signs or symptoms of COVID-19 is defined as an asymptomatic case. Immunological features, including any of the innate immunity pathways (*i.e.*, natural killer (NK) cells, interferon, and other cytokine production), play a role at the onset of infection[14]. Stage I, or the asymptomatic incubation with or without detectable virus, is the period when treatment for improving immunity is given, such as the use of antiserums (ready-made antibodies from survivors), and is undoubtedly crucial[14]. However, due to the initial pathological changes in the target organs, sometimes imaging studies are the only way of detecting problems.

In asymptomatic individuals, this stage begins with inhalation of the SARS-CoV-2 virus replicating in the epithelial cells of the nasal cavity. It is well-known that the virus primarily uses the receptors for ACE2[15]; thus the first affected cells are ciliated cells. Therefore, PCR for SARS-CoV-2 RNA in nasal swabs can diagnose the virus at this point. The virus is then distributed in the lungs, digestive tract, reproductive system, *etc.*, while innate immune tolerance is minimal[15].

It has been shown that asymptomatic persons can be infectious and secrete SARS-CoV-2, promoting the dissemination of COVID-19 – a significant concern from an epidemiological point of view. Moreover, while asymptomatic, some patients present with substantial lung changes, for example, when they seek medical attention. This observation requires a stringent search and examination of the interactions of proven infected persons with COVID-19 to diagnose asymptomatic infections[14].

According to the literature and personal experience of our team, the incidence of asymptomatic occurring COVID-19 infection is much higher, about four times more common than symptomatic moderate to severe ongoing cases[16]. The described histological changes in the respiratory system in an asymptomatic case of COVID-19 infection based on autopsy and biopsy are exceptional[17]. The only

way to examine histological changes, mainly of the lung, in asymptomatic infection in the early stages of the disease is to take a biopsy for other pathological processes, "accidental" sampling of COVID-19, most often in the case of neoplastic diseases in which surgeries were performed for lung tumors at a time when superimposed infections were not recognized[16-20].

The main morphological changes found in routine histopathological examinations in the lungs are edema, proteinaceous exudate, focal reactive hyperplasia of pneumocytes, some with viral inclusions, and polymorphonuclear inflammatory infiltration composed mainly of lymphocytes and multinucleated giant cells. Hyaline membranes are scattered or not apparent in the early (asymptomatic) stage of COVID-19 infection, unlike in acute respiratory distress syndrome (ARDS). In addition, histologically, protein and fibrin exudates can be found in the lung parenchyma, as well as diffuse thickening of the alveolar walls, consisting of proliferating interstitial fibroblasts and type II pneumocystic hyperplasia, with random cell atypia and multinucleated giant cells, indicating varying degrees of the proliferative phase of diffuse alveolar damage. In some areas, an abundance of alveolar macrophages can be found together with type II pneumocystic hyperplasia[17,18,21].

Most patients with COVID-19 infection are diagnosed with pneumonia. The patients who have no symptoms could be transmitters. However, some asymptomatic patients progress quickly, even to ARDS. In asymptomatic patients, radiography has lower sensitivity and specificity than CT. In patients with slight changes, X-ray imaging can appear normal. This is why CT is the preferred method for diagnosis. Based on the published data, to date, almost all patients with COVID-19 have characteristic changes on CT[8,22].

The X-ray of a 60-year-old female patient is presented in Figure 1. The patient had no symptoms, but a positive PCR test was performed because her husband had COVID pneumonia. Her X-ray showed no abnormalities. This is a typical case of an asymptomatic patient with negative radiography.

We also present the CT scan of a 45-year-old male, shown in Figure 2. He had no symptoms but a positive PCR test because he had been in contact with a verified COVID-19 patient. Both lungs showed no abnormalities, no infiltrates, no GGO, and no pleural effusions.

Atypical clinical findings in pregnant women with COVID-19 may increase the difficulty in establishing the diagnosis. Recently, data have demonstrated that pregnant women are more vulnerable to severe COVID-19, the development of complications, and death. CT is the favored approach for detecting pulmonary involvement early, especially in asymptomatic cases[22]. In asymptomatic children or those with atypical presentation of COVID-19, CT may be beneficial, especially in sparing time while waiting for PCR results or false-negative results.

In the case of pregnant women or children, it is always preferred to perform CT instead of waiting because any delay in confirming the diagnosis and management of the disease can be fatal and can contribute to the spread of the virus. Furthermore, the CT results in asymptomatic COVID-19 are usually distinct from the normal appearance, where the most common findings are GGO and consolidations in the lungs[22].

MILD TO MODERATE CASES – TYPICAL COVID-19 PNEUMONIA

The onset of pneumonia in COVID-19 includes extreme antigen presentation, followed by enhanced production of C-reactive protein, D-dimer, and liver amino-transferases, accompanied by infiltrates in the lungs, representing involvement of antigen-presenting cells, T-helper cells, B cells, and NK cells[14].

The virus spreads across the airways in the respiratory tract and further to the gastrointestinal tract. It activates robust innate immune reactions. Nasal secretion, sputum or swabs contain SARS-CoV-2 but also early immune response molecules. Cytokine production during this stage may predict the clinical presentation and the subsequent disease course[23]. Significant amounts of interferon type I can confine the infection within the lungs, which is valid for approximately 80% of affected patients. Most of those with typical COVID-19 pneumonia on conservative symptomatic treatment can stay at home. However, about 20% of infected patients will progress to the next severe stage of the disease. Around 2% will develop life-threatening illnesses[23].

However, we have to keep in mind that COVID-19 pneumonia is a heterogeneous disease. It may include tracheobronchitis, vascular injury, and capillary microthrombi, along with inflammation[23]. Active injury leads to chronic and permanent lung trauma. The late effects of SARS-CoV-2 on the lungs have not been elucidated, but fibrosis development is suggestive.

Histologically, a hallmark of typical viral pneumonia is the interstitial nature of the inflammatory reaction. In addition, the most common morphologic changes in the lungs correlate with ARDS, which is described in the next section (Severe cases of COVID-19). On the other hand, no apparent morphological changes were observed in cardiac tissue due to the direct action of the coronavirus[17]. However, other findings established on necropsy material taken at autopsy are hypertrophy of cardiomyocytes with microscopic evidence of acute ischemia due to hypertensive heart disease and coronary artery atherosclerosis, but no other substantial damage[5].

Interestingly, we documented a case of sinus cavernosus thrombosis in a 49-year-old man hospitalized with COVID-19 pneumonia. One week after hospitalization, he lost vision in his right eye, and

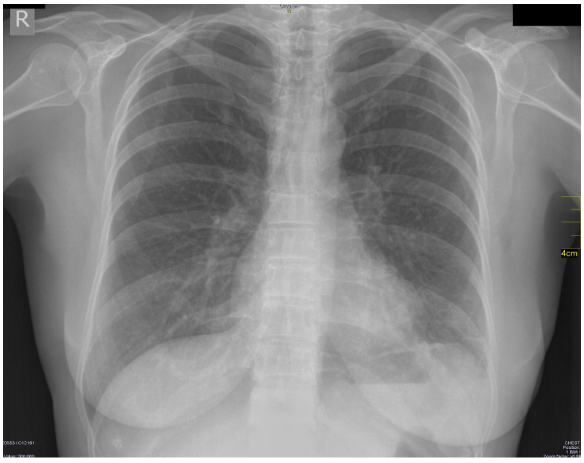

DOI: 10.5495/wjcid.v12.i1.1 **Copyright** ©The Author(s) 2022.

Figure 1 Negative radiography of an asymptomatic patient.

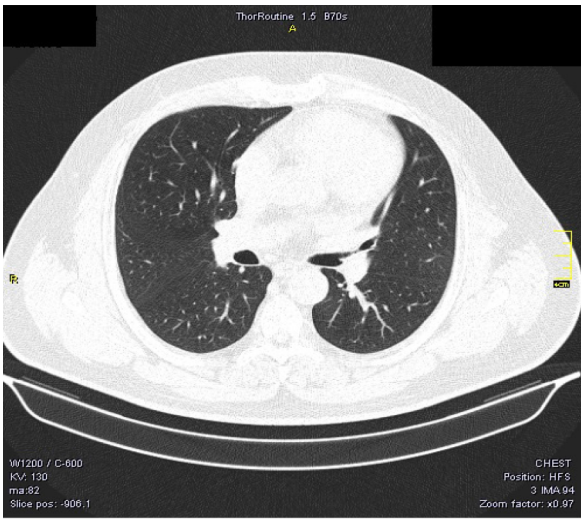

DOI: 10.5495/wjcid.v12.i1.1 **Copyright** ©The Author(s) 2022.

Figure 2 Negative computed tomography of an asymptomatic patient.

presented with exophthalmos and swelling of the soft tissues around the eye. CT with contrast enhancement was performed immediately after the onset of symptoms. Thrombosis of the right sinus cavernosus is presented in Figure 3A and B.

COVID-19 pneumonia is classified as atypical pneumonia because it overlaps with the radiographic findings seen in interstitial pneumonia, including other coronavirus infections (SARS, MERS)[24,25]. Therefore, imaging methods are the first choice for diagnosing COVID-19 pneumonia including CXR and chest CT, with CT being a more sensitive and specific method than CXR, especially in the early stages of the disease[5].

Imaging findings on conventional radiography range from normal findings to diffuse changes in the lung parenchyma. Patients with multiple comorbidities are more likely to have bilateral and diffuse lesions. Findings considered as highly specific for COVID-19 pneumonia on CRX are GGO (Figure 4A) and areas of non-segmental consolidation of parenchyma (Figure 4B) with peripheral and caudal distribution[26]. These findings are most pronounced 10-12 d after the onset of symptoms[27]. Additional findings are confluent ill-defined patchy opacities (Figure 4C), an interstitial lung pattern, decreased lung attenuation, inhomogeneous and linear parenchymal opacities (Figure 4D), and often different features are combined.

On the one hand, for intensive care unit patients, CRX plays a crucial role in detecting disease progression and assessing the position of the individual resuscitation means - endotracheal tubes, drains, and venous sources as it is performed at the patient's bedside with a mobile X-ray machine[26].

On the other hand, CT is a vital component in the diagnosis of suspected COVID-19 infection. CT features vary with the patient's age, immunity status, disease stage, underlying diseases, and drug interventions at the time of scanning[28]. CT findings considered "typical" for COVID-19 pneumonia

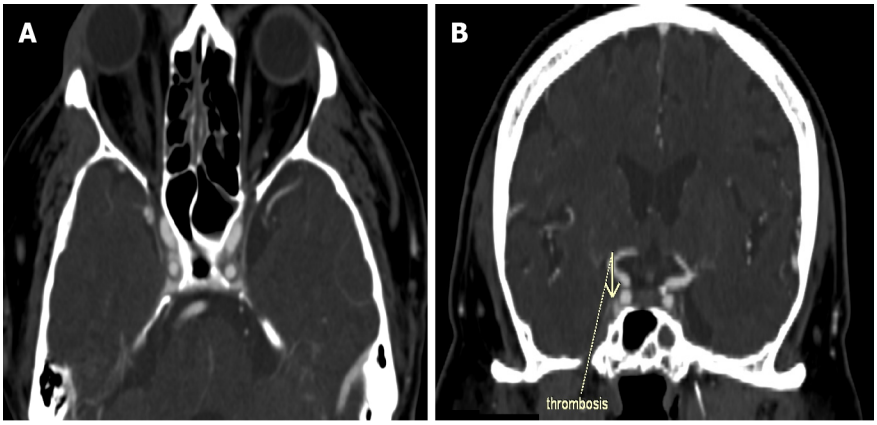

DOI: 10.5495/wjcid.v12.i1.1 **Copyright** ©The Author(s) 2022.

Figure 3 Computed tomography with contrast enhancement. A: Axial slice of thrombosis of the right sinus cavernosus; B: Coronal reconstruction of thrombosis of the right sinus cavernosus.

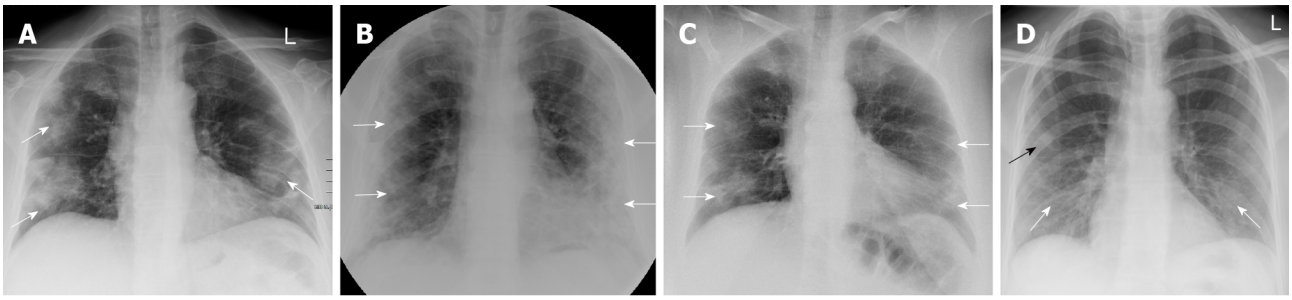

DOI: 10.5495/wjcid.v12.i1.1 **Copyright** ©The Author(s) 2022.

Figure 4 Imaging findings on conventional radiography range from normal findings to diffuse changes in the lung parenchyma. A: Posteroanterior (PA) chest X-ray 7 d after symptom onset. Predominantly peripheral ground glass opacities in both mid and lower zones of the lungs (white arrows); B: PA chest X-ray 11 d after symptom onset. Bilateral dense peripheral and basal air space consolidation (white arrows) more pronounced on the left and loss of lung markings in the mid and lower zones on the left; C: PA chest X-ray 3 d after symptom onset. Bilaterally, approximately proportionally in the middle and lower lung lobes, confluent ill-defined patchy opacities are visualized (white arrows). There is a relative preservation of the central areas of the lungs; D: PA chest X-ray 4 d after symptom onset. Bilaterally, predominantly in the right lower lobe, fine linear opacities (white arrows) are seen. Additionally, small patchy ground glass opacities (black arrow) are visualized in the peripheral region of right middle lobe.

include GGO, parenchymal consolidations, and crazy-paving pattern (Figure 5)[29]. The changes are usually multifocal, bilateral with a peripheral subpleural distribution predominantly in the posterior segments of the inferior lobes[30,31].

A GGO is the most frequent and earliest finding defined as increased attenuation on CT, which does not obscure the bronchovascular structures. It can be observed in three typical patterns: rounded, linear and crazy paving[30] (Figure 6). In the area of GGO, widening of vessels and traction bronchiectasis are commonly seen[32,33]. GGO with reticular interstitial thickening, known as crazy-paving, is defined as thickening of the pulmonary interstitium with thickened interlobular septae and visualization of intralobular pulmonary septae[34]. Crazy paving may be seen with areas of GGO or consolidation in the subacute to chronic phase of the disease[35] (Figure 7).

By definition, consolidation is a homogenous increase in the lung parenchyma's attenuation with obscuration of the underlying vessels (Figure 8) and bronchi[34]. Therefore, it is considered a sign of disease progression, especially in the intermediate and late stages of the disease[30,34].

The distribution of lung abnormalities was recorded as predominantly subpleural (involving mainly the peripheral one-third of the lung), random (without predilection for subpleural or central regions), or diffuse (continuous involvement without respect to lung segments)[33] (Figure 5). Additional CT features of COVID-19 pneumonia include vascular dilation, bronchial wall thickening, and traction bronchiectasis within the areas of GGO, architectural distortion with reticular thickening and subpleural bands formation, halo sign, or reversed halo sign (Figure 9). Changes considered atypical for COVID-19 pneumonia include lobar or segmental consolidations, small nodules (centrilobular lung nodules and tree-in-bud opacities), pulmonary cavitation, lymphadenopathy, and the presence of pleural or pericardial effusions[34].

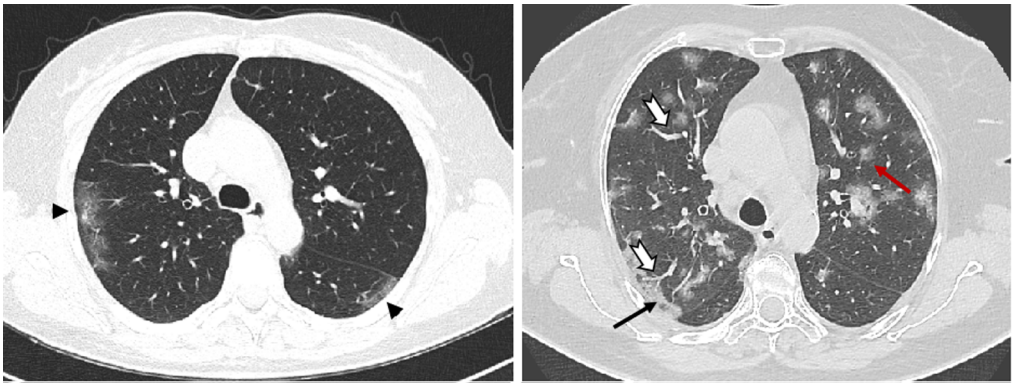

DOI: 10.5495/wjcid.v12.i1.1 **Copyright** ©The Author(s) 2022.

Figure 5 Axial computed tomography images show different patterns of ground glass opacities – round (red arrow), linear (arrowheads) and crazy paving (black arrow) with vascular enlargement (thick white arrow) within ground glass opacities areas.

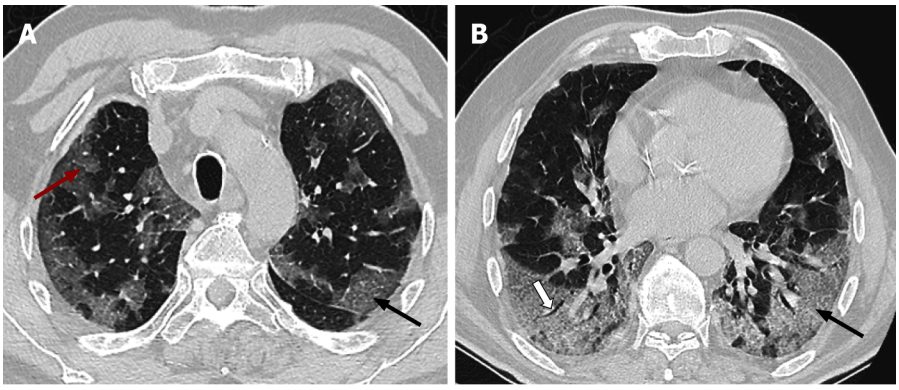

DOI: 10.5495/wjcid.v12.i1.1 **Copyright** ©The Author(s) 2022.

Figure 6 Axial computed tomography scans (7 days after symptom onset) show peripheral bilateral ground-glass opacities. A: Superimposed reticular interstitial thickening (red arrow) within the ground-glass opacities (GGO) giving a 'crazy-paving' appearance (black arrow); B: Air bronchogram (thick arrow) within the GGO.

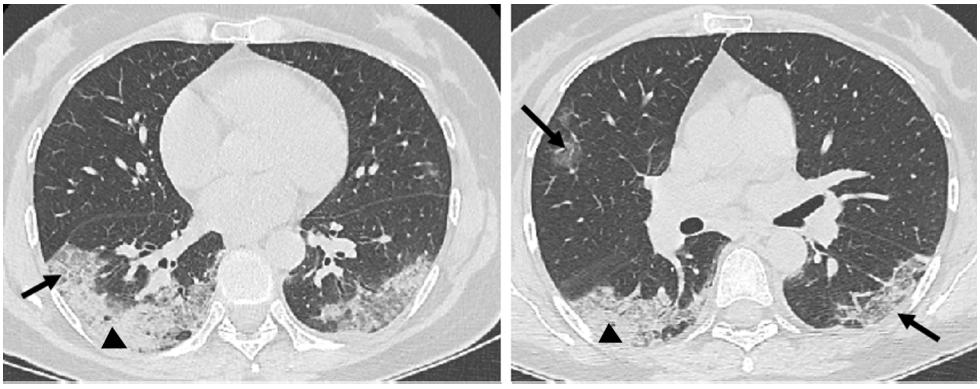

DOI: 10.5495/wjcid.v12.i1.1 **Copyright** ©The Author(s) 2022.

Figure 7 Axial computed tomography images 11 days after symptom onset demonstrate bilateral confluent zones of ground-glass opacities and crazy paving (arrows) with subpleural, predominantly dorsal distribution and with superimposed areas of consolidation (arrowheads), more extensive in the right thoracic half.

CT findings also vary depending on the onset of clinical symptoms. Approximately four stages of COVID-19 on chest CT have been described: (1) Early stage (0-5 d after onset of symptoms) marked by either normal or predominantly GGO (Figure 10); (2) Progressive stage (5-8 d after onset of symptoms) marked by enhanced GGO and a crazy-paving look (Figure 11A and B); (3) Peak stage (9-13 d after onset of symptoms) characterized by progressive consolidation (Figure 11C and D); and (4) Late stage (≥

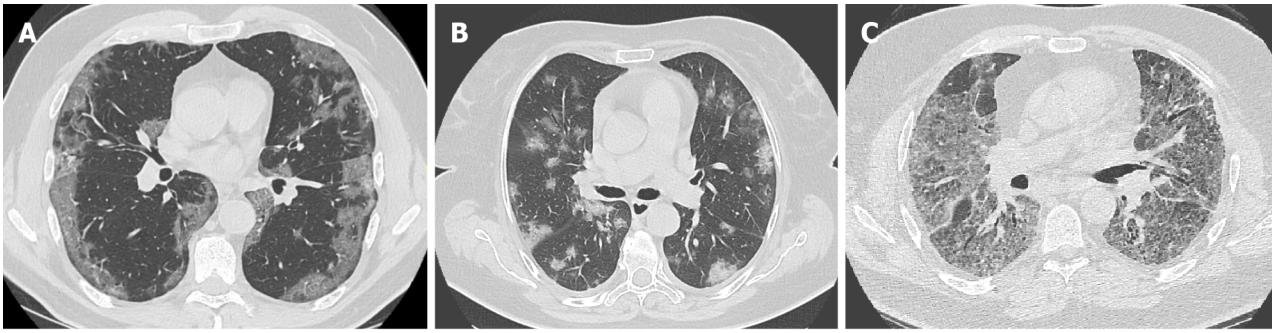

DOI: 10.5495/wjcid.v12.i1.1 **Copyright** ©The Author(s) 2022.

Figure 8 Axial computed tomography images of patients with different time of symptoms onset showing various types of lung abnormalities distribution. A: Subpleural with involvement of peripheral one third of lungs; B: Random with central and subpleural location; C: Diffuse with confluence of changes and continuous involvement.

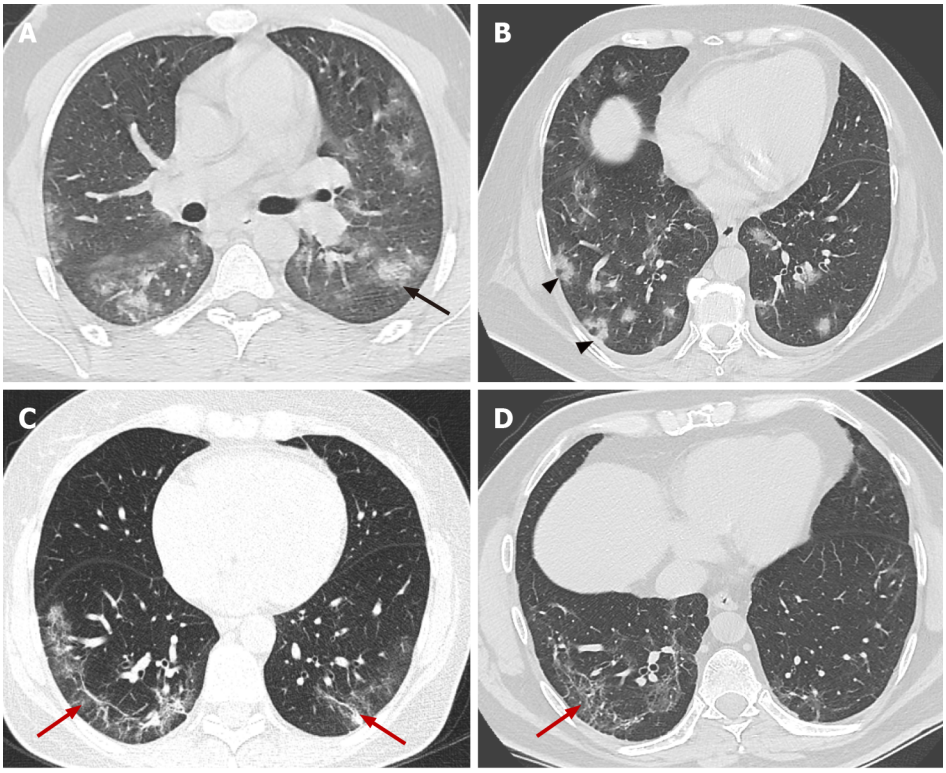

DOI: 10.5495/wjcid.v12.i1.1 **Copyright** ©The Author(s) 2022.

Figure 9 Axial computed tomography images demonstrate features seen in organizing pneumonia. A: Ground-glass opacities (GGO) surrounding small area of consolidation, "halo sign" (black arrow); B: Central GGO surrounded by denser consolidation of crescentic shape, "reverse halo sign" (arrowheads); C and D: Architectural distortion with interstitial thickening and irregular fibrous bands (red arrows).

14 d after the onset of symptoms) denoted by a gradual decrease in consolidation and GGO, although signs of fibrosis (including parenchymal bands, architectural distortion, and traction bronchiectasis) may occur[31,36-39] (Figure 12). It should also be remembered that the temporal development and degree of lung defects are heterogeneous among different individuals, depending on the disease severity[31,36]. Similar findings can be observed in other viral types of pneumonia, pneumonia caused by Mycoplasma or Chlamydia, vasculitis, and connective tissue disease. Therefore, the clinical-laboratory correlation with the radiological finding is essential for the diagnosis of COVID-19 pneumonia.

CT scanning can be a useful tool in evaluating the individual disease burden[40]. The quantitative severity can be assessed using a visual method or software that determines the percentage of affected lung volumes using deep learning algorithms[41,42]. Furthermore, the severity of lung involvement on CT correlates with the severity of the disease. It can be measured by scoring the percentages of each of the five lobes that are involved and can range from 0 (no involvement) to 25 (maximum involvement) when all five lobes show more than 75% involvement[41] (Figure 13).

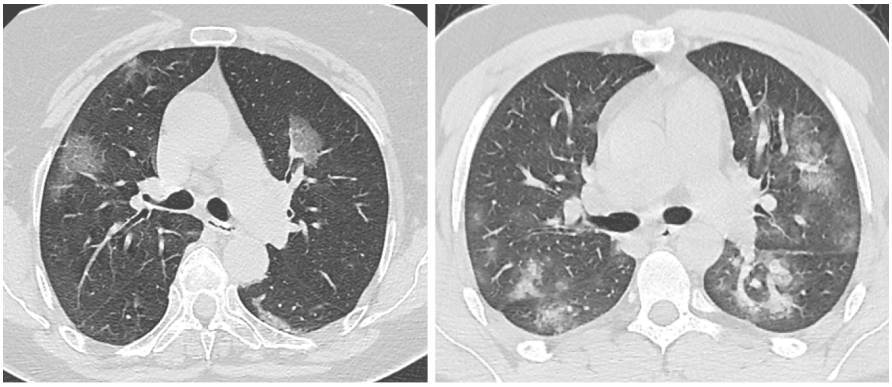

DOI: 10.5495/wjcid.v12.i1.1 **Copyright** ©The Author(s) 2022.

Figure 10 Axial computed tomography images in two different patients 5 days after onset of symptoms show various degree of ground-glass opacities abnormalities (early stage of COVID-19).

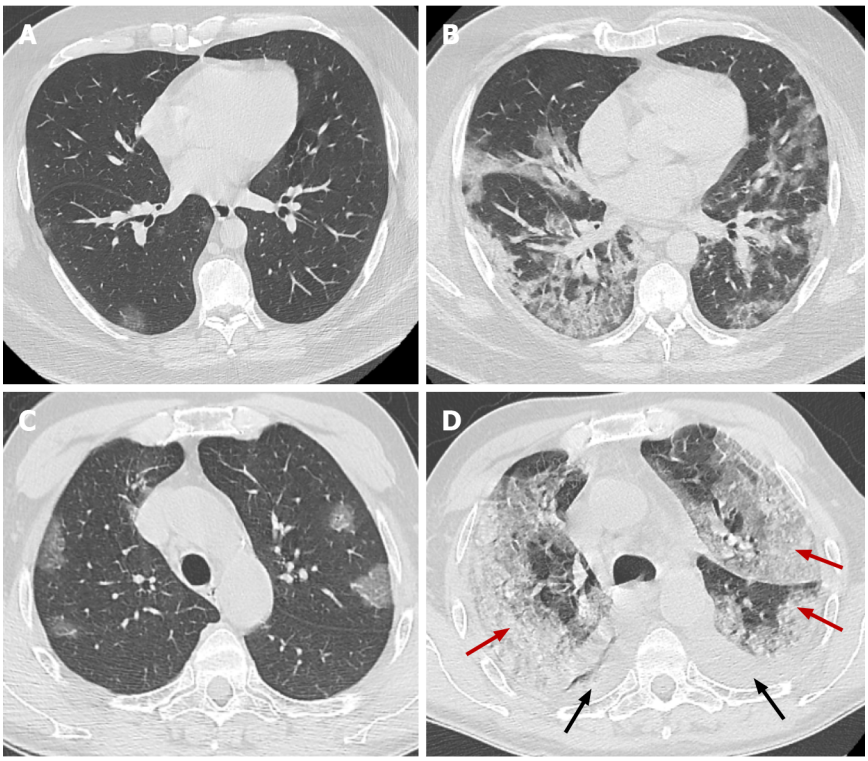

DOI: 10.5495/wjcid.v12.i1.1 **Copyright** ©The Author(s) 2022.

Figure 11 Axial computed tomography images. Axial computed tomography images on day 2 (A) and day 10 (B) from onset of symptoms of patient with clinical worsening demonstrate increased ground-glass opacities with confluence, crazy-paving appearance and typical peripheral subpleural location, early (A) and progressive (B) stage. Axial images from CT on day 5 (C) and day 15 (D) from onset of symptoms of patient with pronounced clinical worsening demonstrate increased ground-glass opacities with confluence, crazy-paving appearance and extensive areas of consolidation (red arrows) with predominant posterior and lateral distribution. In addition, bilateral pleural effusions (black arrows) are noted, early (C) and peak (D) stage.

Lung ultrasound is increasingly used as a complementary method in diagnosing COVID-19 pneumonia. It allows assessment of both the lung parenchyma and the pleural space with the ability of bedside and real-time assessment of pulmonary function and changes. In addition, US can easily distinguish normally aerated from pathologically altered lung parenchyma. The most common findings observed in interstitial pneumonia are irregularly thickened pleura, B-lines, and subpleural consolidations of the parenchyma[43,44].

B-lines are vertical hyperechoic artifacts arising from the pleura that resemble a comet tail (Figure 14A) and move with the lung sliding. The increase in subpleural lung density (in the absence of consolidated tissue) may lead to the coalescence of many vertical artifacts in more extended echogenic patterns and a single homogeneous subpleural echogenic area can be seen. This phenomenon is known as "white lung"[44] (Figure 14B). In addition to B-lines, small, oval subpleural consolidations are visible in the parenchyma (Figure 14C). With disease progression to ARDS, the number of B-lines and

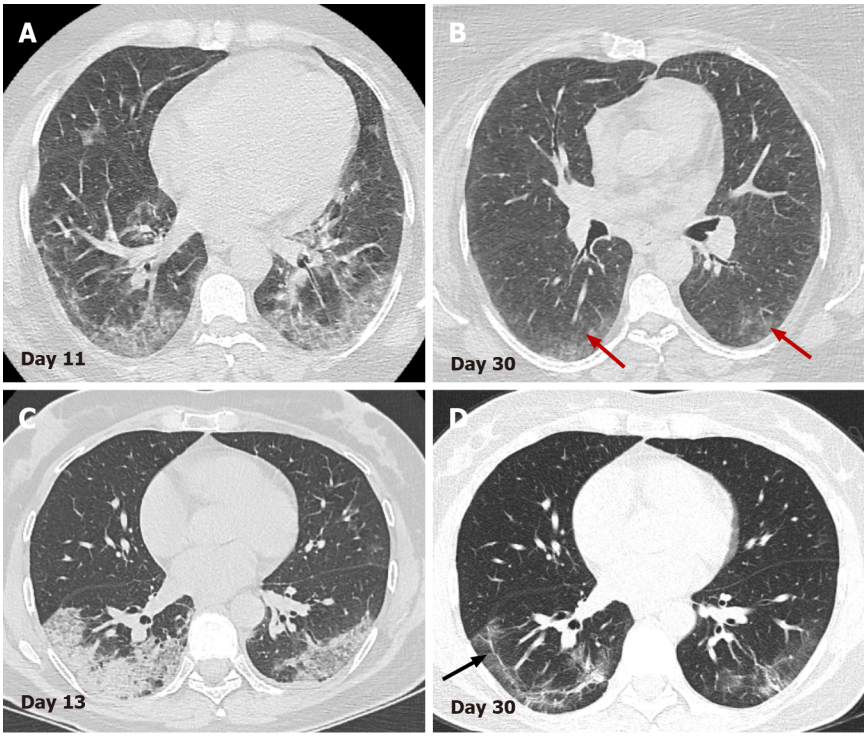

DOI: 10.5495/wjcid.v12.i1.1 **Copyright** ©The Author(s) 2022.

Figure 12 Serial axial computed tomography images. Serial axial computed tomography images in two different patients show gradual decrease of GGO and consolidations in the late stage of disease (B) and (D). In patient 1 (A) and (B) advanced resorption of the abnormalities is seen with very low density GGO at the sight of previous lung changes (red arrows). In patient 2 (C) and (D) architectural distortion with fibrous bands parallel to the pleura (black arrow) and traction bronchiectasis are visualized (arrowheads).

parenchymal consolidations increases with the formation of sizeable gravitational consolidation[44], and the characteristic lung sliding is no longer visible. In the recovery phase of the disease, the consolidations and B-lines gradually disappear. Instead, A-line artifacts found in normally aerated parenchyma reappear and lung sliding is improved.

SEVERE CASES OF COVID-19

ARDS/cytokine storm

In some cases, COVID-19 pneumonia proceeds to the typical complications such as ARDS and cytokine storm. ARDS remains the most frequent immunopathological complication in SARS-CoV-2, SARS-CoV, and MERS-CoV viruses. The cytokine storm is one of the critical pathways for ARDS[45]. Both ARDS and cytokine storm represent an unregulated autoimmune inflammatory response arising from the release of significant quantities of pro-inflammatory cytokines (such as IFNg, IFNa, IL-1β, IL-6, IL-12, IL-18, IL-33, TNF-5-007, TGFβ, *etc.*) and chemokines (C-C Motif Chemokine Ligand 2 (CCL2), CCL3, CCL5, C-X-C motif ligand 8 (CXCL8), CXCL9, CXCL10, *etc.*) from immune or viral-infected cells[46]. Therefore, it is essential that these factors be detected and evaluated early. Thus, the appropriate therapy can be administered.

Histological examination of lung specimens in patients with severe infection is characterized by severe and extensive diffuse alveolar damage, fibromyxoid exudates, interstitial and intra-alveolar edema. However, in one of the cases described in the literature, the respiratory bronchial mucosa was intact, without evidence of squamous metaplasia. This is a significant difference compared with the pathology observed in the first epidemic of SARS[48]. In such patients, it is often found denuded with necrosis of type I pneumocytes and the formation of hyaline membrane and the proliferation of type II pneumocytes, which indicate ARDS in the acute stage without evidence of interstitial organization[17,21]. In addition, there is diffuse thickening of alveolar walls due to congestion, and patchy to mild mononuclear inflammatory infiltrate comprised of lymphocytes, macrophages, and some plasma cells. Perivascular lymphocyte aggregates have also been identified[47]. No eosinophils or neutrophils were identified, but if these are found, they usually suggest secondary bacterial infection[21,47]. Occasionally, in proliferated alveolar epithelial cells, viral inclusions in intranuclear and/or intracytoplasmic and multinucleated syncytial cells with atypical enlarged pneumocytes can be seen characterized by large eosinophilic nuclei with prominent nucleoli and granular cytoplasm (probably representing a viral

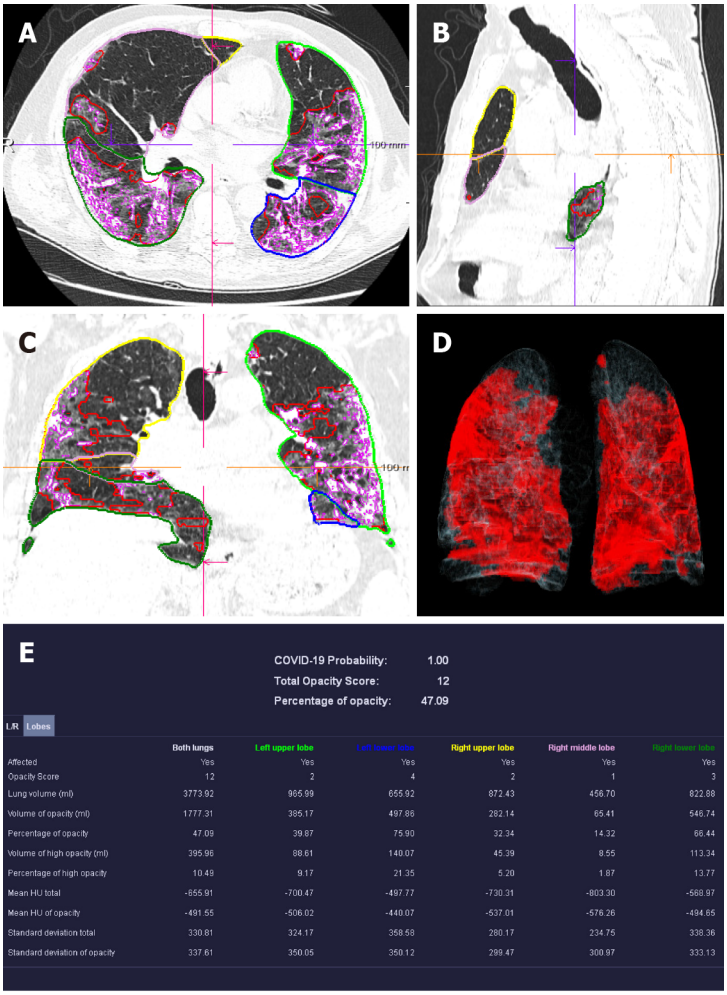

DOI: 10.5495/wjcid.v12.i1.1 **Copyright** ©The Author(s) 2022.

Figure 13 Computed tomography pneumonia analysis (automated lung opacity analysis). A-C: Multi-planar reconstruction views overlaid with delineations of the opacities and the lungs; D: Volume rendering image showing a quick overview of the spatial distribution of the opacities; E: Table with measurements demonstrating relative ("percentage of opacities") and absolute volume of opacities, mean and standard deviation of HU values between lung parenchyma and the detected opacities, separately segmented quantitative results per left and right lung and per lung lobe.

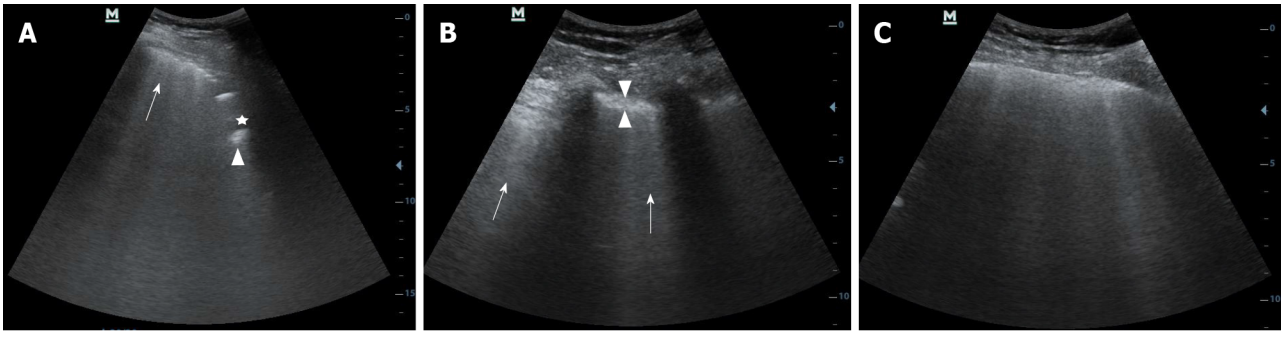

DOI: 10.5495/wjcid.v12.i1.1 **Copyright** ©The Author(s) 2022.

Figure 14 Lung ultrasound image. A: Lung ultrasound image obtained with convex probe shows multiple B-lines (arrow) and subpleural consolidations seen as hypoechoic regions (asterix) that appear tissue-like with an irregular deep border (shredded fractal line) abutting the more aerated lung, which has echogenic artefacts (arrowhead); B: Lung ultrasound image obtained with convex probe. Multiple linear vertical artefacts - B-lines (arrows), and thickened pleural line (between arrowheads) are visualized; C: Lung ultrasound image obtained with convex probe. Multiple confluent B-lines are seen (white lung).

effect similar to that reported in the first SARS epidemic)[17,47-49]. Common in ARDS, pulmonary thrombi and microangiopathy may be noted within a few small pulmonary artery branches and pleural adhesions[21,47]. This thrombotic process may involve activation of megakaryocytes, probably those that are naturally found in the lung, with platelet aggregation and platelet formation, in addition to

fibrin deposition. The formation of small vascular thrombi in the lungs is often accompanied by focal alveolar hemorrhage[47,49].

With regard to imaging, COVID-19 related ARDS is diagnosed when a patient with confirmed COVID-19 infection meets the Berlin 2012 ARDS diagnostic criteria: acute hypoxemic respiratory failure; presentation within one week of worsening respiratory symptoms; bilateral airspace disease on CRX, CT, or US that is not fully explained by effusions, lung collapse, or nodules; and cardiac failure is not the primary cause of acute hypoxemic respiratory failure[50,51]. The risk factors for patients with COVID-19 to develop ARDS in the course of the disease are older age, concomitant conditions – most often hypertension and diabetes, and specific clinical symptoms on initial presentation such as marked dyspnea and fever ≥ 39°C[52]. However, clinical manifestations may be relatively mild regarding the severity of imaging findings in COVID-19[53].

Imaging studies have an essential role in the initial evaluation of the pattern and extent of lung involvement and in the follow-up of hospitalized patients. Chest radiographic findings of ARDS are non-specific and resemble those of typical pulmonary edema or pulmonary hemorrhage with diffuse, patchy or homogeneous, bilateral, and coalescent opacities[54] (Figures 15 and 16). Radiography in the first 24 h of deterioration may be unchanged[55]. CT imaging features depend on the phase of the disease[56]. In the early exudative stage (first week), CT scans usually display a non-homogeneous distribution and ventrodorsal gradient of density. More dense consolidations are observed in dependent regions, extensive GGO, and comparatively regular or hyper-inflated parenchyma (in the case of mechanical ventilation) in non-dependent areas[54] (Figure 17).

In the late fibrotic phase (over two weeks), CT appearance can be variable. Complete resolution may occur in some cases, but the coarse reticular pattern and ground-glass opacification in the anterior (non-dependent) part of the lungs are considered more typical CT features. Pulmonary cysts of varying sizes and bullae have also been reported, which probably developed due to prolonged ventilation[56]. Subsequent imaging studies can show the development of pneumomediastinum, pneumothorax (often hypertensive in mechanically ventilated patients), and subcutaneous emphysema[54] (Figure 18).

Multiorgan failure

The cytokine storm causes ARDS and multiorgan failure, leading to death in severe cases of coronavirus infections[45]. Although COVID-19 is known to cause pulmonary disease, including pneumonia and ARDS, various extrapulmonary manifestations of COVID-19 have been reported, affecting the gastrointestinal tract, brain, heart, kidneys, or muscles. Therefore, imaging helps to estimate the presence of complications and the extend of COVID-19.

Histologically, there is no noticeable viral cytopathic effect on the heart in the case of moderate infection on light microscopy[21,47]. However, liver biopsy specimens in patients with COVID-19 showed moderate fatty degeneration of hepatocytes and mild lobular and portal activity with slight interstitial mononuclear inflammatory infiltrates, indicating that the injury that could have been caused by either COVID-19 infection or drug-induced liver injury.

The pathogenesis of kidney injury due to COVID-19 is not well-described. However, it seems to be multifactorial, involving mechanisms related to systemic hypoxia, coagulation disorders, inflammatory changes, or even cell destruction due to viruses. According to the literature, renal impairment was related to multiple organ failure[57]. Furthermore, post-mortem examination of the kidney from a patient who died of COVID-19 infection demonstrated that viral antigens accumulated in the renal tubules, inducing acute kidney injury[57].

Histological examination confirmed that a diffuse proximal tubular lesion, loss of brush border, non-isometric vacuolar degeneration, and a small area of necrosis were observed. In addition, interstitial inflammation and hemorrhage were found in some of the published cases, probably due to secondary bacterial infection[58]. However, most of these findings are caused by comorbidities. The renal changes described above may be directly due to COVID-19 infection. These pathological observations may only provide a basis for further study and investigation of COVID-19[58].

The main focus of COVID-19 is respiratory system complications, which are also a leading factor determining the severity of the disease course. More and more is known about the pathophysiology of the disease and the mechanism of lung damage. However, the extrapulmonary manifestations of the disease remain unclear, which in some cases is decisive for the disease course[59]. Cardiovascular complications are receiving increasing attention, and according to various studies range from 30 to 78% [60-62]. Cardiovascular disease (CVD) is known to be one of the main risk factors for severe disease. A study of 44672 patients with COVID-19 infection in China showed that a history of concomitant CVD was associated with nearly five-fold higher mortality (10.5% *vs* 2.3%) than patients without a history of CVD[63]. In addition, increasing evidence suggests that the virus may directly affect the cardiovascular system and lead to complications such as myocarditis, acute coronary syndrome, arrhythmias, and venous thromboembolism[64].

Cardiomagnetic resonance imaging (CMR) represents the gold standard in assessing the structure and function of the heart and provides information on the tissue characteristics of the myocardium. That, together with its non-invasive nature and lack of ionizing radiation, makes it essential for both early diagnosis and monitoring of cardiac complications due to COVID-19.

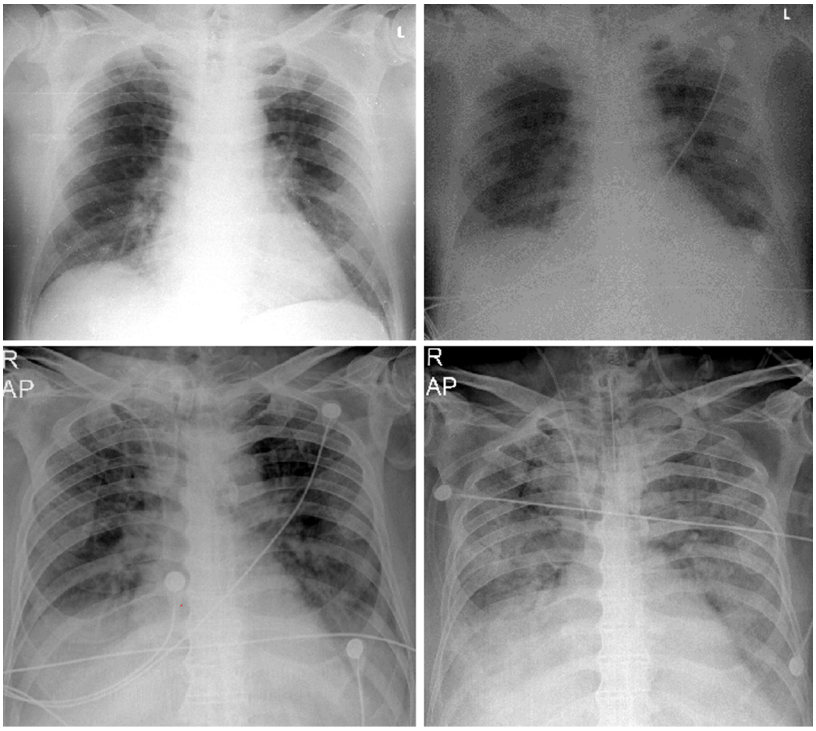

DOI: 10.5495/wjcid.v12.i1.1 **Copyright** ©The Author(s) 2022.

Figure 15 Serial chest X-ray imaging of coronavirus disease-2019 infected 65-year-old man with rapid respiratory deterioration after symptom onset showing progression from lower lung predominant interstitial and airspace opacities on day 1 and day 3 to diffuse and worsening involvement with extensive airspace disease on days 4 and 6.

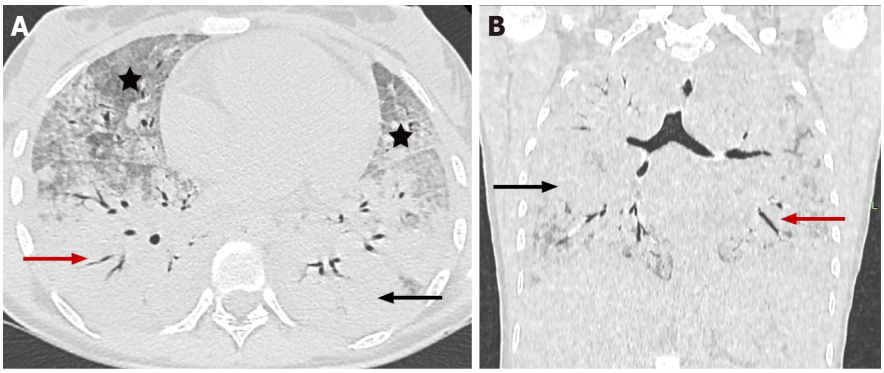

DOI: 10.5495/wjcid.v12.i1.1 **Copyright** ©The Author(s) 2022.

Figure 16 Coronavirus disease-2019 related acute respiratory distress syndrome, early stage. Axial (A) and coronal (B) computed tomography images demonstrate widespread ground glass opacities (asterix) and large areas of consolidation (black arrow) with air bronchogram (red arrow) showing anteroposterior density gradient in both lungs.

The pathogenesis of cardiac damage is currently unclear. However, presumed mechanisms include direct viral invasion, cytokine-mediated injury, a mismatch between needs and oxygen supply, and ischemic impairment resulting from microvascular thrombosis[65,66].

The CMR findings in the acute phase of the disease reported so far are based on small groups of patients. The presence of myocardial edema is a characteristic feature observed in almost all reported cases[67-70]. In a review of 31 publications with 51 patients, only one patient did not have edema at baseline, and two patients developed reversible edema within two weeks[68].

The extent of edema varies - from diffuse to limited to separate segments of the myocardium - most often in the LV inferior wall regions, the mid inferoseptal regions, and the apical region[68]. Another characteristic CMR sign is late gadolinium enhancement (LGE) of the myocardium due to necrosis/fibrosis following nonischemic myocardial injury localized at the sub-epicardial and/or intramural regions in the non-coronary territory. The presence and extent of zones of LGE correlate with the prognosis[68]. An additional feature in the acute phase of the disease is diffuse hypokinesis of the left and/or right ventricle and, much less frequently, segmental hypokinesis[68].

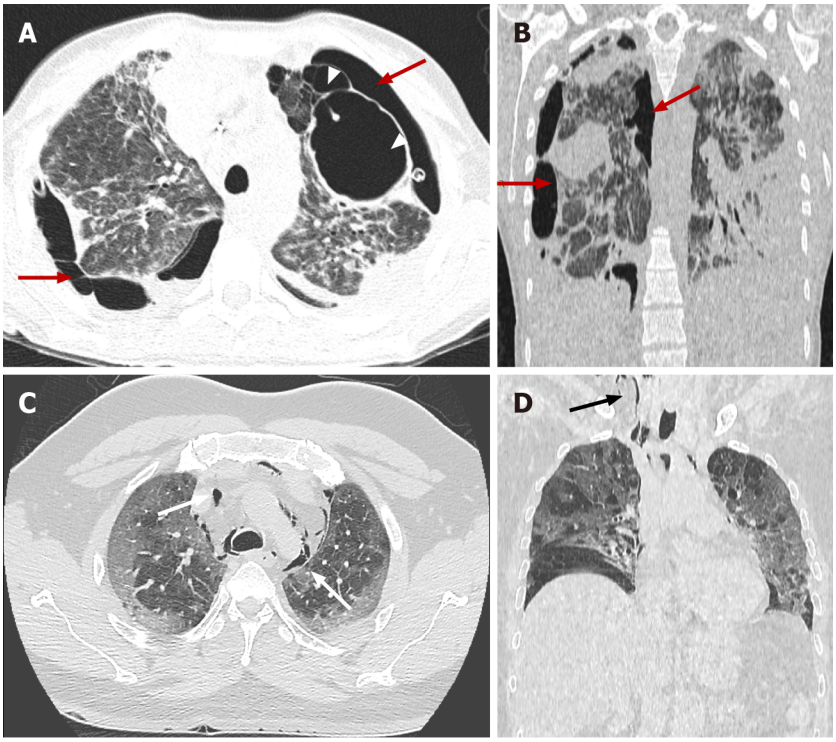

DOI: 10.5495/wjcid.v12.i1.1 **Copyright** ©The Author(s) 2022.

Figure 17 Coronavirus disease-2019 related acute respiratory distress syndrome, late stage. Axial (A) and coronal computed tomography (CT) (B) images demonstrate typical complications in mechanically ventilated patients with subpleural bullae formation (arrowheads) and bilateral pneumothorax (red arrows). Axial (C) and coronal (D) CT images in different patient showing spontaneous pneumomediastinum (white arrows), extending into the neck as subcutaneous emphysema (black arrow).

Similar CMR findings - edema, necrosis/fibrosis, and impaired systolic function are also found in patients following COVID-19 infection[62,67,69-71]. Signs of persistent inflammation with prolonged T2 relaxation time due to edema, prolonged T1 relaxation time and LGE with a different distribution, and pericardial enhancement are seen. In some cases, reduced ejection fraction[62] is found.

Coagulopathy and thrombotic accidents

The cytokine storm is one of the leading causes of disseminated intravascular coagulation (DIC) affecting the entire organism. Pro-inflammatory cytokines, such as TNFa and IL-1, are able to inhibit endogenic anticoagulation. Inflammation injures the endothelium and results in activation of tissue plasminogen activator, which may explain the rise in D-dimer and fibrin degradation products[72,73]. In summary, COVID-19 is associated with a hypercoagulable disease and an elevated risk of thromboembolic complications.

The histological findings in organs other than lungs do not indicate significant changes directly related to COVID-19. However, the most commonly observed histological changes were due to thrombotic microangiopathy involving the lungs, spleen, and kidney. The most common complications which have been described in the literature include acute limb ischemia, aortic and mesenteric thrombosis, myocardial and brain infarction, and DIC[74].

A retrospective study on CTPA reported that pulmonary embolism in COVID-19 patients appears to be primarily distributed in the segmental arteries of the right lung[75]. Furthermore, only the determination of D-dimer and IL-6 at admission to CT scan appears to differentiate patients with pulmonary embolism from patients with a negative CT pulmonary angiogram. However, inter-individual heterogeneity calls for the establishment of cut-off values in COVID-19 patients in future research[76].

The pre-pandemic understanding of the predictive value of perfusion scintigraphy in assessing chronic thromboembolic disease and chronic thromboembolic pulmonary hypertension is well-established. Dhawan *et al*[75] proposed perfusion imaging as a triage tool for post-COVID-19 recovery. They suggested the potential of perfusion imaging to examine the *in situ* thrombotic small vessel signature of COVID-19. It is widely accepted that *in situ* thrombotic microbial pulmonary hypertension is present. Thus, lung perfusion imaging provides a primary triage instrument within the broader panel of investigations to enhance understanding of the natural history of thromboembolic phenomena in COVID-19 and distinguish hemodynamic sequelae from deconditioning dysfunctional breathing-related functional limitations. The authors also suggest that such imaging should be incorporated in routine post-COVID-19 follow-up pathways[75].

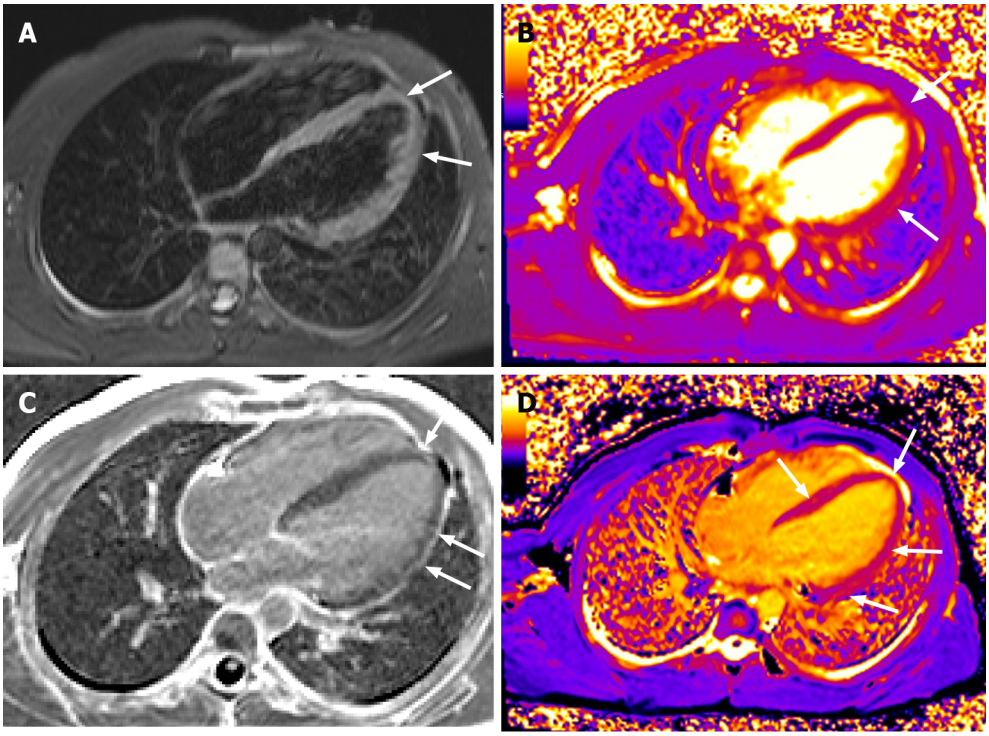

DOI: 10.5495/wjcid.v12.i1.1 **Copyright** ©The Author(s) 2022.

Figure 18 Cardiac magnetic resonance imaging. Horizontal long axis TIRM image (A) displaying high signal in the myocardium at the apex and along the free wall of the left ventricle (LV). Horizontal long axis T2 (B) and T1 (D) mapping depicting prolonged T2 and T1 relaxation times at the same area and in the middle septum (D). Horizontal long axis image post gadolinium administration (C) showing late enhancement at the apex and along the free wall of LV. There is also pericardial enhancement along the free wall of LV.

CONCLUSION

Early observed changes in critical organs such as lungs, kidneys, blood vessels, *etc.*, might benefit the timely and appropriate treatment of COVID-19 to alleviate the complications and avoid fatal outcomes. Along with typical clinical and imaging results, atypical results are also beneficial. Early detection of pathological changes at different stages of life-threatening COVID-19 can improve patient management, treatment, and outcome.

FOOTNOTES

Author contributions: Boyapati A, Chervenkov L, Gulinac M, and Genova K performed the literature review; Chervenkov L, Ilieva E, Gulinac M, and Borisov Y collected and prepared the images from their institutes' database; Genova K, Ilieva E, and Chervenkov L provided the text and explanations of the images; Ilieva E and Velikova T wrote the draft; all the authors wrote additional sections in the paper according to their specialty; Velikova T revised the final draft; all authors revised and approved the final version of the article.

Conflict-of-interest statement: The authors declare that they have no conflict of interest.

Country/Territory of origin: Bulgaria

ORCID number: Elena Ilieva 0000-0003-2016-8591; Alexandra Boyapati 0000-0003-1003-4127; Lyubomir Chervenkov 0000-0002-8380-5992; Milena Gulinac 0000-0001-7970-9378; Jordan Borisov 0000-0001-5842-6096; Kamelia Genova 0000-0002-3168-819X; Tsvetelina Velikova 0000-0002-0593-1272.

S-Editor: Liu JH
L-Editor: Webster JR

P-Editor: Liu JH

REFERENCES

1 **WHO Headquarters**. Clinical management of COVID-19. Interim guidance 2020; last access on 28/01/2021 Available from: https://www.who.int/publications/i/item/WHO-2019-nCoV-clinical-2021-2

2 **Ai T**, Yang Z, Hou H, Zhan C, Chen C, Lv W, Tao Q, Sun Z, Xia L. Correlation of Chest CT and RT-PCR Testing for Coronavirus Disease 2019 (COVID-19) in China: A Report of 1014 Cases. *Radiology* 2020; **296**: E32-E40 [PMID: 32101510 DOI: 10.1148/radiol.2020200642]

3 **Fang Y**, Zhang H, Xie J, Lin M, Ying L, Pang P, Ji W. Sensitivity of Chest CT for COVID-19: Comparison to RT-PCR. *Radiology* 2020; **296**: E115-E117 [PMID: 32073353 DOI: 10.1148/radiol.2020200432]

4 **Lin EC**. Radiation risk from medical imaging. *Mayo Clin Proc* 2010; **85**: 1142-6; quiz 1146 [PMID: 21123642 DOI: 10.4065/mcp.2010.0260]

5 **Borakati A**, Perera A, Johnson J, Sood T. Diagnostic accuracy of X-ray versus CT in COVID-19: a propensity-matched database study. *BMJ Open* 2020; **10**: e042946 [PMID: 33158840 DOI: 10.1136/bmjopen-2020-042946]

6 **Sohail S**. Rational and practical use of imaging in COVID-19 pneumonia. *Pak J Med Sci* 2020; **36**: S130-S133 [PMID: 32582332 DOI: 10.12669/pjms.36.COVID19-S4.2760]

7 **Chervenkov L**, Doykova K, Tsvetkova S. HRCT diagnosis and CORADS classification in patients with COVID-19 infection (2020) Rentgenologiya i radiologiya. ISSN 0486-400X, pp 220-223

8 **Ai T**, Yang Z, Hou H, Zhan C, Chen C, Lv W, Tao Q, Sun Z, Xia L. Correlation of Chest CT and RT-PCR Testing for Coronavirus Disease 2019 (COVID-19) in China: A Report of 1014 Cases. *Radiology* 2020; **296**: E32-E40 [PMID: 32101510 DOI: 10.1148/radiol.2020200642]

9 **Cavagna E**, Muratore F, Ferrari F. Pulmonary Thromboembolism in COVID-19: Venous Thromboembolism or Arterial Thrombosis? *Radiol Cardiothorac Imaging* 2020; **2**: e200289 [PMID: 33778609 DOI: 10.1148/ryct.2020200289]

10 **Revzin MV**, Raza S, Srivastava NC, Warshawsky R, D'Agostino C, Malhotra A, Bader AS, Patel RD, Chen K, Kyriakakos C, Pellerito JS. Multisystem Imaging Manifestations of COVID-19, Part 2: From Cardiac Complications to Pediatric Manifestations. *Radiographics* 2020; **40**: 1866-1892 [PMID: 33136488 DOI: 10.1148/rg.2020200195]

11 **Hameed S**, Elbaaly H, Reid CEL, Santos RMF, Shivamurthy V, Wong J, Jogeesvaran KH. Spectrum of Imaging Findings at Chest Radiography, US, CT, and MRI in Multisystem Inflammatory Syndrome in Children Associated with COVID-19. *Radiology* 2021; **298**: E1-E10 [PMID: 32584166 DOI: 10.1148/radiol.2020202543]

12 **Desai SB**, Pareek A, Lungren MP. Deep learning and its role in COVID-19 medical imaging. *Intell Based Med* 2020; **3**: 100013 [PMID: 33169117 DOI: 10.1016/j.ibmed.2020.100013]

13 **Bai HX**, Wang R, Xiong Z, Hsieh B, Chang K, Halsey K, Tran TML, Choi JW, Wang DC, Shi LB, Mei J, Jiang XL, Pan I, Zeng QH, Hu PF, Li YH, Fu FX, Huang RY, Sebro R, Yu QZ, Atalay MK, Liao WH. Artificial Intelligence Augmentation of Radiologist Performance in Distinguishing COVID-19 from Pneumonia of Other Origin at Chest CT. *Radiology* 2020; **296**: E156-E165 [PMID: 32339081 DOI: 10.1148/radiol.2020201491]

14 **Velikova TV**, Kotsev SV, Georgiev DS, Batselova HM. Immunological aspects of COVID-19: What do we know? *World J Biol Chem* 2020; **11**: 14-29 [PMID: 33024515 DOI: 10.4331/wjbc.v11.i2.14]

15 **Mason RJ**. Pathogenesis of COVID-19 from a cell biology perspective. *Eur Respir J* 2020; **55** [PMID: 32269085 DOI: 10.1183/13993003.00607-2020]

16 **Ouyang W**, Yu J, Zhang J, Xie C. Alert to Potential Contagiousness: A Case of Lung Cancer With Asymptomatic Severe Acute Respiratory Syndrome Coronavirus 2 Infection. *J Thorac Oncol* 2020; **15**: e82-e83 [PMID: 32305592 DOI: 10.1016/j.jtho.2020.04.005]

17 **Tian S**, Hu W, Niu L, Liu H, Xu H, Xiao SY. Pulmonary Pathology of Early-Phase 2019 Novel Coronavirus (COVID-19) Pneumonia in Two Patients With Lung Cancer. *J Thorac Oncol* 2020; **15**: 700-704 [PMID: 32114094 DOI: 10.1016/j.jtho.2020.02.010]

18 **Al-Tawfiq JA**. Asymptomatic coronavirus infection: MERS-CoV and SARS-CoV-2 (COVID-19). *Travel Med Infect Dis* 2020; **35**: 101608 [PMID: 32114075 DOI: 10.1016/j.tmaid.2020.101608]

19 **Joob B**, Wiwanitkit V. Pulmonary Pathology of Early Phase 2019 Novel Coronavirus Pneumonia. *J Thorac Oncol* 2020; **15**: e67 [PMID: 32340677 DOI: 10.1016/j.jtho.2020.03.013]

20 **Zhu J**, Zhang Y, Gao XH, Xi EP. Coronavirus Disease 2019 or Lung Cancer: A Differential Diagnostic Experience and Management Model From Wuhan. *J Thorac Oncol* 2020; **15**: e141-e142 [PMID: 32387713 DOI: 10.1016/j.jtho.2020.04.030]

21 **Barton LM**, Duval EJ, Stroberg E, Ghosh S, Mukhopadhyay S. COVID-19 Autopsies, Oklahoma, USA. *Am J Clin Pathol* 2020; **153**: 725-733 [PMID: 32275742 DOI: 10.1093/ajcp/aqaa062]

22 **Liu H**, Liu F, Li J, Zhang T, Wang D, Lan W. Clinical and CT imaging features of the COVID-19 pneumonia: Focus on pregnant women and children. *J Infect* 2020; **80**: e7-e13 [PMID: 32171865 DOI: 10.1016/j.jinf.2020.03.007]

23 **Borczuk AC**, Salvatore SP, Seshan SV, Patel SS, Bussel JB, Mostyka M, Elsoukkary S, He B, Del Vecchio C, Fortarezza F, Pezzuto F, Navalesi P, Crisanti A, Fowkes ME, Bryce CH, Calabrese F, Beasley MB. COVID-19 pulmonary pathology: a multi-institutional autopsy cohort from Italy and New York City. *Mod Pathol* 2020; **33**: 2156-2168 [PMID: 32879413 DOI: 10.1038/s41379-020-00661-1]

24 **Cleverley J**, Piper J, Jones MM. The role of chest radiography in confirming covid-19 pneumonia. *BMJ* 2020; **370**: m2426 [PMID: 32675083 DOI: 10.1136/bmj.m2426]

25 **Kooraki S**, Hosseiny M, Myers L, Gholamrezanezhad A. Coronavirus (COVID-19) Outbreak: What the Department of Radiology Should Know. *J Am Coll Radiol* 2020; **17**: 447-451 [PMID: 32092296 DOI: 10.1016/j.jacr.2020.02.008]

26 **Cozzi D**, Albanesi M, Cavigli E, Moroni C, Bindi A, Luvarà S, Lucarini S, Busoni S, Mazzoni LN, Miele V. Chest X-ray in

new Coronavirus Disease 2019 (COVID-19) infection: findings and correlation with clinical outcome. *Radiol Med* 2020; **125**: 730-737 [PMID: 32519256 DOI: 10.1007/s11547-020-01232-9]

27 **Wong HYF**, Lam HYS, Fong AH, Leung ST, Chin TW, Lo CSY, Lui MM, Lee JCY, Chiu KW, Chung TW, Lee EYP, Wan EYF, Hung IFN, Lam TPW, Kuo MD, Ng MY. Frequency and Distribution of Chest Radiographic Findings in Patients Positive for COVID-19. *Radiology* 2020; **296**: E72-E78 [PMID: 32216717 DOI: 10.1148/radiol.2020201160]

28 **Jin YH**, Cai L, Cheng ZS, Cheng H, Deng T, Fan YP, Fang C, Huang D, Huang LQ, Huang Q, Han Y, Hu B, Hu F, Li BH, Li YR, Liang K, Lin LK, Luo LS, Ma J, Ma LL, Peng ZY, Pan YB, Pan ZY, Ren XQ, Sun HM, Wang Y, Wang YY, Weng H, Wei CJ, Wu DF, Xia J, Xiong Y, Xu HB, Yao XM, Yuan YF, Ye TS, Zhang XC, Zhang YW, Zhang YG, Zhang HM, Zhao Y, Zhao MJ, Zi H, Zeng XT, Wang XH; , for the Zhongnan Hospital of Wuhan University Novel Coronavirus Management and Research Team, Evidence-Based Medicine Chapter of China International Exchange and Promotive Association for Medical and Health Care (CPAM). A rapid advice guideline for the diagnosis and treatment of 2019 novel coronavirus (2019-nCoV) infected pneumonia (standard version). *Mil Med Res* 2020; **7**: 4 [PMID: 32029004 DOI: 10.1186/s40779-020-0233-6]

29 **Caruso D**, Polidori T, Guido G, Nicolai M, Bracci B, Cremona A, Zerunian M, Polici M, Pucciarelli F, Rucci C, Dominicis C, Girolamo MD, Argento G, Sergi D, Laghi A. Typical and atypical COVID-19 computed tomography findings. *World J Clin Cases* 2020; **8**: 3177-3187 [PMID: 32874972 DOI: 10.12998/wjcc.v8.i15.3177]

30 **Bernheim A**, Mei X, Huang M, Yang Y, Fayad ZA, Zhang N, Diao K, Lin B, Zhu X, Li K, Li S, Shan H, Jacobi A, Chung M. Chest CT Findings in Coronavirus Disease-19 (COVID-19): Relationship to Duration of Infection. *Radiology* 2020; **295**: 200463 [PMID: 32077789 DOI: 10.1148/radiol.2020200463]

31 **Pan F**, Ye T, Sun P, Gui S, Liang B, Li L, Zheng D, Wang J, Hesketh RL, Yang L, Zheng C. Time Course of Lung Changes at Chest CT during Recovery from Coronavirus Disease 2019 (COVID-19). *Radiology* 2020; **295**: 715-721 [PMID: 32053470 DOI: 10.1148/radiol.2020200370]

32 **Kovács A**, Palásti P, Veréb D, Bozsik B, Palkó A, Kincses ZT. The sensitivity and specificity of chest CT in the diagnosis of COVID-19. *Eur Radiol* 2021; **31**: 2819-2824 [PMID: 33051732 DOI: 10.1007/s00330-020-07347-x]

33 **Kanne JP**, Little BP, Chung JH, Elicker BM, Ketai LH. Essentials for Radiologists on COVID-19: An Update-*Radiology* Scientific Expert Panel. *Radiology* 2020; **296**: E113-E114 [PMID: 32105562 DOI: 10.1148/radiol.2020200527]

34 **Hansell DM**, Bankier AA, MacMahon H, McLoud TC, Müller NL, Remy J. Fleischner Society: glossary of terms for thoracic imaging. *Radiology* 2008; **246**: 697-722 [PMID: 18195376 DOI: 10.1148/radiol.2462070712]

35 **Nagpal P**, Narayanasamy S, Vidholia A, Guo J, Shin KM, Lee CH, Hoffman EA. Imaging of COVID-19 pneumonia: Patterns, pathogenesis, and advances. *Br J Radiol* 2020; **93**: 20200538 [PMID: 32758014 DOI: 10.1259/bjr.20200538]

36 **Kwee TC**, Kwee RM. Chest CT in COVID-19: What the Radiologist Needs to Know. *Radiographics* 2020; **40**: 1848-1865 [PMID: 33095680 DOI: 10.1148/rg.2020200159]

37 **Wang Y**, Dong C, Hu Y, Li C, Ren Q, Zhang X, Shi H, Zhou M. Temporal Changes of CT Findings in 90 Patients with COVID-19 Pneumonia: A Longitudinal Study. *Radiology* 2020; **296**: E55-E64 [PMID: 32191587 DOI: 10.1148/radiol.2020200843]

38 **Pan Y**, Guan H, Zhou S, Wang Y, Li Q, Zhu T, Hu Q, Xia L. Initial CT findings and temporal changes in patients with the novel coronavirus pneumonia (2019-nCoV): a study of 63 patients in Wuhan, China. *Eur Radiol* 2020; **30**: 3306-3309 [PMID: 32055945 DOI: 10.1007/s00330-020-06731-x]

39 **Guan CS**, Lv ZB, Yan S, Du YN, Chen H, Wei LG, Xie RM, Chen BD. Imaging Features of Coronavirus disease 2019 (COVID-19): Evaluation on Thin-Section CT. *Acad Radiol* 2020; **27**: 609-613 [PMID: 32204990 DOI: 10.1016/j.acra.2020.03.002]

40 **Francone M**, Iafrate F, Masci GM, Coco S, Cilia F, Manganaro L, Panebianco V, Andreoli C, Colaiacomo MC, Zingaropoli MA, Ciardi MR, Mastroianni CM, Pugliese F, Alessandri F, Turriziani O, Ricci P, Catalano C. Chest CT score in COVID-19 patients: correlation with disease severity and short-term prognosis. *Eur Radiol* 2020; **30**: 6808-6817 [PMID: 32623505 DOI: 10.1007/s00330-020-07033-y]

41 **Li K**, Fang Y, Li W, Pan C, Qin P, Zhong Y, Liu X, Huang M, Liao Y, Li S. CT image visual quantitative evaluation and clinical classification of coronavirus disease (COVID-19). *Eur Radiol* 2020; **30**: 4407-4416 [PMID: 32215691 DOI: 10.1007/s00330-020-06817-6]

42 **Lessmann N**, Sánchez CI, Beenen L, Boulogne LH, Brink M, Calli E, Charbonnier JP, Dofferhoff T, van Everdingen WM, Gerke PK, Geurts B, Gietema HA, Groeneveld M, van Harten L, Hendrix N, Hendrix W, Huisman HJ, Išgum I, Jacobs C, Kluge R, Kok M, Krdzalic J, Lassen-Schmidt B, van Leeuwen K, Meakin J, Overkamp M, van Rees Vellinga T, van Rikxoort EM, Samperna R, Schaefer-Prokop C, Schalekamp S, Scholten ET, Sital C, Stöger JL, Teuwen J, Venkadesh KV, de Vente C, Vermaat M, Xie W, de Wilde B, Prokop M, van Ginneken B. Automated Assessment of COVID-19 Reporting and Data System and Chest CT Severity Scores in Patients Suspected of Having COVID-19 Using Artificial Intelligence. *Radiology* 2021; **298**: E18-E28 [PMID: 32729810 DOI: 10.1148/radiol.2020202439]

43 **Peng QY**, Wang XT, Zhang LN; Chinese Critical Care Ultrasound Study Group (CCUSG). Findings of lung ultrasonography of novel corona virus pneumonia during the 2019-2020 epidemic. *Intensive Care Med* 2020; **46**: 849-850 [PMID: 32166346 DOI: 10.1007/s00134-020-05996-6]

44 **Soldati G**, Smargiassi A, Inchingolo R, Buonsenso D, Perrone T, Briganti DF, Perlini S, Torri E, Mariani A, Mossolani EE, Tursi F, Mento F, Demi L. Is There a Role for Lung Ultrasound During the COVID-19 Pandemic? *J Ultrasound Med* 2020; **39**: 1459-1462 [PMID: 32198775 DOI: 10.1002/jum.15284]

45 **Van de Veerdonk F**, Netea MG, van Deuren M, van den Hoogen FHJ, de Mast Q, Bruggemann R, van der Hoeven H. Kinins and Cytokines in COVID-19: A Comprehensive Pathophysiological Approach. 2020 [DOI: 10.20944/preprints202004.0023.v1]

46 **Li X**, Geng M, Peng Y, Meng L, Lu S. Molecular immune pathogenesis and diagnosis of COVID-19. *J Pharm Anal* 2020; **10**: 102-108 [PMID: 32282863 DOI: 10.1016/j.jpha.2020.03.001]

47 **Fox SE**, Akmatbekov A, Harbert JL, Li G, Quincy Brown J, Vander Heide RS. Pulmonary and cardiac pathology in African American patients with COVID-19: an autopsy series from New Orleans. *Lancet Respir Med* 2020; **8**: 681-686 [PMID: 32473124 DOI: 10.1016/S2213-2600(20)30243-5]

48 **Nicholls JM**, Poon LL, Lee KC, Ng WF, Lai ST, Leung CY, Chu CM, Hui PK, Mak KL, Lim W, Yan KW, Chan KH, Tsang NC, Guan Y, Yuen KY, Peiris JS. Lung pathology of fatal severe acute respiratory syndrome. *Lancet* 2003; **361**: 1773-1778 [PMID: 12781536 DOI: 10.1016/s0140-6736(03)13413-7]

49 **Xu Z**, Shi L, Wang Y, Zhang J, Huang L, Zhang C, Liu S, Zhao P, Liu H, Zhu L, Tai Y, Bai C, Gao T, Song J, Xia P, Dong J, Zhao J, Wang FS. Pathological findings of COVID-19 associated with acute respiratory distress syndrome. *Lancet Respir Med* 2020; **8**: 420-422 [PMID: 32085846 DOI: 10.1016/S2213-2600(20)30076-X]

50 **Gibson PG**, Qin L, Puah SH. COVID-19 acute respiratory distress syndrome (ARDS): clinical features and differences from typical pre-COVID-19 ARDS. *Med J Aust* 2020; **213**: 54-56.e1 [PMID: 32572965 DOI: 10.5694/mja2.50674]

51 **ARDS Definition Task Force**. Ranieri VM, Rubenfeld GD, Thompson BT, Ferguson ND, Caldwell E, Fan E, Camporota L, Slutsky AS. Acute respiratory distress syndrome: the Berlin Definition. *JAMA* 2012; **307**: 2526-2533 [PMID: 22797452 DOI: 10.1001/jama.2012.5669]

52 **Wu C**, Chen X, Cai Y, Xia J, Zhou X, Xu S, Huang H, Zhang L, Du C, Zhang Y, Song J, Wang S, Chao Y, Yang Z, Xu J, Chen D, Xiong W, Xu L, Zhou F, Jiang J, Bai C, Zheng J, Song Y. Risk Factors Associated With Acute Respiratory Distress Syndrome and Death in Patients With Coronavirus Disease 2019 Pneumonia in Wuhan, China. *JAMA Intern Med* 2020; **180**: 934-943 [PMID: 32167524 DOI: 10.1001/jamainternmed.2020.0994]

53 **Li X**, Ma X. Acute respiratory failure in COVID-19: is it "typical" ARDS? *Crit Care* 2020; **24**: 198 [PMID: 32375845 DOI: 10.1186/s13054-020-02911-9]

54 **Zompatori M**, Ciccarese F, Fasano L. Overview of current lung imaging in acute respiratory distress syndrome. *Eur Respir Rev* 2014; **23**: 519-530 [PMID: 25445951 DOI: 10.1183/09059180.00001314]

55 **Desai SR**. Acute respiratory distress syndrome: imaging of the injured lung. *Clin Radiol* 2002; **57**: 8-17 [PMID: 11798197 DOI: 10.1053/crad.2001.0889]

56 **Sheard S**, Rao P, Devaraj A. Imaging of acute respiratory distress syndrome. *Respir Care* 2012; **57**: 607-612 [PMID: 22472500 DOI: 10.4187/respcare.01731]

57 **Duarte PMA**, Bastos Filho FAG, Duarte JVA, Duarte BA, Duarte IA, Lemes RPG, Duarte FB. Renal changes in COVID-19 infection. *Rev Assoc Med Bras (1992)* 2020; **66**: 1335-1337 [PMID: 33174922 DOI: 10.1590/1806-9282.66.10.1335]

58 **Su H**, Yang M, Wan C, Yi LX, Tang F, Zhu HY, Yi F, Yang HC, Fogo AB, Nie X, Zhang C. Renal histopathological analysis of 26 postmortem findings of patients with COVID-19 in China. *Kidney Int* 2020; **98**: 219-227 [PMID: 32327202 DOI: 10.1016/j.kint.2020.04.003]

59 **Babapoor-Farrokhran S**, Gill D, Walker J, Rasekhi RT, Bozorgnia B, Amanullah A. Myocardial injury and COVID-19: Possible mechanisms. *Life Sci* 2020; **253**: 117723 [PMID: 32360126 DOI: 10.1016/j.lfs.2020.117723]

60 **Guo T**, Fan Y, Chen M, Wu X, Zhang L, He T, Wang H, Wan J, Wang X, Lu Z. Cardiovascular Implications of Fatal Outcomes of Patients With Coronavirus Disease 2019 (COVID-19). *JAMA Cardiol* 2020; **5**: 811-818 [PMID: 32219356 DOI: 10.1001/jamacardio.2020.1017]

61 **Giustino G**, Croft LB, Stefanini GG, Bragato R, Silbiger JJ, Vicenzi M, Danilov T, Kukar N, Shaban N, Kini A, Camaj A, Bienstock SW, Rashed ER, Rahman K, Oates CP, Buckley S, Elbaum LS, Arkonac D, Fiter R, Singh R, Li E, Razuk V, Robinson SE, Miller M, Bier B, Donghi V, Pisaniello M, Mantovani R, Pinto G, Rota I, Baggio S, Chiarito M, Fazzari F, Cusmano I, Curzi M, Ro R, Malick W, Kamran M, Kohli-Seth R, Bassily-Marcus AM, Neibart E, Serrao G, Perk G, Mancini D, Reddy VY, Pinney SP, Dangas G, Blasi F, Sharma SK, Mehran R, Condorelli G, Stone GW, Fuster V, Lerakis S, Goldman ME. Characterization of Myocardial Injury in Patients With COVID-19. *J Am Coll Cardiol* 2020; **76**: 2043-2055 [PMID: 33121710 DOI: 10.1016/j.jacc.2020.08.069]

62 **Puntmann VO**, Carerj ML, Wieters I, Fahim M, Arendt C, Hoffmann J, Shchendrygina A, Escher F, Vasa-Nicotera M, Zeiher AM, Vehreschild M, Nagel E. Outcomes of Cardiovascular Magnetic Resonance Imaging in Patients Recently Recovered From Coronavirus Disease 2019 (COVID-19). *JAMA Cardiol* 2020; **5**: 1265-1273 [PMID: 32730619 DOI: 10.1001/jamacardio.2020.3557]

63 **Wu Z**, McGoogan JM. Characteristics of and Important Lessons From the Coronavirus Disease 2019 (COVID-19) Outbreak in China: Summary of a Report of 72 314 Cases From the Chinese Center for Disease Control and Prevention. *JAMA* 2020; **323**: 1239-1242 [PMID: 32091533 DOI: 10.1001/jama.2020.2648]

64 **Driggin E**, Madhavan MV, Bikdeli B, Chuich T, Laracy J, Biondi-Zoccai G, Brown TS, Der Nigoghossian C, Zidar DA, Haythe J, Brodie D, Beckman JA, Kirtane AJ, Stone GW, Krumholz HM, Parikh SA. Cardiovascular Considerations for Patients, Health Care Workers, and Health Systems During the COVID-19 Pandemic. *J Am Coll Cardiol* 2020; **75**: 2352-2371 [PMID: 32201335 DOI: 10.1016/j.jacc.2020.03.031]

65 **Bavishi C**, Bonow RO, Trivedi V, Abbott JD, Messerli FH, Bhatt DL. Special Article - Acute myocardial injury in patients hospitalized with COVID-19 infection: A review. *Prog Cardiovasc Dis* 2020; **63**: 682-689 [PMID: 32512122 DOI: 10.1016/j.pcad.2020.05.013]

66 **Lippi G**, Lavie CJ, Sanchis-Gomar F. Cardiac troponin I in patients with coronavirus disease 2019 (COVID-19): Evidence from a meta-analysis. *Prog Cardiovasc Dis* 2020; **63**: 390-391 [PMID: 32169400 DOI: 10.1016/j.pcad.2020.03.001]

67 **Inciardi RM**, Lupi L, Zaccone G, Italia L, Raffo M, Tomasoni D, Cani DS, Cerini M, Farina D, Gavazzi E, Maroldi R, Adamo M, Ammirati E, Sinagra G, Lombardi CM, Metra M. Cardiac Involvement in a Patient With Coronavirus Disease 2019 (COVID-19). *JAMA Cardiol* 2020; **5**: 819-824 [PMID: 32219357 DOI: 10.1001/jamacardio.2020.1096]

68 **Ho JS**, Sia CH, Chan MY, Lin W, Wong RC. Coronavirus-induced myocarditis: A meta-summary of cases. *Heart Lung* 2020; **49**: 681-685 [PMID: 32861884 DOI: 10.1016/j.hrtlng.2020.08.013]

69 **Blondiaux E**, Parisot P, Redheuil A, Tzaroukian L, Levy Y, Sileo C, Schnuriger A, Lorrot M, Guedj R, Ducou le Pointe H. Cardiac MRI in Children with Multisystem Inflammatory Syndrome Associated with COVID-19. *Radiology* 2020; **297**: E283-E288 [PMID: 32515676 DOI: 10.1148/radiol.2020202288]

70 **Clark DE**, Parikh A, Dendy JM, Diamond AB, George-Durrett K, Fish FA, Fitch W, Hughes SG, Soslow JH. COVID-19 Myocardial Pathology Evaluated Through scrEening Cardiac Magnetic Resonance (COMPETE CMR). *medRxiv* 2020 [PMID: 32908996 DOI: 10.1101/2020.08.31.20185140]

71 **Huang L**, Zhao P, Tang D, Zhu T, Han R, Zhan C, Liu W, Zeng H, Tao Q, Xia L. Cardiac Involvement in Patients

Recovered From COVID-2019 Identified Using Magnetic Resonance Imaging. *JACC Cardiovasc Imaging* 2020; **13**: 2330-2339 [PMID: 32763118 DOI: 10.1016/j.jcmg.2020.05.004]

72 **Levi M**, Thachil J, Iba T, Levy JH. Coagulation abnormalities and thrombosis in patients with COVID-19. *Lancet Haematol* 2020; **7**: e438-e440 [PMID: 32407672 DOI: 10.1016/S2352-3026(20)30145-9]

73 **Belen-Apak FB**, Sarıalioğlu F. Pulmonary intravascular coagulation in COVID-19: possible pathogenesis and recommendations on anticoagulant/thrombolytic therapy. *J Thromb Thrombolysis* 2020; **50**: 278-280 [PMID: 32372336 DOI: 10.1007/s11239-020-02129-0]

74 **Avila J**, Long B, Holladay D, Gottlieb M. Thrombotic complications of COVID-19. *Am J Emerg Med* 2021; **39**: 213-218 [PMID: 33036855 DOI: 10.1016/j.ajem.2020.09.065]

75 **Dhawan RT**, Gopalan D, Howard L, Vicente A, Park M, Manalan K, Wallner I, Marsden P, Dave S, Branley H, Russell G, Dharmarajah N, Kon OM. Beyond the clot: perfusion imaging of the pulmonary vasculature after COVID-19. *Lancet Respir Med* 2021; **9**: 107-116 [PMID: 33217366 DOI: 10.1016/S2213-2600(20)30407-0]

76 **Espallargas I**, Rodríguez Sevilla JJ, Rodríguez Chiaradía DA, Salar A, Casamayor G, Villar-Garcia J, Rodó-Pin A, Marsico S, Carbullanca S, Ramal D, Del Carpio LA, Gayete Á, Maiques JM, Zuccarino F. CT imaging of pulmonary embolism in patients with COVID-19 pneumonia: a retrospective analysis. *Eur Radiol* 2021; **31**: 1915-1922 [PMID: 32964337 DOI: 10.1007/s00330-020-07300-y]

World Journal of Clinical Infectious Diseases

Submit a Manuscript: https://www.f6publishing.com

World J Clin Infect Dis 2022 April 26; 12(1): 20-32

DOI: 10.5495/wjcid.v12.i1.20

ISSN 2220-3176 (online)

ORIGINAL ARTICLE

Basic Study

Mutations of the *brpR* and *brpS* genes affect biofilm formation in *Staphylococcus aureus*

Allison Zank, Lillian Schulte, Xavier Brandon, Lauren Carstensen, Amy Wescott, William R Schwan

Specialty type: Infectious diseases

Provenance and peer review: Unsolicited article; Externally peer reviewed.

Peer-review model: Single blind

Peer-review report's scientific quality classification

Grade A (Excellent): 0
Grade B (Very good): B
Grade C (Good): 0
Grade D (Fair): 0
Grade E (Poor): E

P-Reviewer: Barik S, Sun Y

Received: September 2, 2021
Peer-review started: September 2, 2021
First decision: November 22, 2021
Revised: December 3, 2021
Accepted: February 12, 2022
Article in press: February 12, 2022
Published online: April 26, 2022

Allison Zank, Lillian Schulte, Xavier Brandon, Lauren Carstensen, Amy Wescott, William R Schwan, Department of Microbiology, University of Wisconsin-La Crosse, La Crosse, WI 54601, United States

Corresponding author: William R Schwan, PhD, Professor, Department of Microbiology, University of Wisconsin-La Crosse, 1725 State St, La Crosse, WI 54601, United States. wschwan@uwlax.edu

Abstract

BACKGROUND

In the United States, *Staphylococcus aureus* (*S. aureus*) kills tens of thousands of individuals each year and the formation of a biofilm contributes to lethality. Biofilm-associated infections are hard to treat once the biofilm has formed. A new stilbene drug, labeled SK-03-92, was shown to kill *S. aureus* and affected transcription of two genes tied to a putative two-component system (TCS) we have named *brpR* (biofilm regulating protein regulator) and *brpS* (biofilm regulating protein sensor).

AIM

To determine if BrpR and BrpS regulate biofilm formation, *brpR* and *brpS* mutants were assessed using biofilm assays compared to wild-type *S. aureus*.

METHODS

A combination of biofilm and quantitative real-time-polymerase chain reaction assays were used. In addition, bioinformatic software tools were also utilized.

RESULTS

Significantly more biofilm was created in the brpR and brpS mutants *vs* wild-type cells. Quantitative real-time polymerase chain reactions showed the *brpS* mutant had differences in transcription of biofilm associated genes that were eight-fold higher for *srtA*, two-fold lower for *lrgA*, and 1.6-fold higher for *cidA* compared to wild-type. Bioinformatic analysis demonstrated that the *S. aureus* brpR/brpS TCS had homology to streptococcal late-stage competence proteins involved in cell-death, increased biofilm production, and the development of persister cells.

CONCLUSION

Our study suggests that *brpR/brpS* is a TCS that may repress *S. aureus* biofilm production and be linked to late-stage competence in *S. aureus*.

Key Words: Biofilm; Two-component system; Stilbene; *Staphylococcus aureus*; Late-stage competence; SK-03-92

Core Tip: *Staphylococcus aureus* is a primary cause of skin/soft tissue infections. In this study, we have shown that two previously uncharacterized genes, *brpR* and *brpS*, encode proteins that we believe comprise a two-component system that regulates biofilm formation in *S. aureus*.

Citation: Zank A, Schulte L, Brandon X, Carstensen L, Wescott A, Schwan WR. Mutations of the *brpR* and *brpS* genes affect biofilm formation in *Staphylococcus aureus*. *World J Clin Infect Dis* 2022; 12(1): 20-32
URL: https://www.wjgnet.com/2220-3176/full/v12/i1/20.htm
DOI: https://dx.doi.org/10.5495/wjcid.v12.i1.20

INTRODUCTION

Staphylococcus aureus (*S. aureus*) is a significant pathogen of humans, causing more than 700000 skin/soft tissue infections, nearly 120000 bloodstream infections, and close to 20000 deaths *per* year in the United States[1-3]. Because drug resistance within this species continues to increase, new drugs are needed to treat human infections. Our research group has developed a new stilbene drug labeled SK-03-92 with efficacy against all Gram-positive bacteria that were tested, including methicillin-resistant *S. aureus*[4]. An mRNA microarray was performed on SK-03-92 treated *vs* untreated *S. aureus* cells to try to elucidate the mechanism of action of the drug[5]. From this microarray, the genes for a putative two-component system (TCS) (annotated as *MW2284/MW2285*) were the most downregulated at the transcriptional level. Moreover, transcription of the *srtA* gene (encoding sortase A) was upregulated and the *lrgA* gene encoding an anti-holin was downregulated following SK-03-92 treatment. Additionally, SK-03-92 treatment led to a high degree of persister cells and greater biofilm formation. Because of the effect on biofilm formation, the *MW22284* gene was labeled *brpR* (biofilm regulating protein regulator) and the *MW2285* gene was labeled *brpS* (biofilm regulating protein sensor).

Transcriptional changes of the *srtA* and *lrgA* genes as well as high numbers of persister cells suggested that SK-03-92 treatment may induce late-stage competence in *S. aureus*. Although competence allows DNA uptake to occur in heavily stressed cells, transformation is only one effect of bacterial competence. During early competence, which occurs prior to transformation, a large proportion of the stressed bacterial population die *via* holin-induced autolysis[6]. It is this phenomenon that supplies environmental DNA (eDNA) to the remaining cells for DNA uptake. Additionally, the surplus eDNA provides scaffolding for the rapid formation of a biofilm[7]. The final stage of natural competence is metabolic dormancy[8]. Current estimates show that only the youngest 1% of the original population survive to become a dormant cell. Thus, when faced with resource competition, a thriving bacterial colony has the ability to rapidly transform itself into a small group of latent (*i.e.* persister) cells living within a biofilm. These surviving cells re-emerge once environmental resources again become plentiful. This is one strategy used by bacterial cells to survive antibiotic challenge and re-infect the host[9].

The initiation of competence has been shown to rely on a symphony of genetic switches that begin to harmonize when short-sequence amino acids, known as competence stimulating pheromones (CSPs) bind to certain specific membrane proteins. The initiation of the CSP alarmone response has been well characterized in streptococcal species[10]. These membrane proteins are autoinducers that comprise one half of a specific TCS[11]. In *Streptococcus pneumoniae* (*S. pneumoniae*) and *Streptococcus mutans* (*S. mutans*), this response is initiated following the interaction with self-produced autoinducing pheromones known as CSPs, which are short, 14 residue peptides. The CSP is then received by the membrane bound sensor kinase ComD (*S. pneumoniae*)[12] or BrsM (*S. mutans*)[13]. Next, ComD or BrsM phosphorylate the cytoplasmic response regulator ComE (*S. pneumoniae*)[12] or BrsR (*S. mutans*)[13], which ultimately controls programmed cell death and persistence. In *S. aureus*, neither the CSP nor the TCS by which CSPs are received have yet been identified.

In this study, we have shown that mutations of the *brpR* and *brpS* genes in *S. aureus* strain Newman showed greater biofilm formation and transcriptional changes of the *srtA* and *lrgA* genes than wild-type *S. aureus*. Furthermore, we have used bioinformatic tools to show that the *brpR/brpS* TCS has homology to the BrsR/BrsM[13] and ComE/ComD[12] late-stage competence TCSs in *S. mutans* and *S. pneumoniae*, respectively. These findings suggest that the *brpR/brpS* TCS may be specific for the reception and resultant signal cascade of a molecule that induces late-stage competence in *S. aureus*.

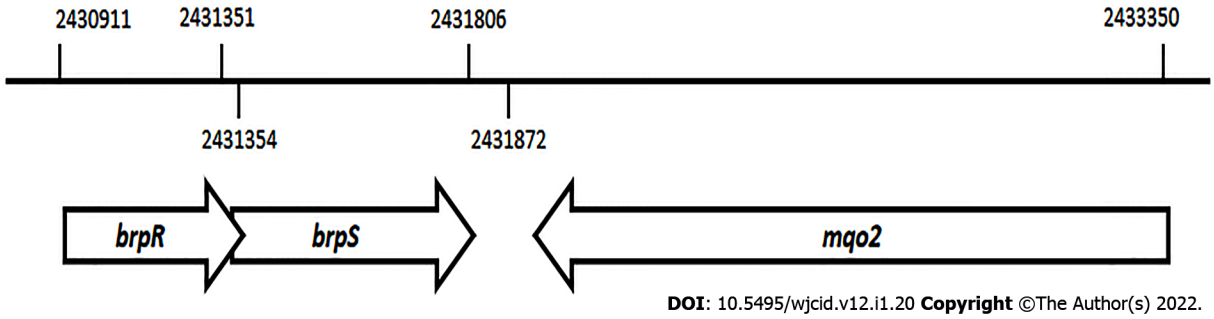

DOI: 10.5495/wjcid.v12.i1.20 **Copyright** ©The Author(s) 2022.

Figure 1 Schematic representation of the chromosomal position and organization of the *brpR*, *brpS*, and *mqo2* genes in the *Staphylococcus aureus* strain MW2 genome.

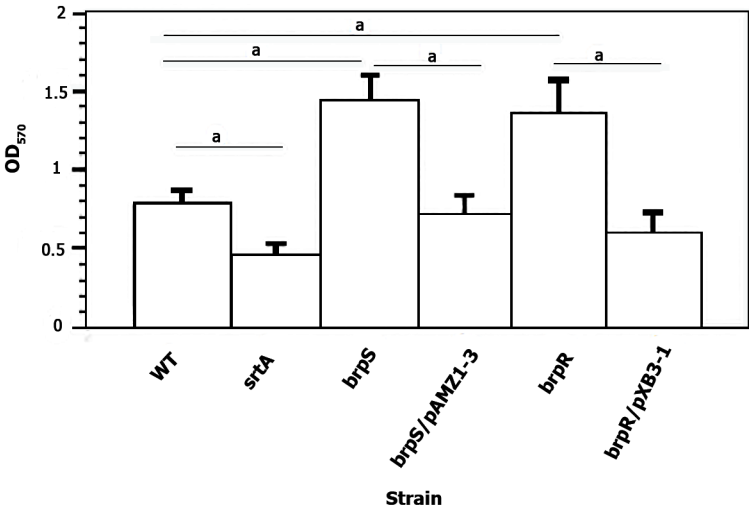

DOI: 10.5495/wjcid.v12.i1.20 **Copyright** ©The Author(s) 2022.

Figure 2 Effect of *brpR* and *brpS* mutations and complementation on *Staphylococcus aureus* biofilm formation. All experiments represent the mean ± SD from five different runs done in triplicate for each strain. Biofilm formation was done on wild-type *Staphylococcus aureus* (*S. aureus*) strain Newman (WT, open column), *S. aureus* Newman *srtA* mutant (black column), *S. aureus* Newman *brpS* mutant (right striped column), *S. aureus* Newman *brpS* mutant/pAMZ1-3 (left striped column), *S. aureus* Newman *brpR* mutant (dark right striped column), and *S. aureus* Newman *brpR* mutant/pXB31 (dark left striped column). Differences were statistically compared by analysis of variance where $^{a}P < 0.001$.

MATERIALS AND METHODS

Bacterial strains, plasmids, and growth conditions

All of the bacterial strains and plasmids used in this study are shown in Table 1. The *S. aureus* parent strain Newman was isolated from a human infection[14]. The JE2 strain, created by the University of Nebraska Medical Center, is the *S. aureus* parent strain USA300 LAC CA-MRSA cured of its plasmids [15]. Strains NE272 (*brpS mutant*), NE671 (*brpR mutant*), and NE1787 (*srtA mutant*) are erythromycin-resistant (Em^R) mutants representing part of the Nebraska Transposon Mutant Library created by the University of Nebraska Medical Center by *mariner* transposon mutagenesis[15] and obtained from the Network on Antimicrobial Resistance in *S. aureus* (NARSA) strain repository (Table 1). The *E. coli* strain DH5α is a cloning strain with mutations that enable high-efficiency transformation[16]. *S. aureus* strain RN4220 is a transformation efficient strain of *S. aureus*[17].

To clone the *brpR* and *brpS* genes for complementation studies, plasmid pALC2073 was used. This plasmid carries ampicillin and chloramphenicol resistance genes, *E. coli* and Gram-positive origins of replication, and a *xyl/tetO* tetracycline inducible promoter[18].

All media was purchased from Thermo Fisher Scientific (Thermo Fisher Scientific, Pittsburgh, PA, United States). All antibiotics were purchased from Sigma-Aldrich (Sigma-Aldrich, St. Louis, MO, United States). *E. coli* strains were grown in Luria (LB) broth shaken at 250 rpm at 37 °C or on Luria agar (LA) incubated at 37 °C. The *E. coli* strains carrying the pALC2073 plasmid were selected for in media containing 100 μg/mL ampicillin.

All *S. aureus* strains were grown in brain heart infusion (BHI) broth with 1% (wt/vol) glucose (BHI-G) or trypticase soy broth shaken at 250 rpm at 37 °C. Agar grown *S. aureus* cultures were passaged on BHI agar at 37 °C. The *mariner* transposon mutant strains were grown in media with 5 μg/mL of

Table 1 Bacterial strains and plasmids used in this study

Bacterial strain	Description	Ref.
E. coli		
DH5	Transformation efficient *E. coli* strain	[16]
S. aureus		
Newman	*S. aureus* clinical isolate	[14]
JE2	*S. aureus* USA300 MRSA strain	[15]
NE272	*S. aureus* JE2 *brpS*::*mariner* mutant	[15]
NE671	*S. aureus* JE2 *brpR*::*mariner* mutant	[15]
NE1787	*S. aureus* JE2 *srtA*::*mariner* mutant	[15]
RN4220	Transformation-efficient *S. aureus* strain	[17]
Newman *brpR*	*S. aureus* Newman *brpR*::*mariner* mutant	This study
Newman *brpS*	*S. aureus* Newman *brpS*::*mariner* mutant	This study
Newman *srtA*	*S. aureus* Newman *srtA*::*mariner* mutant	This study
Plasmids		
pXB3-1	pALC2073 plasmid with the *brpR* gene inserted	This study
pALC2073	Cloning vector with Ap^r, Cm^r, and Tc^r genes, and a Tc-inducible promoter	[18]
pAMZ1-3	pALC2073 plasmid with the *brpS* gene inserted	This study

erythromycin (Em^5). *S. aureus* strains carrying the pALC2073, pXB3-1, or pAMZ1-3 plasmid were selected for in media containing 10 μg/mL of chloramphenicol (Cm^{10}). To induce the *xyl*/*tetO* promoter on the pXB3-1 and pAMZ1-3 plasmids, tetracycline at 0.25 μg/mL was added to the growth medium.

Transduction of S. aureus

The *brpR*::*mariner*, *brpS*::*mariner*, and *srtA*::*mariner* mutations were transduced into strain Newman using the a ϕ80a bacteriophage[19]. The transductants were then selected for on BHI agar containing Em^5. All mutations were verified by polymerase chain reaction (PCR) and biofilm assays.

Construction of brpS and brpR complementing plasmids

The *brpR* complementing plasmid was constructed using the pALC2073 backbone[18]. Isolation of pALC2073 plasmid DNA followed the manufacturer's instructions for the Qiagen QiaPrep plasmid isolation kit (Qiagen, Germantown, MD, United States). The full-length coding region of the *S. aureus* strain MW2 *brpR* gene was PCR amplified using the MW2284I/MW2284M primers (Integrated DNA Technologies, Coralville, IA, United States; Table 2) and the following PCR conditions: 35 cycles, 94 °C 1 min, 57 °C 1 min, 72 °C 1 min. *S. aureus* strain MW2 chromosomal DNA served as a template. The *brpR* DNA was amplified to have a *Kpn*I site on the 5′ end and an *Eco*RI site on the 3′ end. PCR amplified *brpR* gene product was digested with *Kpn*I and *Eco*RI (New England Biolabs, Ipswich, MA, United States), and then ligated with *Kpn*I/*Eco*RI cut pALC2073 plasmid DNA using T_4 DNA ligase (New England Biolabs). Ligated DNA was transformed into *E. coli* strain DH5α cells[16]. Transformants were selected on LA containing 100 μg/mL ampicillin, and one resulting plasmid, plasmid pXB3-1, was used for further experiments.

A recombinant *brpS* complementing plasmid was also constructed. Isolation of pALC2073 plasmid DNA used the same plasmid isolation kit described above. The full-length coding region of the *S. aureus* strain MW2 *brpS* gene was PCR amplified using the GEX-5XB/GEX-5XC primers (Table 2) and the following PCR conditions: 35 cycles, 94 °C 1 min, 57 °C 1 min, 72 °C 1 min. *S. aureus* strain MW2 chromosomal DNA was used as the template. The *brpS* DNA was amplified to have a *Kpn*I site on the 5′ end and an *Eco*RI site on the 3′ end. PCR amplified *brpS* gene product was digested with *Kpn*I and *Eco*RI (New England Biolabs), and then ligated with *Kpn*I/*Eco*RI cut pALC2073 plasmid DNA using T_4 DNA ligase (New England Biolabs) immediately downstream from the tetracycline-inducible *xyl/tetO* promoter on pALC2073. Ligated DNA was transformed into *E. coli* strain DH5α cells[16]. Transformants were selected on LA containing 100 mg/mL ampicillin, and one resulting plasmid, plasmid pAMZ1-3, was used for further experiments.

Plasmid DNA from *E. coli* was purified with a Qiagen Plasmid Miniprep Kit (Qiagen) and electroporated into the *S. aureus* strain RN4220[20] using a GenePulser, (Bio-Rad, Hercules, CA, United States) under the following conditions: 100 W capacitance, 25 mF resistance, 2.5 kV charge voltage, 4 s.

Table 2 Primers used in this study

Primer	Sequence
GEX-5XC	5′- CCTAGGAGATCTCTTTCTGTC -3′
GEX-5XB	5′- GTTAATTTTACTAAACTTAAG -3′
MW2284I	5′- GAGCAGGTACCATGATGAAACTCAATTTATTTATCAATGCAAAAG-3′
MW2284M	5′- CAGCGAATTCTCAATGGTGATGGTGATGTATTGATAATCGCTCCTTTATAGATTTTAAAA -3′
CidA1	5′- TGCAACGATACATGTTCCTATG -3′
CidA2	5′- CTACAACTAGGAATCATCATTGTG -3′
LrgA1	5′- GCATCAAAACCAGCACACTTT -3′
LrgA2	5′- GACTTCGCCTAACTTAACAGC -3′
SaFtsZ1	5′- GGTGTAGGTGGTGGCGGTAA -3′
SaFtsZ2	5′- TCATTGGCGTAGATTTGTC -3′
SrtA1	5′- TCGCTGGTGTGGTACTTATC -3′
SrtA2	5′- CAGGTGTTGCTGGTCCTGGA -3′

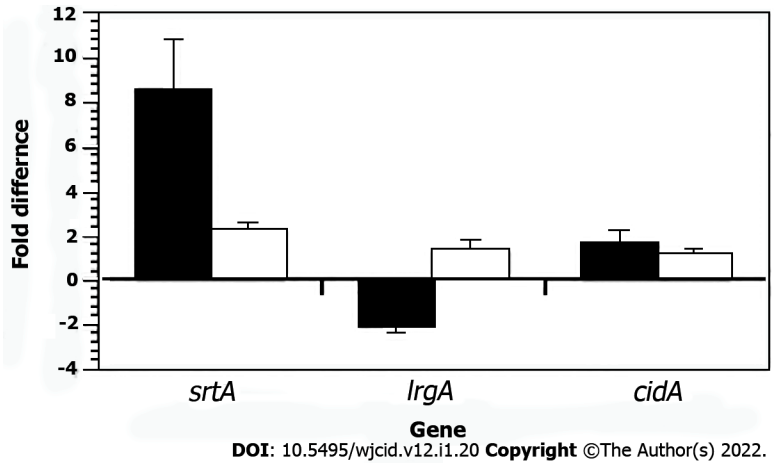

DOI: 10.5495/wjcid.v12.i1.20

Figure 3 Quantitative reverse transcribed-polymerase chain reaction results of *Staphylococcus aureus* Newman *cidA*, *lrgA*, and *srtA* transcription in wild-type bacteria (standardized to 0) compared to a *Staphylococcus aureus* Newman *brpS* mutant (black column) and the complemented *brpS* mutant (white column). The data represents the mean ± SD from three separate runs.

Transformants were selected for on BHI agar containing Cm^{10} after one hour of expression in BHI broth. Finally, plasmid DNA was re-isolated from one *S. aureus* strain RN4200 transformant carrying either the pXB3-1 or pAMZ1-3 plasmid using the method noted above with one alteration. The *S. aureus* cells were incubated with 50 µL of lysostaphin (10 mg/mL; Remel, San Diego, CA, United States) for 60 min at 37 °C prior to the first step to facilitate lysis of the staphylococcal cells. Each isolated plasmid DNA sample was then cut with the *Kpn*I and *EcoR*I restriction endonucleases to verify the insertion. The *S. aureus* strain Newman was then transformed with 10 mL of pXB3-1 or pAMZ1-3 plasmid DNA using electroporation as outlined above and transformants selected for on BHI agar containing Cm^{10}.

Biofilm assays

To determine the effect of the *brpR* and *brpS* mutations on the ability of *S. aureus* Newman to form a biofilm, biofilm assays were performed[21]. Briefly, cultures of the *S. aureus* were grown at 37 °C with shaking (250 rpm) overnight in BHIG broth with the appropriate antibiotic(s). Each strain was then diluted 1:100 in BHI-G and 220 µL of the solution was placed in microtiter wells in triplicate in a 96-well microtiter plate. The microtiter plates were statically incubated for 24 h at 37 °C to allow a biofilm to form. Each well was then rinsed three times with sterile water. The biofilms were then allowed to settle (10 min), stained with crystal violet dye (0.1% wt/vol) for 10 min, and then washed with sterile water. After allowing the well contents to dry fully in a sterile hood, the dried contents were incubated in 33% acetic acid at room temperature for 30 min. The contents of the well were vigorously curettaged. The optical densities were measured on a SpectraMax M3 96-well microtiter plate reader (Molecular

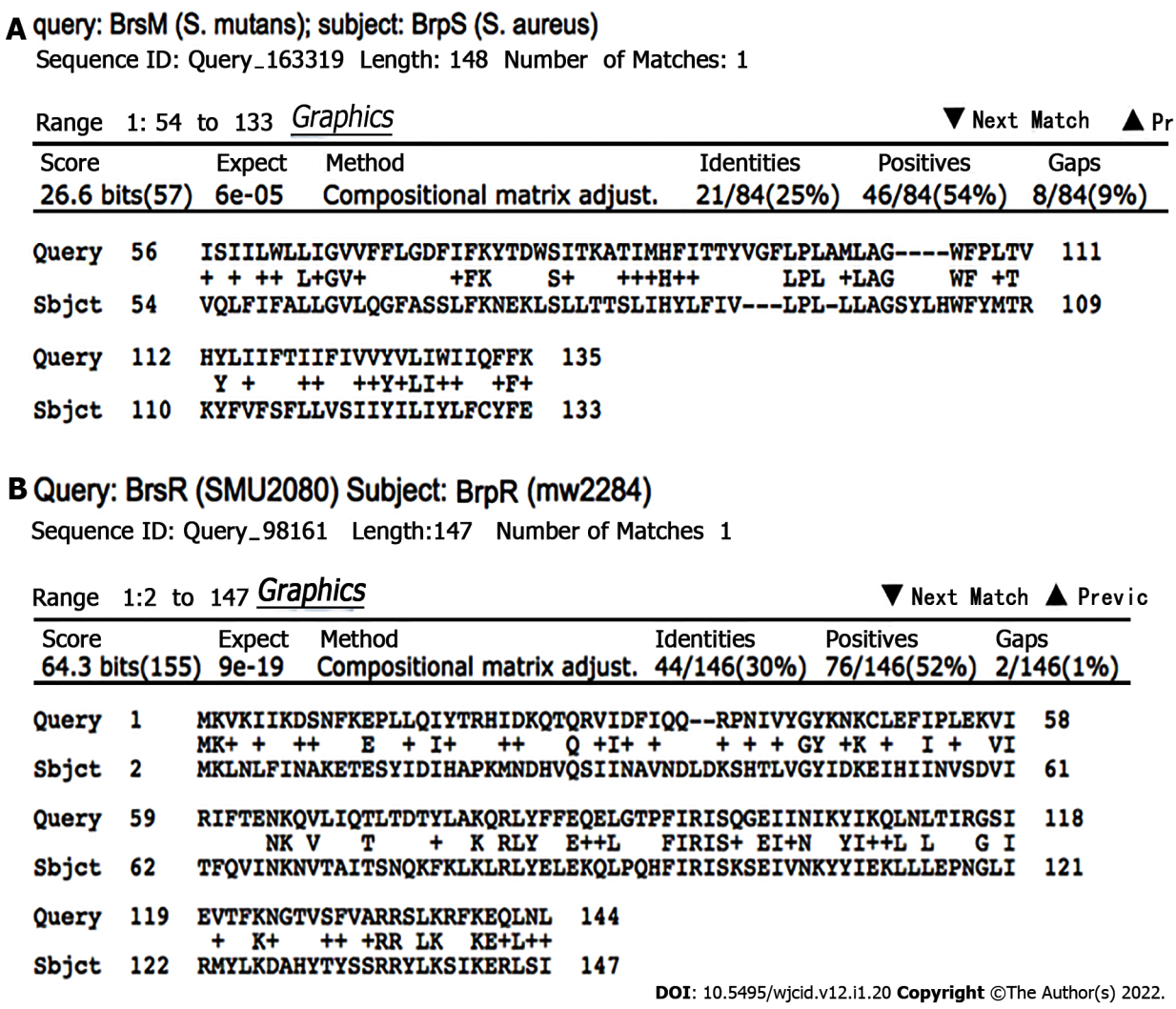

DOI: 10.5495/wjcid.v12.i1.20

Figure 4 Bioinformatic comparison of the BrsRM proteins of *Streptococcus mutans* with the BrpRS proteins of *Staphylococcus aureus*. A: BrsM, a two-component system membrane protein responsible for activating competence in response to sensing competitor organisms within a niche, shares sequence similarity with BrpS; B: BrsR, which is the cognate response regulator to BrsM, shares sequence similarity with BrpR. BLASTp NCBI. Algorithm parameters: Max target sequences = 100, automatically adjusted parameters for short input sequences, expect threshold = 10, word size = 3, max matches in a query range = 0, matrix = BLOSUM62, gap costs = 11 existence and 1 extension, and a conditional compositional score matrix adjustment.

Devices, San Jose, CA, United States) at an optical density of 570 nm. In addition to wild-type Newman cells, Newman *brpR* and Newman *brpS* mutant strains as well as *brpR* and *brpS* mutants containing the pXB3-1 or pAMZ1-3 plasmids were tested and compared with a Newman *srtA* transposon mutant strain that served as a negative control. To achieve statistical significance, the biofilm assays were performed a minimum of five times in triplicate for each strain.

Quantitative real-time PCR

Total RNA was isolated from *S. aureus* strains grown to early logarithmic phase in BHI broth with shaking (250 rpm) incubated at 37 °C using a High Pure RNA Isolation kit ΔΔ(Roche Diagnostics, Indianapolis, IN, United States) with an additional lysostaphin treatment step to help lyse the *S. aureus* cell walls and a DNase I digestion to digest contaminating DNA. To confirm RNA concentration and ensure the integrity of each RNA sample, an aliquot of each RNA sample was analyzed on a Nanodrop machine (Thermo Scientific, Waltham, MA, United States) and electrophoresed through 0.8% agarose gels. The cDNA for each strain was then synthesized from 2 μg of total RNA according to manufacturer's instruction using a First-Strand Synthesis kit (Life Technologies, Carlsbad, CA, United States). All quantitative real-time PCR (qRT-PCR) trials were performed according to manufacturer's instruction using the iTaq Universal SYBR Supermix kit (BioRad, Hercules, CA, United States). Oligonucleotide primers that targeted the *ftsZ*, *srtA*, *lrgA*, and *cidA* genes were synthesized (Table 2) by Integrated DNA Technologies. To perform qRT-PCR, the minimum information for publication of quantitative real-time PCR experiments guidelines were followed and the *ftsZ* housekeeping gene was used as a standardization control[22]. All replicates were performed at least three times on a CFX96 qPCR instrument (BioRad, Hercules, CA, United States) under the following conditions: 94 °C, 20 s; 55

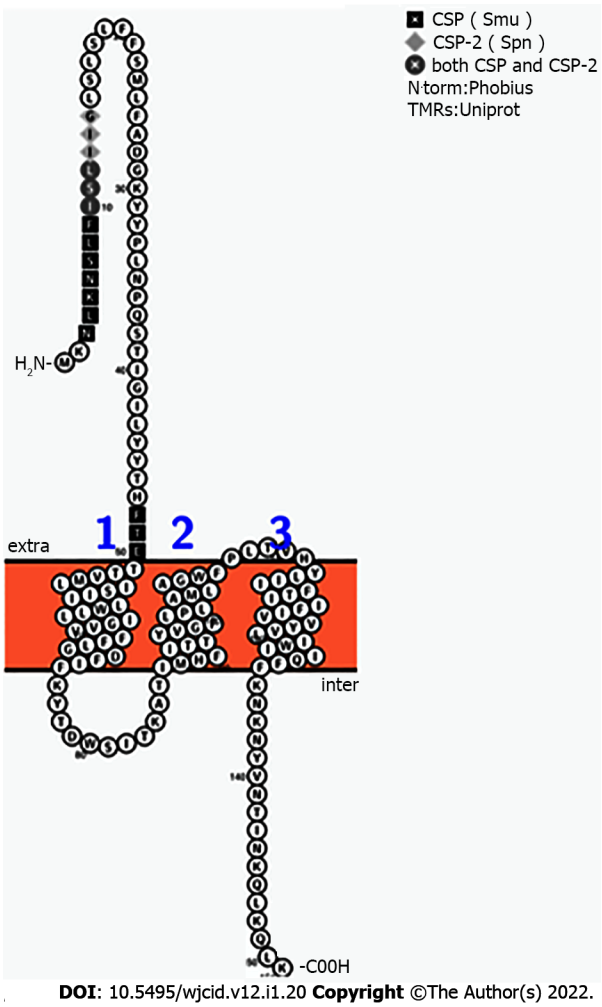

DOI: 10.5495/wjcid.v12.i1.20

Figure 5 Highlight of amino acid residues shared by competence stimulating pheromone, competence stimulating pheromone-2, and BrpS. The predicted exterior segment of BrpS, which spans N'-1-MKNLKNSLFISLIIGLSLSLFFSMLFADGKYYPLNPQSTIGILYYTHFT-50-C', was compared to competence stimulating pheromone (CSP) and CSP-2 by BLASTp. The competence stimulating peptides of *Streptococcus mutans* (1-SGSLSTFFRLFNRSFTQA-18, CSP) and *Streptococcus pneumoniae* (1-EMRISRIILDFLFLRKK-17, CSP-2) has 56% similarity to CSP and 30% similarity to CSP-2. CSP: Competence stimulating pheromone.

°C, 30 s; and 72 °C, 1 min for 35 cycles. The level of target gene transcript from each strain was estimated against the *ftsZ* gene standard curve. Additionally, crossover points for all genes were standardized to the crossover points for *ftsZ* in each sample using the $2^{-\Delta\Delta CT}$ formula[23].

Bioinformatic tools

The sequenced genomes of *S. aureus* strains MW2 and Newman used in this study are publicly available on GenBank (NCBI, genome assembly ASM1126v1)[24-26]. The protein annotations for all of the bacterial strains included in this study were found on BioCyc or GenBank[26,27]. BioCyc was also used to search for brpRS homologs downstream of the *mqo2* gene. The UniProt Consortium was used to obtain amino acid FASTA sequences[28]. Domain motifs were sought using NetPHOS, ExPASy, Prosite, and GenomeNet[28-30]. Protter was used to two-dimensionally visualize brpS and brsM[31]. I-TASSER and PyMOL were used together to three dimensionally visualize BrpR and BrpS[32,33]. I-TASSER and PyMol were also used to visually verify DNA binding in residues predicted by DP-Bind[34]. Finally, protein sequence homology analyses were performed by BLASTp (NCBI) with the following parameters: Max target sequences = 100, automatically adjusted parameters for short input sequences, expect threshold = 10, word size = 3, max matches in a query range = 0, matrix = BLOSUM62, gap costs = 11 existence and 1 extension, and a conditional compositional score matrix adjustment[35].

Statistical analysis

Calculation of the means, standard deviations, and paired Student's t-tests were performed using Microsoft Excel. $P < 0.05$ were considered significant.

RESULTS

Alignment of the brpS/brpR genes

An alignment of the *brpR* and *brpS* genes that encode the BrpR and BrpS proteins is seen on the *S. aureus* MW2 genome sequence (Figure 1)[24]. These genes overlap in a unidirectional in-tandem sequence. The overlapping *brpRS* genes lie just 66 base pairs upstream from the *mqo2* gene, encoding one of the two malate: Quinone oxidoreductases (MQO2) produced by *S. aureus*. The bi-functional MQO2 protein is able to generate oxaloacetate through an oxidation of malate as well as donate electrons to the electron transport chain[36].

Mutations in the brpR and brpS genes cause greater biofilm formation in S. aureus

To confirm biofilm formation was linked to BrpR and BrpS, individual *brpR* and *brpS* mutations were moved to the *S. aureus* strain JE2 background[15] to the *S. aureus* strain Newman *via* transduction. Biofilm production of both mutants was compared to the unmutated wild-type *S. aureus* Newman strain. Significantly more biofilm material was produced by the *brpS* and *brpR* mutants (1.8-fold and 1.73-fold higher, respectively, $P < 0.001$) compared to wild-type. Complementation of the *brpR* and *brpS* mutants caused biofilm expression to either return to wild-type levels or there was less biofilm material formed (Figure 2). The *srtA* mutant displayed a 1.73-fold decline in the biofilm forming ability compared to the wild-type strain ($P < 0.001$). This suggested that the putative BrpRS TCS may repress *S. aureus* biofilm production.

Transcription of srtA and lrgA are regulated by a brpS mutation

Previously, we showed *srtA* transcription was elevated and *lrgA* transcription was lower after SK-03-92 treatment of *S. aureus* cells compared to untreated cells[5]. The *srtA* gene encodes sortase A[37] and the *lrgA* gene encodes an anti-holin[38] that are important for the formation of biofilms[39,40]. Total RNA was collected during the mid-exponential growth phase from the *S. aureus* Newman *brpS* mutant, *S. aureus* Newman *brpS* mutant containing the pAMZ1-3 plasmid, and wild-type S. *aureus* Newman cells Each RNA sample was converted to cDNA for qRT-PCRs analysis. The *brpS* mutant displayed 8.5-fold higher *srtA* transcription ($P < 0.008$), 2-fold lower *lrgA* transcription ($P < 0.016$), and 1.6-fold higher *cidA* transcription ($P < 0.43$) *vs* the wild-type strain (Figure 3). Complementation of the *brpS* mutation caused *srtA* transcription to drop to a 2.2-fold increase, a 1.3-fold increase in *lrgA* transcription, and a 1.2-fold increase in *cidA* transcription. These results demonstrated that transcription of some biofilm-associated genes was regulated by a mutation in the *brpS* gene.

BrpR/BrpS homology to other TCS proteins

BrpR and BrpS homologs were identified by BLAST analyses in multiple Gram-positive bacterial pathogens, including *Bacillus cereus, Clostridioides difficile, Enterococcus faecalis, Lactobacillus species, Staphylococcus haemolyticus, Streptococcus pneumoniae* ComD/ComE, *and S. mutans* BrsR/BrsM as well as three other bacterial species (*Escherichia coli* YehT/YehU, *Mycobacterium tuberculosis* YehT/YehU, and *Chlamydia trachomatis*)[26,35]. Of these, the *S. mutans* BrsR/BrsM TCS that senses CSP and then induces late-stage competence showed the highest homology (Figure 4)[12].

Putative structures of the BrpS protein

S. aureus BrpS and *S. mutans* BrsM have a similar arrangement of reactive residues. Lysine, serine, threonine, histidine, tyrosine, and glutamic acid residues were illuminated on a 2-dimensional Protter-generated image of each protein (Figure 5)[29]. This mapping suggested that BrpS and BrsM are partitioned into distinct functional domains separated by the membrane. Functionality appears to occur at the intercellular loop (staphylococcal N'-76-KYTDWSITKAT-86-C'), at the extracellular loop (staphylococcal N'-108-PLTVHY-113-C'), and within a single reactive residue near the membrane at K135 (staphylococcal) within the C'-terminal tail region.

Additionally, the region at the N'-terminus of brpS displays sequence homology with the secreted *S. mutans* and *S. pneumoniae* CSPs (Figure 6). The segment of brpS spanning the regions from N'-1-MKNLKNSLFISLIIGLSLSLFFSMLFADGKYYPLNPQSTIGILYYTHFT-50-C' showed 56% similarity with CSP (*S. mutans*, 1-SGSLSTFFRLFNRSFTQ A-18) and 30% similarity to CSP-2 (*S. pneumoniae*, 1-EMRISRIILDFLFLRKK-17).

DISCUSSION

S. aureus causes 65% of biofilm-associated infections *per* year[40,41]. Biofilms provide a defense against host immune defenses as well as most antibiotics. An understanding of what regulates *S. aureus* biofilm formation could lead to treatment options that target this process in *S. aureus*.

Both sortase A (SrtA) and antiholin (LrgA) are important *S. aureus* proteins needed for creation and maintenance of biofilms. Sortase A promotes the covalent anchoring of surface proteins to the cell wall

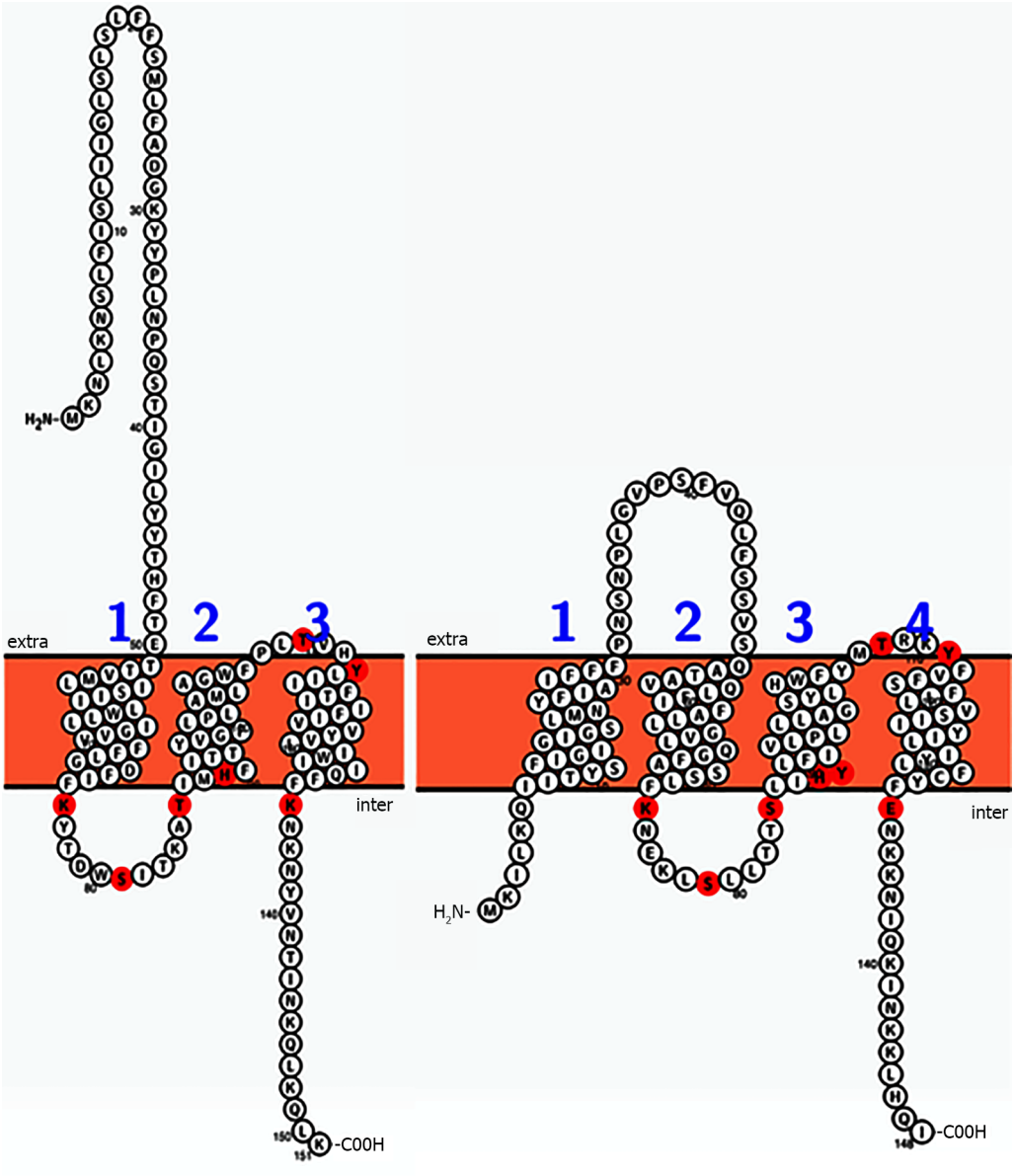

DOI: 10.5495/wjcid.v12.i1.20

Figure 6 Comparison of the sequences and predicted topologies of the putative two-component system membrane sensor BrpS (left, *Staphylococcus aureus*) and BrsM (right, *Streptococcus mutans*). According to this prediction, residues likely to be reactive (red) are topologically arranged in similar loci among both proteins. Intra is proposed to correspond with the cytoplasmic space, and extra is proposed to correspond with the extracellular milieu of the cell. Figures generated by Protter.

of *S. aureus*[42] that are important in the first stage of biofilm formation. Cell death releases eDNA that is tied to holin/antiholin action. An integral part of mature *S. aureus* biofilms is eDNA[7]. The function of the antiholin LrgA is to prevent cell autolysis by complexing with CidA holins[38,43].

In this study, we have shown that mutations in either the *brpR* or *brpS* gene cause an increase in biofilm formation as well as transcriptional changes of the *srtA* and *lrgA* genes, which are linked events. Previous studies with transposon mutants of what was an uncharacterized gene, that we have named *brpS*, displayed better biofilm formation than the wild-type strain[44,45]. Strains with a mutated *lrgA* gene have also been shown to produce increased levels of biofilms[46]. Another study has shown that cell lysis caused eDNA to be rapidly produced that could act as a scaffolding for newly forming biofilms [10].

The *in silico* data; biofilm results with the *brpR* and *brpS* mutants; and the data from the transcript abundance changes of the *lrgA*, *srtA*, *brpR*, and *brpS* genes suggest that BrpR/BrpS comprise a TCS that may be involved in late-stage competence. From the *in silico* analysis, we speculate that the BrpR protein (that possesses an apparent LytTR DNA binding-motif[47]) may repress *srtA* transcription. Other proteins that have LytTR motifs, such as BrsR and ComE, have been shown to have multifunctional activities tied to activation and repression[47-49]. Further analysis is required to show that BrpR is capable of binding to this region.

From the data presented, we speculate that BrpS is a receptor for a CSP-like pheromone secreted by *S. aureus* as a response to competition for resources. The leader peptide of BrpS may function to competitively antagonize the extracellular receptor portion of BrpS from the CSPs of competitive species, such as *S. mutans* and *S. pneumoniae,* that inhabit the human upper respiratory tract.

A number of previously completed studies focused on biofilm production and bacterial cell viability due to interactions with CSP-like pheromones. A study by Zhang *et al*[49] demonstrated that within *S. mutans* there was a 76.3% decline in cell viability and biofilm mass increased by 89.3% following the addition of CSP to bacterial growth media[49]. In addition, supernatant collected from *S. mutans* that was co-cultured with *Aggregatibacter actinomycetemcomitans* caused a 1.3-fold rise in biofilm production within *S. mutans*[50]. Ample evidence of cell death after CSP exposure has been documented by several studies, however, biofilm production has not been normalized to the viable bacterial cells that remain [51-53]. Nevertheless, a number of Gram-positive bacterial species show cell viability and subsequent biofilm production correlate with the level of CSP added to the media. Further studies should be done to assess the actual increase in biofilm formation by taking into account the findings that competence is accompanied by massive cellular death.

We also believe that there may be a connection between metabolic dormancy and the BrpR/BrpS TCS. If malate production is interrupted after BrpR binds to the sigma factor binding sites, malate conversion to oxalacetate would be halted. As a consequence of this interruption, any acetyl groups generated by acetyl-CoA would not interact with citrate within the citric-acid cycle. Thus, too much acetyl-CoA would arise within the cell. Because these functional groups would be liberated, it is possible that there would be an epigenetic modification and BrpR would be rapidly released from the *srtA* gene enhancer region. By freeing BrpR from the *srtA* gene enhancer region, additional BrpR molecules would be available to interact with sigma factors, blocking transcription of *brpRS* that would lead to even less transcription of the *mqo2* gene. The work by Zhang *et al*[54] used profiling of lysine acetylomes in *S. aureus* and *E. coli* to identify a sequence motif, which supports our idea that BrpR may epigenetically block DNA-binding[54]. As part of that study, 412 proteins and 1361 lysine sites were cross-referenced against each other, which led to a conserved motif, N'-RLYELExQLxxxFIRISKxxEIVN-C', being identified. BrpR has this conserved motif, which is very well conserved among a number of bacterial species. By shutting down malate expression, persister cells could form suddenly as a response to late-stage competence or treatment with the SK-03-92 drug. Thus, BrpR repression of malate production could be connected to formation of persister cells that is a feature of late-stage competence.

CONCLUSION

Our study suggests that BrpR/BrpS is a TCS that may repress *S. aureus* biofilm production and be linked to late-stage competence in *S. aureus*.

ARTICLE HIGHLIGHTS

Research background

Staphylococcus aureus (*S. aureus*) is a primary cause of skin/soft tissue infections. Biofilm formation is a key component of *S. aureus* pathogenesis. Thus, an understanding of what regulates biofilm formation in *S. aureus* is important.

Research motivation

We were interested in characterizing two open reading frames that we thought were tied to biofilm formation in *S. aureus*.

Research objectives

Determine if mutations in the *brpR* and *brpS* genes affected biofilm formation and what the respective proteins had homologies with.

Research methods

We used biofilm assays and quantitative real-time-polymerase chain reaction (qRT-PCR) analysis to test *brpR* and *brpS* mutants compared to the parent strain of *S. aureus*. Bioinformatic tools were used to determine what roles the BrpR and BrpS proteins may play in *S. aureus* cells.

Research results

The biofilm and qRT-PCR analyses demonstrated that mutations in the *brpR* and *brpS* genes affected biofilm formation in *S. aureus* and led to transcriptional differences in key biofilm-related genes as compared to the parent strain. Further, the BrpR and BrpS proteins share homologies with proteins

involved in late-stage competence in streptococcal species.

Research conclusions

BrpR/BrpS are likely a new two-component system which regulates biofilm formation in *S. aureus*.

Research perspectives

A better understanding of a new regulator of *S. aureus* biofilm formation has been identified.

ACKNOWLEDGEMENTS

We wish to thank Jean Lee, Ambrose Cheung, Jo Handelsman, and NARSA for bacterial strains and plasmids used in this study as well as Jennifer Klein and the Molecular Biology Laboratory students who ran some of the qRT-PCRs.

FOOTNOTES

Author contributions: Zank A, Wescott A, and Schwan WR designed the research study; Zank A, Schulte L, Brandon X, Carstensen L, Wescott A, and Schwan WR performed the research; Zank A, Brandon X, and Schwan WR contributed new plasmids; Zank A, and Schwan WR analyzed the data and wrote the manuscript; and all authors have read and approved the final manuscript.

Supported by National Science Foundation Graduate Research Program to Zank A, No. 0002016179620.

Institutional review board statement: No humans or samples from human were used in this study.

Institutional animal care and use committee statement: No animals were used in this study.

Conflict-of-interest statement: Schwan WR holds a composition of matter and use patent covering the SK-03-92 Lead compound.

Data sharing statement: The authors will share their data with whomever asks.

Country/Territory of origin: United States

ORCID number: Allison Zank 0000-0001-6264-853X; Lillian Schulte 0000-0003-4175-0193; Xavier Brandon 0000-0002-2108-793X; Lauren Carstensen 0000-0002-3976-9023; Amy Wescott 0000-0002-3581-3365; William R Schwan 0000-0003-3076-1815.

S-Editor: Fan JR
L-Editor: A
P-Editor: Cai YX

REFERENCES

1 **Suaya JA**, Mera RM, Cassidy A, O'Hara P, Amrine-Madsen H, Burstin S, Miller LG. Incidence and cost of hospitalizations associated with *Staphylococcus aureus* skin and soft tissue infections in the United States from 2001 through 2009. *BMC Infect Dis* 2014; **14**: 296 [PMID: 24889406 DOI: 10.1186/1471-2334-14-296]

2 **Klein EY**, Sun L, Smith DL, Laxminarayan R. The changing epidemiology of methicillin-resistant *Staphylococcus aureus* in the United States: a national observational study. *Am J Epidemiol* 2013; **177**: 666-674 [PMID: 23449778 DOI: 10.1093/aje/kws273]

3 **Klein EY**, Mojica N, Jiang W, Cosgrove SE, Septimus E, Morgan DJ, Laxminarayan R. Trends in methicillin-resistant *Staphylococcus aureus* hospitalizations in the United States, 2010-2014. *Clin Infect Dis* 2017; **65**: 1921-1923 [PMID: 29020322 DOI: 10.1093/cid/cix640]

4 **Schwan WR**, Kabir MS, Kallaus M, Krueger S, Monte A, Cook JM. Synthesis and minimum inhibitory concentrations of SK-03-92 against *Staphylococcus aureus* and other gram-positive bacteria. *J Infect Chemother* 2012; **18**: 124-126 [PMID: 21739106 DOI: 10.1007/s10156-011-0273-7]

5 **Schwan WR**, Polanowski R, Dunman PM, Medina-Bielski S, Lane M, Rott M, Lipker L, Wescott A, Monte A, Cook JM,

Baumann DD, Tiruveedhula VVNPB, Witzigmann CM, Mikel C, Rahman MT. Identification of *Staphylococcus aureus* cellular pathways affected by the stilbenoid lead drug SK-03-92 using a microarray. *Antibiotics (Basel)* 2017; **6** [PMID: 28892020 DOI: 10.3390/antibiotics6030017]

6 **Rice KC**, Bayles KW. Molecular control of bacterial death and lysis. *Microbiol Mol Biol Rev* 2008; **72**: 85-109, table of contents [PMID: 18322035 DOI: 10.1128/MMBR.00030-07]

7 **Okshevsky M**, Meyer RL. The role of extracellular DNA in the establishment, maintenance and perpetuation of bacterial biofilms. *Crit Rev Microbiol* 2015; **41**: 341-352 [PMID: 24303798 DOI: 10.3109/1040841X.2013.841639]

8 **Wood TK**, Knabel SJ, Kwan BW. Bacterial persister cell formation and dormancy. *Appl Environ Microbiol* 2013; **79**: 7116-7121 [PMID: 24038684 DOI: 10.1128/AEM.02636-13]

9 **Zhang Y**. Persisters, persistent infections and the Yin-Yang model. *Emerg Microbes Infect* 2014; **3**: e3 [PMID: 26038493 DOI: 10.1038/emi.2014.3]

10 **Dufour D**, Lévesque CM. Bacterial behaviors associated with the quorum-sensing peptide pheromone ('alarmone') in streptococci. *Future Microbiol* 2013; **8**: 593-605 [PMID: 23642115 DOI: 10.2217/fmb.13.23]

11 **Cozzone AJ**. ATP-dependent protein kinases in bacteria. *J Cell Biochem* 1993; **51**: 7-13 [PMID: 8432746 DOI: 10.1002/jcb.240510103]

12 **Pestova EV**, Håvarstein LS, Morrison DA. Regulation of competence for genetic transformation in *Streptococcus pneumoniae* by an auto-induced peptide pheromone and a two-component regulatory system. *Mol Microbiol* 1996; **21**: 853-862 [PMID: 8878046 DOI: 10.1046/j.1365-2958.1996.501417.x]

13 **Xie Z**, Okinaga T, Niu G, Qi F, Merritt J. Identification of a novel bacteriocin regulatory system in *Streptococcus mutans*. *Mol Microbiol* 2010; **78**: 1431-1447 [PMID: 21143316 DOI: 10.1111/j.1365-2958.2010.07417.x]

14 **Duthie ES**, Lorenz LL. Staphylococcal coagulase; mode of action and antigenicity. *J Gen Microbiol* 1952; **6**: 95-107 [PMID: 14927856 DOI: 10.1099/00221287-6-1-2-95]

15 **Fey PD**, Endres JL, Yajjala VK, Widhelm TJ, Boissy RJ, Bose JL, Bayles KW. A genetic resource for rapid and comprehensive phenotype screening of nonessential *Staphylococcus aureus* genes. *mBio* 2013; **4**: e00537-e00512 [PMID: 23404398 DOI: 10.1128/mBio.00537-12]

16 **Hanahan D**. Studies on transformation of *Escherichia coli* with plasmids. *J Mol Biol* 1983; **166**: 557-580 [PMID: 6345791 DOI: 10.1016/s0022-2836(83)80284-8]

17 **Novick RP**. The Staphylococcus as a molecular genetic system. "Molecular Biology of the Staphylococci" R. P. Novick ed, pp. 1–40, VCH Publishers: New York, NY, USA, 1990

18 **Bateman BT**, Donegan NP, Jarry TM, Palma M, Cheung AL. Evaluation of a tetracycline-inducible promoter in *Staphylococcus aureus* in vitro and in vivo and its application in demonstrating the role of sigB in microcolony formation. *Infect Immun* 2001; **69**: 7851-7857 [PMID: 11705967 DOI: 10.1128/IAI.69.12.7851-7857.2001]

19 **Kloss WE**, Pattee PA. Transduction analysis of the histidine region in *Staphylococcus aureus*. *J Gen Microbiol* 1965; **39**: 195-207 [PMID: 14324965 DOI: 10.1099/00221287-39-2-195]

20 **Iandolo JJ**, Kraemer GR. High frequency transformation of *Staphylococcus aureus* by electroporation. *Curr Microbiol* 1990; **21**: 373-376 [DOI: 10.1007/BF02199440]

21 **Stepanović S**, Vuković D, Jezek P, Pavlović M, Svabic-Vlahović M. Influence of dynamic conditions on biofilm formation by staphylococci. *Eur J Clin Microbiol Infect Dis* 2001; **20**: 502-504 [PMID: 11561809 DOI: 10.1007/s100960100534]

22 **Bustin SA**, Benes V, Garson JA, Hellemans J, Huggett J, Kubista M, Mueller R, Nolan T, Pfaffl MW, Shipley GL, Vandesompele J, Wittwer CT. The MIQE guidelines: minimum information for publication of quantitative real-time PCR experiments. *Clin Chem* 2009; **55**: 611-622 [PMID: 19246619 DOI: 10.1373/clinchem.2008.112797]

23 **Livak KJ**, Schmittgen TD. Analysis of relative gene expression data using real-time quantitative PCR and the 2(-Delta Delta C(T)) Method. *Methods* 2001; **25**: 402-408 [PMID: 11846609 DOI: 10.1006/meth.2001.1262]

24 **Baba T**, Takeuchi F, Kuroda M, Yuzawa H, Aoki K, Oguchi A, Nagai Y, Iwama N, Asano K, Naimi T, Kuroda H, Cui L, Yamamoto K, Hiramatsu K. Genome and virulence determinants of high virulence community-acquired MRSA. *Lancet* 2002; **359**: 1819-1827 [PMID: 12044378 DOI: 10.1016/s0140-6736(02)08713-5]

25 **Baba T**, Bae T, Schneewind O, Takeuchi F, Hiramatsu K. Genome sequence of *Staphylococcus aureus* strain Newman and comparative analysis of staphylococcal genomes: polymorphism and evolution of two major pathogenicity islands. *J Bacteriol* 2008; **190**: 300-310 [PMID: 17951380 DOI: 10.1128/JB.01000-07]

26 **Clark K**, Karsch-Mizrachi I, Lipman DJ, Ostell J, Sayers EW. GenBank. *Nucleic Acids Res* 2016; **44**: D67-D72 [PMID: 26590407 DOI: 10.1093/nar/gkv1276]

27 **Karp PD**, Billington R, Caspi R, Fulcher CA, Latendresse M, Kothari A, Keseler IM, Krummenacker M, Midford PE, Ong Q, Ong WK, Paley SM, Subhraveti P. The BioCyc collection of microbial genomes and metabolic pathways. *Brief Bioinform* 2019; **20**: 1085-1093 [PMID: 29447345 DOI: 10.1093/bib/bbx085]

28 **UniProt Consortium T**. UniProt: the universal protein knowledgebase. *Nucleic Acids Res* 2018; **46**: 2699 [PMID: 29425356 DOI: 10.1093/nar/gky092]

29 **Omasits U**, Ahrens CH, Müller S, Wollscheid B. Protter: interactive protein feature visualization and integration with experimental proteomic data. *Bioinformatics* 2014; **30**: 884-886 [PMID: 24162465 DOI: 10.1093/bioinformatics/btt607]

30 **Blom N**, Sicheritz-Pontén T, Gupta R, Gammeltoft S, Brunak S. Prediction of post-translational glycosylation and phosphorylation of proteins from the amino acid sequence. *Proteomics* 2004; **4**: 1633-1649 [PMID: 15174133 DOI: 10.1002/pmic.200300771]

31 **de Castro E**, Sigrist CJ, Gattiker A, Bulliard V, Langendijk-Genevaux PS, Gasteiger E, Bairoch A, Hulo N. ScanProsite: detection of PROSITE signature matches and ProRule-associated functional and structural residues in proteins. *Nucleic Acids Res* 2006; **34**: W362-W365 [PMID: 16845026 DOI: 10.1093/nar/gkl124]

32 **Yang J**, Yan R, Roy A, Xu D, Poisson J, Zhang Y. The I-TASSER Suite: protein structure and function prediction. *Nat Methods* 2015; **12**: 7-8 [PMID: 25549265 DOI: 10.1038/nmeth.3213]

33 **Delano WL**. The PyMOL Molecular Graphics System, Version 1.2r3pre, Schrödinger, LLC.

34 **Hwang S**, Gou Z, Kuznetsov IB. DP-Bind: a web server for sequence-based prediction of DNA-binding residues in DNA-

binding proteins. *Bioinformatics* 2007; **23**: 634-636 [PMID: 17237068 DOI: 10.1093/bioinformatics/btl672]
35 **Altschul SF**, Gish W, Miller W, Myers EW, Lipman DJ. Basic local alignment search tool. *J Mol Biol* 1990; **215**: 403-410 [PMID: 2231712 DOI: 10.1016/S0022-2836(05)80360-2]
36 **Molenaar D**, van der Rest ME, Petrović S. Biochemical and genetic characterization of the membrane-associated malate dehydrogenase (acceptor) from *Corynebacterium glutamicum*. *Eur J Biochem* 1998; **254**: 395-403 [PMID: 9660197 DOI: 10.1046/j.1432-1327.1998.2540395.x]
37 **Mazmanian SK**, Liu G, Ton-That H, Schneewind O. *Staphylococcus aureus* sortase, an enzyme that anchors surface proteins to the cell wall. *Science* 1999; **285**: 760-763 [PMID: 10427003 DOI: 10.1126/science.285.5428.760]
38 **Ranjit DK**, Endres JL, Bayles KW. *Staphylococcus aureus* CidA and LrgA proteins exhibit holin-like properties. *J Bacteriol* 2011; **193**: 2468-2476 [PMID: 21421752 DOI: 10.1128/JB.01545-10]
39 **Kavanaugh JS**, Flack CE, Lister J, Ricker EB, Ibberson CB, Jenul C, Moormeier DE, Delmain EA, Bayles KW, Horswill AR. Identification of extracellular DNA-binding proteins in the biofilm matrix. *mBio* 2019; **10** [PMID: 31239382 DOI: 10.1128/mBio.01137-19]
40 **Archer NK**, Mazaitis MJ, Costerton JW, Leid JG, Powers ME, Shirtliff ME. *Staphylococcus aureus* biofilms: properties, regulation, and roles in human disease. *Virulence* 2011; **2**: 445-459 [PMID: 21921685 DOI: 10.4161/viru.2.5.17724]
41 **Otto M**. Staphylococcal biofilms. *Curr Top Microbiol Immunol* 2008; **322**: 207-228 [PMID: 18453278 DOI: 10.1007/978-3-540-75418-3_10]
42 **Marraffini LA**, Dedent AC, Schneewind O. Sortases and the art of anchoring proteins to the envelopes of gram-positive bacteria. *Microbiol Mol Biol Rev* 2006; **70**: 192-221 [PMID: 16524923 DOI: 10.1128/MMBR.70.1.192-221.2006]
43 **Sadykov MR**, Bayles KW. The control of death and lysis in staphylococcal biofilms: a coordination of physiological signals. *Curr Opin Microbiol* 2012; **15**: 211-215 [PMID: 22221897 DOI: 10.1016/j.mib.2011.12.010]
44 **Kadurugamuwa JL**, Sin L, Albert E, Yu J, Francis K, DeBoer M, Rubin M, Bellinger-Kawahara C, Parr TR Jr, Contag PR. Direct continuous method for monitoring biofilm infection in a mouse model. *Infect Immun* 2003; **71**: 882-890 [PMID: 12540570 DOI: 10.1128/IAI.71.2.882-890.2003]
45 **Xiong YQ**, Willard J, Kadurugamuwa JL, Yu J, Francis KP, Bayer AS. Real-time in vivo bioluminescent imaging for evaluating the efficacy of antibiotics in a rat *Staphylococcus aureus* endocarditis model. *Antimicrob Agents Chemother* 2005; **49**: 380-387 [PMID: 15616318 DOI: 10.1128/AAC.49.1.380-387.2005]
46 **Brunskill EW**, Bayles KW. Identification of LytSR-regulated genes from *Staphylococcus aureus*. *J Bacteriol* 1996; **178**: 5810-5812 [PMID: 8824633 DOI: 10.1128/jb.178.19.5810-5812.1996]
47 **Okinaga T**, Xie Z, Niu G, Qi F, Merritt J. Examination of the *hdrRM* regulon yields insight into the competence system of *Streptococcus mutans*. *Mol Oral Microbiol* 2010; **25**: 165-177 [PMID: 20536745 DOI: 10.1111/j.2041-1014.2010.00574.x]
48 **Kreth J**, Hung DCI, Merritt J, Perry J, Zhu L, Goodman SD, Cvitkovitch DG, Shi W, Qi F. The response regulator ComE in *Streptococcus mutans* functions both as a transcription activator of mutacin production and repressor of CSP biosynthesis. *Microbiology (Reading)* 2007; **153**: 1799-1807 [PMID: 17526837 DOI: 10.1099/mic.0.2007/005975-0]
49 **Zhang K**, Ou M, Wang W, Ling J. Effects of quorum sensing on cell viability in *Streptococcus mutans* biofilm formation. *Biochem Biophys Res Commun* 2009; **379**: 933-938 [PMID: 19138664 DOI: 10.1016/j.bbrc.2008.12.175]
50 **Szafrański SP**, Deng ZL, Tomasch J, Jarek M, Bhuju S, Rohde M, Sztajer H, Wagner-Döbler I. Quorum sensing of *Streptococcus mutans* is activated by *Aggregatibacter actinomycetemcomitans* and by the periodontal microbiome. *BMC Genomics* 2017; **18**: 238 [PMID: 28320314 DOI: 10.1186/s12864-017-3618-5]
51 **Qi F**, Kreth J, Lévesque CM, Kay O, Mair RW, Shi W, Cvitkovitch DG, Goodman SD. Peptide pheromone induced cell death of *Streptococcus mutans*. *FEMS Microbiol Lett* 2005; **251**: 321-326 [PMID: 16165324 DOI: 10.1016/j.femsle.2005.08.018]
52 **Ween O**, Gaustad P, Håvarstein LS. Identification of DNA binding sites for ComE, a key regulator of natural competence in *Streptococcus pneumoniae*. *Mol Microbiol* 1999; **33**: 817-827 [PMID: 10447890 DOI: 10.1046/j.1365-2958.1999.01528.x]
53 **Perry JA**, Cvitkovitch DG, Lévesque CM. Cell death in *Streptococcus mutans* biofilms: a link between CSP and extracellular DNA. *FEMS Microbiol Lett* 2009; **299**: 261-266 [PMID: 19735463 DOI: 10.1111/j.1574-6968.2009.01758.x]
54 **Zhang Y**, Wu ZX, Wan XL, Liu P, Zhang JB, Ye Y, Zhao YM, Tan MJ. Comprehensive profiling of lysine acetylome in *Staphylococcus aureus*. *Sci China Chem* 2014; **57**: 732-738 [DOI: 10.1007/s11426-014-5100-4]

World Journal of Clinical Infectious Diseases

Submit a Manuscript: https://www.f6publishing.com

World J Clin Infect Dis 2022 April 26; 12(1): 33-40

DOI: 10.5495/wjcid.v12.i1.33

ISSN 2220-3176 (online)

CASE REPORT

Pericarditis following COVID-19 vaccination: Two case reports

Justyna Fydrych, Amanda Paige Hughes, Said Abuhasna, Endale Mekonen

Specialty type: Infectious diseases

Provenance and peer review: Unsolicited article; Externally peer reviewed.

Peer-review model: Single blind

Peer-review report's scientific quality classification

Grade A (Excellent): 0
Grade B (Very good): B
Grade C (Good): C
Grade D (Fair): D
Grade E (Poor): 0

P-Reviewer: Ciccone MM, Spartalis M, Wong CP

Received: July 2, 2021
Peer-review started: July 2, 2021
First decision: October 18, 2021
Revised: November 13, 2021
Accepted: January 25, 2022
Article in press: January 25, 2022
Published online: April 26, 2022

Justyna Fydrych, Department of Pharmacy, Advocate Trinity Hospital, Chicago, IL 60617, United States

Amanda Paige Hughes, Department of Pharmacy, Advocate Aurora Health, Chicago, IL 60617, United States

Said Abuhasna, Department of Critical Care, Advocate Trinity Hospital, Chicago, IL 60617, United States

Endale Mekonen, Department of Infectious Disease, Advocate Trinity Hospital, Chicago, IL 60617, United States

Corresponding author: Justyna Fydrych, PharmD, Pharmacist, Department of Pharmacy, Advocate Trinity Hospital, 2320 E 93rd St, Chicago, IL 60617, United States.
jfydry2@gmail.com

Abstract

BACKGROUND

Coronavirus disease 2019 (COVID-19) is a highly contagious viral illness which conventionally manifests with primarily respiratory symptoms and less commonly with cardiac involvement in various forms, such as pericarditis. Myocarditis and pericarditis have been reported in a variety of live and attenuated vaccines, such as smallpox and influenza. As of October 2021, no cases of pericarditis associated with COVID-19 vaccination have been published. We present two healthy male patients who present post COVID-19 vaccination with pericarditis diagnoses.

CASE SUMMARY

A 21-year-old male with no significant past medical history presented with myalgia, chills, mild headache, and chest pain for two days. Patient received the Moderna COVID-19 vaccine the day prior to symptom onset. On presentation, electrocardiogram (ECG) revealed sinus rhythm with ST elevation, and troponin was elevated. Emergent cardiac catheterization was not significant for abnormalities. The primary diagnosis was acute pericarditis, and the patient was discharged on colchicine and indomethacin. Additionally, a 35-year-old male with no pertinent past medical history presented with fever, chills, weakness, nausea, vomiting, diarrhea, and retrosternal chest pain for three days. He received the Moderna COVID-19 vaccine four days prior to symptom onset. On presentation, troponin was elevated, and ECG revealed mild ST elevation. Left ventricular dysfunction with ejection fraction of 41% was reported on transthoracic echocardiogram. Patient was started on ibuprofen and colchicine for diagnosis of

myopericarditis.

CONCLUSION
These case reports highlight a potential unintended consequence, pericarditis, associated with COVID-19 vaccination that may not warrant invasive cardiac intervention.

Key Words: Pericarditis; Myocarditis; COVID-19; COVID-19 vaccine; Myopericarditis; Case report

Core Tip: Coronavirus disease 2019 (COVID-19) manifests with primarily respiratory symptoms and less commonly with cardiac involvement. Myocarditis and pericarditis have been reported in a variety of live and attenuated vaccines. However, to our knowledge, there are no published cases associated with COVID-19 vaccination as of October 2021. We present two cases of pericarditis following COVID-19 vaccination. Both patients were treated with colchicine and non-steroidal anti-inflammatory agents but with varying degrees of invasive work-up. The first patient had emergent cardiac catheterization, while the second patient underwent computed tomographic angiography of the coronary arteries. Neither patient required intervention, thus questioning the necessity of cardiac catheterization.

Citation: Fydrych J, Hughes AP, Abuhasna S, Mekonen E. Pericarditis following COVID-19 vaccination: Two case reports. *World J Clin Infect Dis* 2022; 12(1): 33-40
URL: https://www.wjgnet.com/2220-3176/full/v12/i1/33.htm
DOI: https://dx.doi.org/10.5495/wjcid.v12.i1.33

INTRODUCTION

On January 9, 2020, the World Health Organization announced a mysterious Coronavirus-related pneumonia in Wuhan, China[1]. Shortly after, cases were identified across the globe and quarantines were ordered to help prevent transmission. Despite early prevention efforts of social distancing and donning masks, coronavirus disease 2019 (COVID-19) was relentless[1]. As of November 2021, there are over 250 million confirmed cases and over five million deaths attributed to COVID-19[2]. The development of a vaccine was the light at the end of the tunnel but not without some associated risks.

Cardiac complications, such as myocarditis and pericarditis, after immunizations are extremely rare events in both younger and older patients but have been reported following smallpox, diphtheria, tetanus, polio, human papillomavirus (HPV), and influenza vaccines[3-6]. Through a PubMed search of pericarditis associated with the COVID-19 vaccine, no published cases have been identified. However, recently, the possible link between myocarditis and the COVID-19 vaccine has been under investigation by the Israel Health Ministry[7]. Sixty-two cases of myocarditis in young males were identified, but at this time, no conclusions have been made. The European Medicines Agency and United States Centers for Disease Control and Prevention (CDC) are also investigating the link between pericarditis and myocarditis with the COVID-19 vaccine, but no association has been found[8,9].

Here below, we present two cases of pericarditis in two young adult males following Moderna COVID-19 vaccination. A 21-year-old healthy male presenting three days post vaccination, and a 35-year-old male presenting seven days post vaccination. The purpose of this case report is to highlight an atypical response to the COVID-19 vaccine.

CASE PRESENTATION

Chief complaints

Case 1: In April 2021, a 21-year-old man was admitted to the hospital with myalgia, chills, mild headache, and chest pain for two days.

Case 2: In February 2021, a 35-year-old man presented to the emergency department with fever, chills, weakness, nausea, vomiting, diarrhea, and retrosternal chest pain for three days.

History of present illness

Case 1: Chest pain was rated three out of ten which worsened on inspiration and described as pleuritic in nature. The patient received the first dose of the Moderna COVID-19 vaccine series the day prior to

symptom onset. No associated diaphoresis or arm pain. No tenderness on palpation. No history of known COVID-19 infection or current fevers, nausea, vomiting, diarrhea, abdominal pain, shortness of breath, cough, extremity swelling, travel, or sick contacts.

Case 2: He received his first Moderna COVID-19 vaccine four days prior to symptom onset. Patient denies recent travel, sick contacts, COVID-19 exposure, or symptoms associated with COVID-19.

History of past illness

Case 1: The patient has no pertinent past medical history or surgeries.

Case 2: Past medical history significant for obesity, chronic allergic rhinitis, and previous COVID-19 infection reported several months prior to vaccination.

Personal and family history

No tobacco, illicit drugs, or alcohol use reported. No family history of heart disease for either of the two cases.

Physical examination

Case 1: In the emergency department (ED), on physical examination, no rub, normal rate, and regular rhythm noted.

Case 2: In the ED, on physical exam, the patient was noted to be tachycardic but otherwise had no abnormal physical exam findings, including pericardial rub.

Laboratory examinations

Case 1: Troponin was elevated at 15.2 ng/mL, creatinine kinase elevated at 657 units/L, C-Reactive Protein (CRP) elevated at 6.3 mg/dL, and erythrocyte sedi-mentation rate (ESR) mildly elevated at 24 mm/hr. Toxicology screen was negative. COVID-19, respiratory syncytial virus (RSV), and Influenza were negative using a sample obtained from a nasopharyngeal swab tested on Cepheid Xpert Xpress severe acute respiratory syndrome coronavirus 2/influenza/RSV reverse transcriptase polymerase chain reaction (SARS-CoV-2/Flu/RSV RT-PCR).

Case 2: Troponin was elevated at 7.58 ng/mL, CRP elevated at 26.8 mg/dL, and ESR elevated at 96 mm/hr. White blood cell (WBC) count was also elevated at 20.4 K/mcL. Bacterial and viral infectious etiologies were ruled out including COVID-19, RSV, influenza, bocavirus, adenovirus, parainfluenza, metapneumovirus, rhinovirus, enterovirus, *Mycoplasma pneumoniae*, and *Chlamydophila pneumoniae* using a sample from a nasopharyngeal swab tested on Cepheid Xpert Xpress SARS-CoV-2/Flu/RSV RT-PCR and Multiplex RT PCR amplification followed by Liquid Bead Array Hybridization. Hepatitis and human immunodeficiency viruses were also ruled out *via* antibody and antigen testing. Blood cultures had no growth.

Imaging examinations

Case 1: Chest X-ray was unremarkable with clear lungs and normal heart size. Transthoracic echocardiogram (TTE) demonstrated an ejection fraction (EF) of 65% without wall motion abnormalities and no pericardial effusion. Original electrocardiogram (ECG) reported sinus rhythm with ST elevation (Figure 1A). On repeat ECG, there was disproportionate worsening of ST elevation in inferior leads with development of new ST depression in aVL lead, so the patient was worked up for acute inferior myocardial infarction to rule out obstructive etiology. Emergent cardiac catheterization demonstrated 40% stenosis of the midsegment of the left anterior descending artery (LAD), though the remaining coronary arteries appeared to be disease-free and no interventions warranted.

Case 2: Chest X-ray and computed tomographic angiography (CTA) of the chest with contrast were both unremarkable. ECG demonstrated mild diffuse ST/T elevation (Figure 1B). On TTE, left ventricular dysfunction with EF of 41% reported.

FINAL DIAGNOSIS

Case 1: The primary diagnosis was acute pericarditis.

Case 2: The final diagnosis was myopericarditis complicated by acute kidney injury (AKI) secondary to intravenous (IV) contrast.

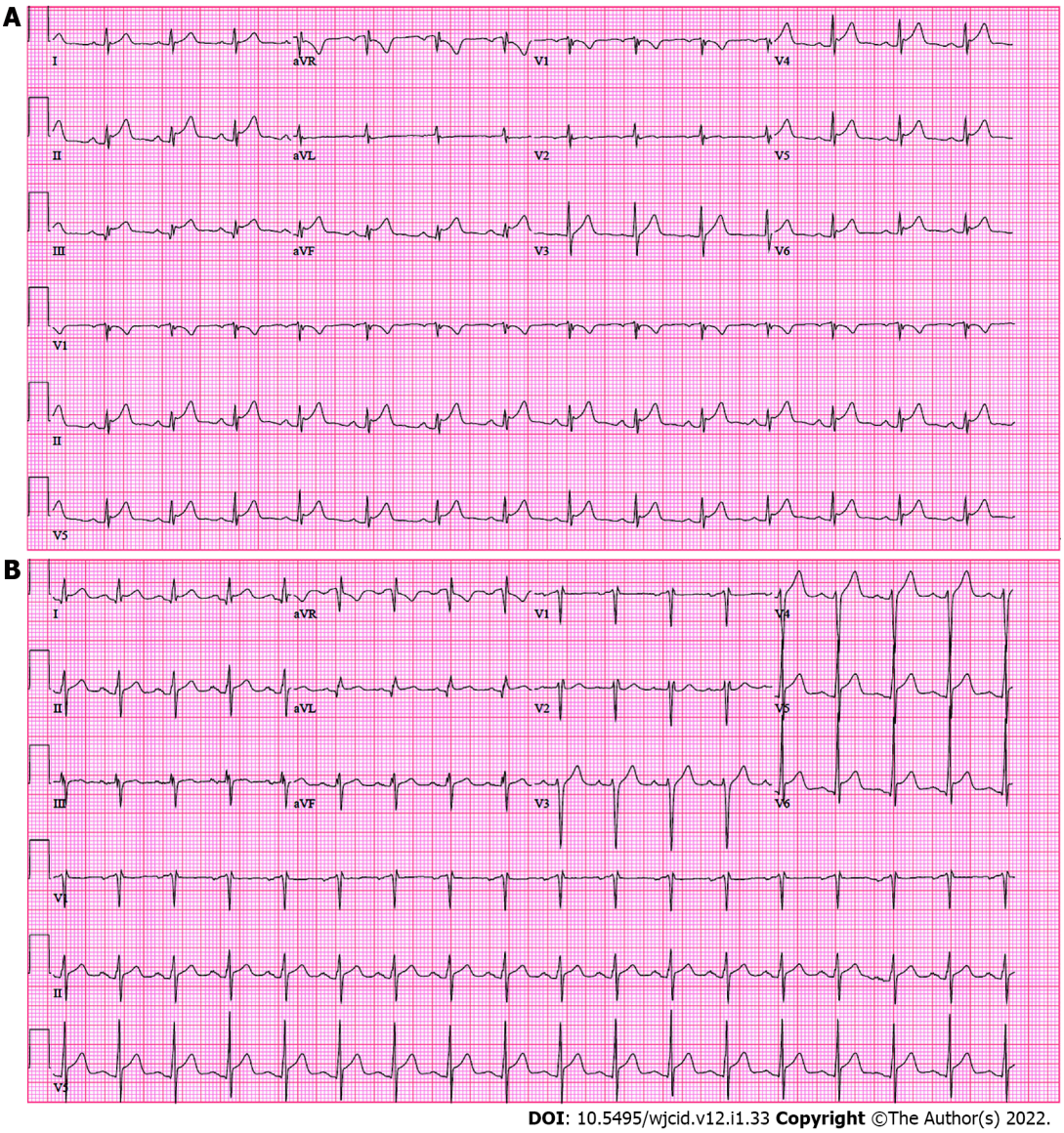

DOI: 10.5495/wjcid.v12.i1.33

Figure 1 Electrocardiogram of 21-year-old male (A) and 35-year-old male (B) showing ST elevation.

TREATMENT

Case 1: The patient was started on colchicine, indomethacin, and aspirin. He was discharged the following day on aspirin, colchicine for 14 d, and an indomethacin taper over 28 d.

Case 2: The patient was given acetaminophen and ketorolac in the ED. Cardiology was consulted and started the patient on ibuprofen and colchicine for myopericarditis. Ibuprofen was changed to prednisone due to contrast induced AKI. Colchicine and prednisone were continued for five additional days on discharge with instruction to follow-up with cardiology outpatient. Carvedilol and sacubitril/valsartan were initiated based on left ventricular dysfunction with plans to monitor and titrate outpatient. No antimicrobials were administered, and leukocytosis spontaneously resolved.

OUTCOME AND FOLLOW-UP

Case 1: Upon discharge, an appointment was scheduled with a new primary care provider with instruction to obtain a cardiologist referral. During follow-up with cardiology three months after discharge, repeat TTE was unremarkable with normal function and no regional wall motion abnormalities. Troponin, CRP, and ESR were normal as well. No further work-up or cardiology follow-up warranted. To our knowledge, there were no complications or readmissions associated with pericarditis following discharge.

Case 2: The patient's course was complicated by AKI secondary to IV contrast which extended his hospitalization to four days. Coronary CTA was later completed outpatient with no notable findings. To our knowledge, there were no complications or readmissions associated with pericarditis following discharge.

DISCUSSION

As of November 2021, over three billion individuals are fully vaccinated for COVID-19[10]. Common side effects of the COVID-19 vaccine are pain, redness, and swelling of the injection site, fatigue, headache, muscle pain, chills, fever, and nausea. No case reports of pericarditis as a side effect of COVID-19 vaccines have been published as of November 2021. A hypothesized mechanism of action of vaccine induced myopericarditis is an autoimmune reaction that typically occurs after seven days. Our patients presented within seven days post vaccination; therefore, this mechanism is unlikely[11]. A possible mechanism for male predominance in myocarditis/pericarditis is presumably related to variations in sex hormones. Estrogen is thought to inhibit proinflammatory T cells, resulting in a decrease in immune related responses. Pericarditis in females may also be underdiagnosed, which could explain the male predominance[12].

On the contrary, active COVID-19 infection presenting as pericarditis and endocarditis have been reported[13,14]. A systematic review conducted in December 2020 identified 34 COVID-19 patients with pericarditis reported, and 62% were diagnosed with myopericarditis[15]. Pericarditis in COVID-19 patients is still poorly understood. A proposed explanation is the binding of the SARS-CoV-2 Spike protein to angiotensin-converting enzyme 2 which can be found on the heart. Thus, there is potential cause for myocarditis, pericardial effusion, and pericarditis[13,15].

While no case reports were published to our knowledge, as of May 2021, 133 cases of pericarditis and 119 cases of myocarditis had been reported to the CDC Vaccine Adverse Event Reporting System (VAERS)[16]. Cases of pericarditis were reported following each of the Food and Drug Administration approved COVID-19 vaccines Pfizer (67), Moderna (54), and Johnson and Johnson (12). Pfizer was the first vaccine to be approved as well as the most common manufacturer associated with reported pericarditis cases, followed by Moderna, then Johnson and Johnson. Of the 133 pericarditis cases, 77 reported cases are males, 53 are females, and 3 were not reported. The average age for males was 44.6 years old and ranged from 16 to 84 years old. The average age for females was 54.5 years old and ranged from 20 to 85 years old. The mean ages are likely falsely elevated based on vaccine rollout and earlier access to patients 65 years and older in the general public. The average reported time to symptom onset is 7.4 d and ranges from 0 to 63 d. Our patient cases consist of two males that are below the mean reported age and below the average time to symptom onset. As of November 2021, the number of adverse events with the word "pericarditis" associated with the COVID-19 vaccine has since substantially increased to 15895 reports[16].

Acute pericarditis is most commonly caused by viral infections and has been reported in patients with active COVID-19 infections[14,17-19]. Our case report is unique because we present two individuals diagnosed with pericarditis post COVID-19 vaccination who tested negative for active COVID-19 infection. Pericarditis is diagnosed when at least two of the four following criteria are present: Pericarditic chest pain, pericardial rubs, new widespread ST elevation or PR depression on ECG, or pericardial effusion[20]. Additional supporting findings include elevation of cardiac inflammatory markers and evidence of pericardial inflammation by imaging[20]. Both of our patients presented with ST elevation, pericarditic chest pain, along with several elevated cardiac inflammatory markers. In the second case, ECG does not show the typical patterns of acute pericarditis (*i.e.* diffuse ST elevations with PR depressions), which are often seen hours to days after symptom onset during the first stage. Considering the patient presented seven days post-vaccination and three days after symptom onset, it is plausible any atypical ECG patterns had since normalized. Neither patient had diagnosed cardiac history, infectious causes, noninfectious causes, or past medical history to predispose them to pericarditis; therefore, we believe these episodes of acute pericarditis are secondary to the COVID-19 vaccine.

Patients presenting with COVID-19 and elevated troponins often have worse outcomes[21]. However, if patients present following COVID-19 immunization with elevated cardiac inflammatory markers, ST elevation, but not diagnosed with COVID-19, should cardiac catheterization be standard of care? The 21-year-old patient was taken for emergent cardiac catheterization and was found to have 40% stenosis of the midsegment of the LAD, but remaining coronary arteries appeared to be disease-free. No lesions were identified, and no interventions warranted. While no complications occurred with this patient, possible complications of invasive cardiac catheterization include infection, vascular complications, bleeding, stroke, myocardial infarction, and death[22]. The 35-year-old patient did not undergo cardiac catheterization but did receive a CTA of the chest and coronary arteries instead, which was unremarkable. It is unknown if the pericarditis cases reported to CDC VAERS warranted catheterization or other invasive testing. But of the 133 individuals reported, 86 were hospitalized, 46 were not hospitalized, and one unknown, which leads us to believe many cases self-resolved without seeking out

higher level of care.

Our patient cases do have inherent limitations. In the second case, since the patient reported a previous diagnosis of COVID-19, it is impossible to completely rule out myopericarditis as a complication from previous infection. The patient tested negative for active infection on admission, but past COVID-19 test results could not be found in the electronic medical record, so an exact date of infection is unknown. To our knowledge, neither patient has received the second immunization in the series; therefore, we are unable to assess outcomes when re-challenged with the second dose. Additionally, due to a lack of endomyocardial biopsy, a histopathological diagnosis for pericarditis or myocarditis cannot be confirmed. Both patients presented to a community hospital where there was not access to cardiac MRI, and based on rapid clinical improvement, myocardial biopsy was not warranted. Furthermore, other causes of pericarditis cannot be completely ruled out. The first patient tested negative for COVID-19, influenza, and RSV. Other infectious causes are less likely but were not tested for. COVID-19, RSV, influenza, bocavirus, adenovirus, parainfluenza, metapneumovirus, rhinovirus, enterovirus, *Mycoplasma pneumoniae*, and *Chlamydophila pneumoniae* were ruled out for the second patient, making viral and bacterial causes unlikely. Neither of these patients have a significant past medical history, including no likely medication causes, no trauma, nor autoimmune conditions. We also do not have long-term follow-up, thus no long-term outcomes for either patient. Despite these limitations, both patients scored a 5 on the Naranjo Algorithm, or Adverse Drug Reaction Probability Scale, resulting in a probable association. The reaction "followed a reasonable temporal sequence after a drug, followed a recognized response to the suspected drug, was confirmed by withdrawal but not by exposure to the drug, and could not be reasonably explained by the known characteristics of the patient's clinical state." [23].

During the time of these cases, the new mRNA COVID-19 vaccinations were under emergency use authorization. It is important to note, despite the skepticism and fear surrounding these novel vaccines, the benefits greatly outweigh the risk of rare side effects, including pericarditis and myocarditis. In fact, the CDC has reported the rare incidence of myocarditis/pericarditis as about 12.6 cases per million doses of second-dose mRNA vaccines in those age 12 to 39 years old (0.0000126%)[12]. However, a study investigating cardiovascular sequelae in COVID-19 infected patients revealed that 5.0% developed new-onset myocarditis and 1.5% developed pericarditis; therefore, there is much higher risk from active infection than vaccination[24]. The COVID-19 mRNA vaccines reduce the rate of severe infections, hospitalizations, and death from COVID-19. In a study conducted at five Veteran Affairs Medical Centers, mRNA vaccines were 86.8% effective at preventing COVID-19 associated hospitalizations in those who were over the age of 18 years old[25]. Most episodes of pericarditis are uncomplicated and can be managed in the outpatient setting[18]. Therefore, these cases should alleviate the fear of vaccine associated adverse effects and help guide the public on when to seek care.

CONCLUSION

Despite our findings and presumed correlation of COVID-19 vaccination and pericarditis, this should not deter individuals from being vaccinated, especially given the reported cardiac involvement from COVID-19 infections. Immunizations are essential for public health and achieving population immunity. Rather, these cases are intended to bring awareness to a potential etiology of pericarditis that should be considered in the differential that might not warrant invasive interventions with substantial risks. Further research and trials are needed to assess the linkage between COVID-19 vaccination and cardiac injury. Our cases highlight the importance of recognizing the possibility of COVID-19 vaccine side effects presenting as pericardial injury in young otherwise healthy individuals. The question remains, is cardiac catheterization necessary for every patient who presents with pericarditis secondary to COVID-19 vaccination?

FOOTNOTES

Author contributions: Fydrych J and Hughes AP contributed equally to data collection, research, and manuscript development; Abuhasna S and Mekonen E contributed equally to patient care, interpretation of diagnostics and manuscript review; all authors have read and approved the final manuscript.

Informed consent statement: Informed written consent was obtained from the patients for publication of this report and any accompanying images.

Conflict-of-interest statement: The authors declare that they have no conflict of interest to report.

CARE Checklist (2016) statement: The authors have read the CARE Checklist (2016). The manuscript was prepared and revised according to the CARE Checklist (2016).

Country/Territory of origin: United States

ORCID number: Justyna Fydrych 0000-0003-3140-406X; Amanda Paige Hughes 0000-0003-1771-2189; Said Abuhasna 0000-0003-2072-2011; Endale Mekonen 0000-0001-7495-7487.

S-Editor: Li X
L-Editor: A
P-Editor: Li X

REFERENCES

1 A Timeline of COVID-19 Developments in 2020. Published online 2021. Available from: https://www.ajmc.com/view/a-timeline-of-covid19-developments-in-2020
2 **World Health Organization**. WHO Coronavirus (COVID-19) Dashboard. Published online 2020. Available from: https://covid19.who.int/
3 **Mei R**, Raschi E, Forcesi E, Diemberger I, De Ponti F, Poluzzi E. Myocarditis and pericarditis after immunization: Gaining insights through the Vaccine Adverse Event Reporting System. *Int J Cardiol* 2018; **273**: 183-186 [PMID: 30236504 DOI: 10.1016/j.ijcard.2018.09.054]
4 **Nalca A**, Zumbrun EE. ACAM2000: the new smallpox vaccine for United States Strategic National Stockpile. *Drug Des Devel Ther* 2010; **4**: 71-79 [PMID: 20531961 DOI: 10.2147/dddt.s3687]
5 **Hawkes D**, Lea CE, Berryman MJ. Answering human papillomavirus vaccine concerns; a matter of science and time. *Infect Agent Cancer* 2013; **8**: 22 [PMID: 23758825 DOI: 10.1186/1750-9378-8-22]
6 **Boccara F**, Benhaiem-Sigaux N, Cohen A. Acute myopericarditis after diphtheria, tetanus, and polio vaccination. *Chest* 2001; **120**: 671-672 [PMID: 11502677 DOI: 10.1378/chest.120.2.671]
7 Israel assesses myocarditis cases linked to Pfizer-BioNTech COVID-19 vaccine. Pharmaceutical Technology. Published 2021. Available from: https://www.pharmaceutical-technology.com/news/israel-myocarditis-pfizer-vaccine/
8 **European Medicines Agency**. COVID-19 vaccine safety update. 28 January 2021. Available from: https://www.ema.europa.eu/en/documents/COVID-19-vaccine-safety-update/COVID-19-vaccine-safety-update-comirnaty-january-2021_en.pdf
9 **Achenbach J**, Sun LH. CDC probes rare cases of heart inflammation in vaccinated teens, young adults. Published 2021. Available from: https://www.washingtonpost.com/health/2021/05/24/heart-inflammation-coronavirus-vaccines-young-adults/
10 **World Health Organization**. Coronavirus disease (COVID-19): Vaccines. Published 2021. Available from: https://www.who.int/news-room/q-a-detail/coronavirus-disease-(COVID-19)-vaccines?adgroupsurvey=%7Badgroupsurvey%7D&gclid=Cj0KCQiA6Or_BRC_ARIsAPzuer84gbbRGBKcj2M76A-THyhJcXvZZ0wFZ80kdlnNVP1YeeK6J4T1C5UaAn1tEALw_wcB
11 **O'Leary ST**, Maldonado YA. Myocarditis After SARS-CoV-2 Vaccination: True, True, and… Related? *Pediatrics* 2021; 148: e2021052644 [PMID: 34088761 DOI: 10.1542/peds.2021-052644]
12 **Bozkurt B**, Kamat I, Hotez PJ. Myocarditis With COVID-19 mRNA Vaccines. *Circulation* 2021; **144**: 471-484 [PMID: 34281357 DOI: 10.1161/CIRCULATIONAHA.121.056135]
13 COVID-19 as a Possible Cause of Myocarditis and Pericarditis. Am Coll Cardiol. Published online 2021. Available from: https://www.acc.org/latest-in-cardiology/articles/2021/02/05/19/37/COVID-19-as-a-possible-cause-of-myocarditis-and-pericarditis
14 **Kumar R**, Kumar J, Daly C, Edroos SA. Acute pericarditis as a primary presentation of COVID-19. *BMJ Case Rep* 2020; **13**: e237617 [PMID: 32816925 DOI: 10.1136/bcr-2020-237617]
15 **Diaz-Arocutipa C**, Saucedo-Chinchay J, Imazio M. Pericarditis in patients with COVID-19: a systematic review. *J Cardiovasc Med (Hagerstown)* 2021; **22**: 693-700 [PMID: 33927144 DOI: 10.2459/JCM.0000000000001202]
16 The Vaccine Adverse Event Reporting System (VAERS) Request. Available from: https://wonder.cdc.gov/vaers.html
17 **de Meester A**, Luwaert R, Chaudron JM. Symptomatic pericarditis after influenza vaccination: report of two cases. *Chest* 2000; **117**: 1803-1805 [PMID: 10858422 DOI: 10.1378/chest.117.6.1803]
18 **Tingle LE**, Molina D, Calvert CW. Acute pericarditis. *Am Fam Physician* 2007; **76**: 1509-1514 [PMID: 18052017]
19 **Tung-Chen Y**. Acute pericarditis due to COVID-19 infection: An underdiagnosed disease? *Med Clin (Barc)* 2020; **155**: 44-45 [PMID: 32446685 DOI: 10.1016/j.medcli.2020.04.007]
20 **Adler Y**, Charron P, Imazio M, Badano L, Barón-Esquivias G, Bogaert J, Brucato A, Gueret P, Klingel K, Lionis C, Maisch B, Mayosi B, Pavie A, Ristic AD, Sabaté Tenas M, Seferovic P, Swedberg K, Tomkowski W; ESC Scientific Document Group. 2015 ESC Guidelines for the diagnosis and management of pericardial diseases: The Task Force for the Diagnosis and Management of Pericardial Diseases of the European Society of Cardiology (ESC)Endorsed by: The European Association for Cardio-Thoracic Surgery (EACTS). *Eur Heart J* 2015; **36**: 2921-2964 [PMID: 26320112 DOI: 10.1093/eurheartj/ehv318]

21 **Sandoval Y**, Januzzi JL Jr, Jaffe AS. Cardiac Troponin for Assessment of Myocardial Injury in COVID-19: JACC Review Topic of the Week. *J Am Coll Cardiol* 2020; **76**: 1244-1258 [PMID: 32652195 DOI: 10.1016/j.jacc.2020.06.068]

22 **Wanamaker BL**, Seth MM, Sukul D, Dixon SR, Bhatt DL, Madder RD, Rumsfeld JS, Gurm HS. Relationship Between Troponin on Presentation and In-Hospital Mortality in Patients With ST-Segment-Elevation Myocardial Infarction Undergoing Primary Percutaneous Coronary Intervention. *J Am Heart Assoc* 2019; **8**: e013551 [PMID: 31547767 DOI: 10.1161/JAHA.119.013551]

23 Adverse Drug Reaction Probability Scale (Naranjo) in Drug Induced Liver Injury. 2019 May 4. In: LiverTox: Clinical and Research Information on Drug-Induced Liver Injury [Internet]. Bethesda (MD): National Institute of Diabetes and Digestive and Kidney Diseases; 2012- [PMID: 31689026]

24 **Buckley BJR**, Harrison SL, Fazio-Eynullayeva E, Underhill P, Lane DA, Lip GYH. Prevalence and clinical outcomes of myocarditis and pericarditis in 718,365 COVID-19 patients. *Eur J Clin Invest* 2021; **51**: e13679 [PMID: 34516657 DOI: 10.1111/eci.13679]

25 **Bajema KL**, Dahl RM, Prill MM, Meites E, Rodriguez-Barradas MC, Marconi VC, Beenhouwer DO, Brown ST, Holodniy M, Lucero-Obusan C, Rivera-Dominguez G, Morones RG, Whitmire A, Goldin EB, Evener SL, Tremarelli M, Tong S, Hall AJ, Schrag SJ, McMorrow M, Kobayashi M, Verani JR, Surie D; SUPERNOVA COVID-19; Surveillance Group; Surveillance Platform for Enteric and Respiratory Infectious Organisms at the VA (SUPERNOVA) COVID-19 Surveillance Group. Effectiveness of COVID-19 mRNA Vaccines Against COVID-19-Associated Hospitalization - Five Veterans Affairs Medical Centers, United States, February 1-August 6, 2021. *MMWR Morb Mortal Wkly Rep* 2021; **70**: 1294-1299 [PMID: 34529636 DOI: 10.15585/mmwr.mm7037e3]

World Journal of Clinical Infectious Diseases

Submit a Manuscript: https://www.f6publishing.com

World J Clin Infect Dis 2022 April 26; 12(1): 41-46

DOI: 10.5495/wjcid.v12.i1.41

ISSN 2220-3176 (online)

CASE REPORT

Unusual cause of hemorrhagic pleural effusion: A case report

Kee Tat Lee, Kar Nim Leong, Ting Soo Chow, Peng Shyan Wong

Specialty type: Infectious diseases

Provenance and peer review: Unsolicited article; Externally peer reviewed.

Peer-review model: Single blind

Peer-review report's scientific quality classification

Grade A (Excellent): 0
Grade B (Very good): 0
Grade C (Good): C, C, C
Grade D (Fair): D
Grade E (Poor): 0

P-Reviewer: Schoenhagen P, United States; Shiryajev YN, Russia

Received: January 6, 2022
Peer-review started: January 6, 2022
First decision: February 21, 2022
Revised: March 6, 2022
Accepted: April 3, 2022
Article in press: April 3, 2022
Published online: April 26, 2022

Kee Tat Lee, Department of Medicine, Hospital Sultanah Bahiyah, Alor Setar 05460, Kedah, Malaysia

Kar Nim Leong, Ting Soo Chow, Peng Shyan Wong, Infectious Disease Unit, Department of Medicine, Hospital Pulau Pinang, Georgetown 10990, Pulau Pinang, Malaysia

Corresponding author: Kee Tat Lee, MD, MRCP, Doctor, Department of Medicine, Hospital Sultanah Bahiyah, Km6, Jalan Langgar, Alor Setar 05460, Kedah, Malaysia.
keetat.lee@gmail.com

Abstract

BACKGROUND

Infected aortic aneurysms are uncommon and difficult to treat. We present a case of infected aortic aneurysm with recurrent nontyphoidal *Salmonella* bacteremia.

CASE SUMMARY

A 68-year-old gentleman presented with non-specific symptoms and was found to have nontyphoidal *Salmonella* bacteremia and was treated with intravenous ceftriaxone. However his condition did not improve, and he developed a multiloculated right pleural effusion. Thoracocentesis was done to drain hemorrhagic pleural fluid. Chest computed tomography demonstrated descending thoracic aorta saccular aneurysm with periaortic hematoma likely due to recent bleed and extending to the right pleural cavity. He was referred to cardiothoracic surgery team and was planned for medical therapy in view of hemodynamic stability and no evidence of active leakage. He completed intravenous antibiotic for 5 wk and refused surgical intervention. Unfortunately, he was admitted twice for recurrent nontyphoidal *Salmonella* bacteremia. Finally, he agreed for surgical intervention and underwent endovascular aortic repair 3 mo later. Postoperatively, his condition remained stable with no recurrence of infection.

CONCLUSION

Our case highlights the importance of high index of suspicion of infected aortic aneurysm in patients with *Salmonella* bacteremia with high-risk factors such as atherosclerosis.

Key Words: Infected aneurysm; Aorta; Nontyphoidal *Salmonella*; Pleural effusion; Case report

Core Tip: Infected aortic aneurysm is a rare condition with high mortality. Our aim of this case report is to highlight the importance of high index of suspicion of infected aortic aneurysm in patients with *Salmonella* bacteremia with additional literature review to help clinician in the management of this disease. Medical therapy alone in this condition is associated with poor outcome.

Citation: Lee KT, Leong KN, Chow TS, Wong PS. Unusual cause of hemorrhagic pleural effusion: A case report. *World J Clin Infect Dis* 2022; 12(1): 41-46
URL: https://www.wjgnet.com/2220-3176/full/v12/i1/41.htm
DOI: https://dx.doi.org/10.5495/wjcid.v12.i1.41

INTRODUCTION

Infected aneurysm is a rare disease associated with significant morbidity and mortality. Initial symptoms are non-specific, and due to lack of conclusive signs and symptoms, patients are often subjected to various investigations until a diagnosis is made. Standard treatment consists of antibiotic therapy and open surgery with surgical debridement and vascular reconstruction. However, there are no clear guidelines or randomized controlled trial on the best approach for the management of this condition. We report a patient with nontyphoidal *Salmonella* infected aortic aneurysm who was treated with medical therapy initially and complicated with recurrence. He was successfully treated with endovascular aortic repair and was well during follow-up with no recurrence of infection. Relevant literature is reviewed.

CASE PRESENTATION

Chief complaints

A 68-year-old man presented to our hospital with fever associated with lethargy, reduced oral intake, and dyspnea.

History of present illness

The patient's presenting symptoms had lasted for 1 wk.

History of past illness

His medical illness includes diabetes mellitus, hypertension, ischemic heart disease, and chronic kidney disease.

Personal and family history

No relevant family history.

Physical examination

He was febrile and required the support of face mask oxygen during presentation. Examination revealed reduced air entry over right lower zone with bilateral lower zone crepitations.

Laboratory examinations

Laboratory results showed white blood cell count of 16 × 10^9/L, hemoglobin level of 8.3 g/dL, urea 16.9 mmol/L, and creatinine 301 μmol/L.

Imaging examinations

Chest X-ray on admission showed blunted right costophrenic angle (Figure 1).

PROGRESS

He was admitted to the medical ward with the diagnosis of pneumonia and acute on chronic kidney disease. He was started on intravenous (IV) ceftriaxone 2 g daily. Blood culture on admission was positive for nontyphoidal *Salmonella spp*. During the course of admission, he became more tachypneic, and right thoracocentesis was done in view of worsening pleural effusion, which drained out 250 mL of blood stained fluid. Lung ultrasound showed multiseptated right pleural effusion. Despite ultrasound guided pigtail drainage of right pleural effusion, his condition did not improve. Chest computed

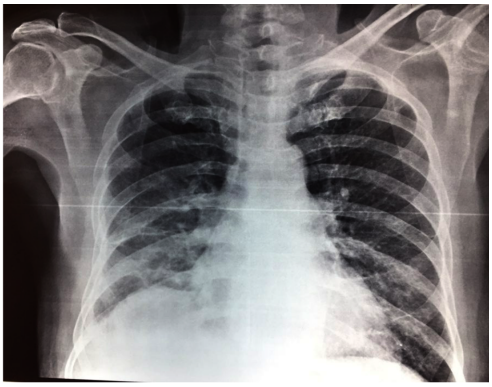

DOI: 10.5495/wjcid.v12.i1.41

Figure 1 Chest X-ray on admission showed right pleural effusion.

tomography (CT) demonstrated descending thoracic aorta saccular aneurysm with periaortic hematoma (Figure 2), likely due to recent bleed, and extending to the right pleural cavity. Pleural fluid culture was negative.

FINAL DIAGNOSIS

Salmonella infected aortic aneurysm.

TREATMENT

He was referred to cardiothoracic surgery team and was planned for medical therapy in view of hemodynamical stability and no evidence of active leakage. There were multiple changes in his antibiotics regimen due to persistent fever (which included ceftazidime, piperacillin-tazobactam, meropenem, and cefepime). He completed 5 wk of antibiotics and was planned for a CT angiography of aorta at a later date to decide on surgical intervention.

OUTCOME AND FOLLOW-UP

Unfortunately, the patient was readmitted 2 mo later with abdominal discomfort and unable to pass motion for 1 wk. Abdominal X-ray demonstrated dilated large intestine. CT abdomen and pelvis showed descending thoracic aorta saccular aneurysm (slightly larger) with features suggestive of superimposed infection of periaortic hematoma; size of aneurysm: 2.4 cm × 3.6 cm and fecal laden bowels with features of impending intestinal obstruction. No obvious bowel related mass was seen. He was treated conservatively for the ileus, which resolved after 1 d. Blood culture on this admission was positive again for nontyphoidal *Salmonella spp*. Echocardiogram did not show any vegetations. He completed 6 wk of IV ampicillin and was discharged well. A repeated CT scan after 2 mo showed resolved periaortic hematoma; however, the patient refused surgical intervention and was given lifelong prophylactic oral antibiotic. Unfortunately, patient presented again with second recurrence after 1 mo, and blood culture was positive again for non-typhoidal *Salmonella*. He completed IV antibiotic and finally agreed for surgical intervention. He underwent endovascular aortic repair, and his condition remained stable with no recurrence of infection during his last follow-up after 2 years.

DISCUSSION

Infected aneurysm is a serious clinical condition. The term mycotic aneurysm was first described by William Osler in 1885[1], however the nomenclature of mycotic aneurysm *vs* infected aneurysm remains controversial as a majority of infected aneurysms are due to bacterial infection. Etiology of infected aneurysm includes direct bacterial inoculation, bacteremic seeding of existing intimal injury, atherosclerotic plaque, or preexisting aneurysm, contiguous infection, or septic emboli from heart, which can occlude vasa vasorum of blood vessel and lead to infected aneurysm.

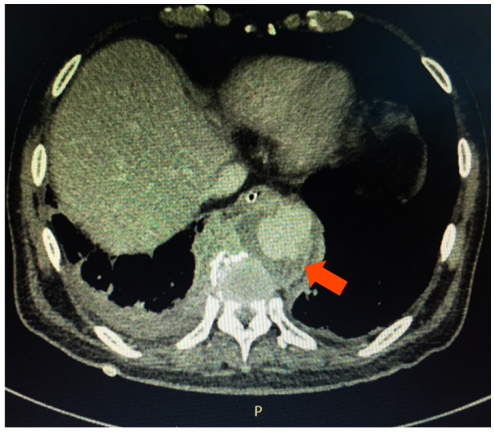

DOI: 10.5495/wjcid.v12.i1.41

Figure 2 Chest computed tomography showed descending thoracic saccular aneurysm with periaortic hematoma (arrow).

Infected aortic aneurysm is a rare but life-threatening condition with devastating outcomes. Initial clinical presentations are often non-specific; therefore, misdiagnosis is common. Infected aortic aneurysms may manifest as vague pain at the back, chest, or abdomen. Some patients may present as pyrexia of unknown origin and remain undiagnosed until rupture of aneurysm. In our patient, he was only diagnosed with infected aortic aneurysm after 3 wk of admission.

Salmonella species and *Staphylococcus aureus* are the most common pathogens of infected aortic aneurysm, followed by other organisms such as *Streptococci* species, *Treponema pallidum*, and *Mycobacterium spp*[2-4]. In East Asia, gram negative bacteria related infected aortic aneurysm is more prevalent, where *Salmonella* species are the most common organisms[2,3,5,6]. It is important to obtain a microbiological diagnosis given the need for protracted courses of antimicrobial therapy. However, blood cultures are negative in around 50% of cases[5,7,8]. Initial empirical treatment is often required and guided by the most likely infecting organism according to the individual and clinical circumstances. It is also prudent to use antibiotics judiciously as prolonged broad spectrum antibiotics may lead to development of antimicrobial resistance. *Salmonella* has a strong affinity for large blood vessels and can easily adhere to the damaged vascular wall, strongly affecting the natural course of the disease. However, studies showed that non-*Salmonella* infections are associated with higher aneurysm-related complications and mortality after treatment[9].

The study by Oderich *et al*[10], with 43 patients with infected aortic aneurysm, found that the risk factors of aneurysm-related death were extensive periaortic infection, female gender, *Staphylococcus aureus* infection, aneurysm rupture, and suprarenal aneurysm location. Another larger series done in Taiwan reported that the independent predictors of aneurysm-related death were advanced age, non-*Salmonella* infection, and non-surgical treatment[2].

Until now, there are no randomized clinical trials to guide the management of infected aneurysm. Therapy mainly includes the control of infections by antibiotic and surgical debridement with or without reconstruction of arterial circulation. Management strategies are primarily based upon clinical experience guided by case series. The optimal duration of antibiotic therapy remains inconclusive. Most studies recommend at least 6 wk of antibiotic and stopping only when there is no longer clinical and laboratory evidence of ongoing sepsis[11,12].

Medical therapy alone is associated with devastating outcomes, with in-hospital mortality of 50% [13]. Since infected aortic aneurysm is at high risk of rupture, surgical treatment is encouraged in the absence of absolute contraindications. Open surgery with extensive debridement of infected tissue and *in situ* or extra-anatomical reconstruction has been the gold standard treatment. However, it is associated with high risk of morbidity and mortality[3,14-16]. Recently, endovascular techniques has become an emerging treatment alternative, especially in the treatment of patients at prohibitive risk for open surgery. Few studies have shown that endovascular treatment of infected aortic aneurysm is feasible and that it is a durable treatment option for high risk patients[17,18]. Luo *et al*[18] reported that survival at 1 mo, 6 mo, 1 year, and 5 year was 90%, 82%, 71%, and 53%, respectively. In addition, a European multicenter study of endovascular treatment for infected aortic aneurysm also showed similar results[17].

CONCLUSION

Infected aortic aneurysm is a rare clinical entity with high mortality. Due to non-specificity of the early symptoms, misdiagnosis is common. Our case highlights the importance of high index of suspicion of

infected aortic aneurysm in patient with recurrent nontyphoidal *Salmonella* bacteremia. Endovascular technique has become an emerging treatment option.

ACKNOWLEDGEMENTS

We thank the Director-General of Health Malaysia for the permission to present these findings.

FOOTNOTES

Author contributions: Lee KT, Chow TS, and Wong PS were involved in data analysis; Lee KT, Leong KN, Chow TS, and Wong PS contributed to conception of the study and drafting, critically revising, and providing final approval of the manuscript.

Informed consent statement: Written consent for publication has been obtained from the patient.

Conflict-of-interest statement: The authors declare that there is no conflict of interest.

CARE Checklist (2016) statement: The authors have read the CARE Checklist (2016) and the manuscript was prepared according to the checklist.

Country/Territory of origin: Malaysia

ORCID number: Kee Tat Lee 0000-0003-3638-2541; Kar Nim Leong 0000-0002-0175-6059; Ting Soo Chow 0000-0001-6175-1818; Peng Shyan Wong 0000-0003-1913-6648.

S-Editor: Wang LL
L-Editor: Filipodia
P-Editor: Wang LL

REFERENCES

1 **Osler W**. The Gulstonian Lectures, on Malignant Endocarditis. *Br Med J* 1885; **1**: 467-470 [PMID: 20751186 DOI: 10.1136/bmj.1.1262.467]
2 **Lin CH**, Hsu RB. Primary Infected Aortic Aneurysm: Clinical Presentation, Pathogen, and Outcome. *Acta Cardiol Sin* 2014; **30**: 514-521 [PMID: 27122829 DOI: 10.6515/acs20140630a]
3 **Hsu RB**, Chen RJ, Wang SS, Chu SH. Infected aortic aneurysms: clinical outcome and risk factor analysis. *J Vasc Surg* 2004; **40**: 30-35 [PMID: 15218459 DOI: 10.1016/j.jvs.2004.03.020]
4 **Jackman JD Jr**, Radolf JD. Cardiovascular syphilis. *Am J Med* 1989; **87**: 425-433 [PMID: 2679075 DOI: 10.1016/s0002-9343(89)80826-5]
5 **Hsu RB**, Tsay YG, Wang SS, Chu SH. Surgical treatment for primary infected aneurysm of the descending thoracic aorta, abdominal aorta, and iliac arteries. *J Vasc Surg* 2002; **36**: 746-750 [PMID: 12368720 DOI: 10.1067/mva.2002.126557]
6 **Kan CD**, Lee HL, Yang YJ. Outcome after endovascular stent graft treatment for mycotic aortic aneurysm: a systematic review. *J Vasc Surg* 2007; **46**: 906-912 [PMID: 17905558 DOI: 10.1016/j.jvs.2007.07.025]
7 **Johnson JR**, Ledgerwood AM, Lucas CE. Mycotic aneurysm. New concepts in therapy. *Arch Surg* 1983; **118**: 577-582 [PMID: 6687676 DOI: 10.1001/archsurg.1983.01390050053010]
8 **Maeda H**, Umezawa H, Goshima M, Hattori T, Nakamura T, Umeda T, Shiono M. Primary infected abdominal aortic aneurysm: surgical procedures, early mortality rates, and a survey of the prevalence of infectious organisms over a 30-year period. *Surg Today* 2011; **41**: 346-351 [PMID: 21365414 DOI: 10.1007/s00595-010-4279-z]
9 **Wang JH**, Liu YC, Yen MY, Wang JH, Chen YS, Wann SR, Cheng DL. Mycotic aneurysm due to non-typhi salmonella: report of 16 cases. *Clin Infect Dis* 1996; **23**: 743-747 [PMID: 8909837 DOI: 10.1093/clinids/23.4.743]
10 **Oderich GS**, Panneton JM, Bower TC, Cherry KJ Jr, Rowland CM, Noel AA, Hallett JW Jr, Gloviczki P. Infected aortic aneurysms: aggressive presentation, complicated early outcome, but durable results. *J Vasc Surg* 2001; **34**: 900-908 [PMID: 11700493 DOI: 10.1067/mva.2001.118084]
11 **Clough RE**, Black SA, Lyons OT, Zayed HA, Bell RE, Carrell T, Waltham M, Sabharwal T, Taylor PR. Is endovascular repair of mycotic aortic aneurysms a durable treatment option? *Eur J Vasc Endovasc Surg* 2009; **37**: 407-412 [PMID: 19211280 DOI: 10.1016/j.ejvs.2008.11.025]
12 **Deipolyi AR**, Rho J, Khademhosseini A, Oklu R. Diagnosis and management of mycotic aneurysms. *Clin Imaging* 2016;

40: 256-262 [PMID: 26995583 DOI: 10.1016/j.clinimag.2015.11.011]

13 **Hsu RB**, Chang CI, Wu IH, Lin FY. Selective medical treatment of infected aneurysms of the aorta in high risk patients. *J Vasc Surg* 2009; **49**: 66-70 [PMID: 18848757 DOI: 10.1016/j.jvs.2008.08.004]

14 **Müller BT**, Wegener OR, Grabitz K, Pillny M, Thomas L, Sandmann W. Mycotic aneurysms of the thoracic and abdominal aorta and iliac arteries: experience with anatomic and extra-anatomic repair in 33 cases. *J Vasc Surg* 2001; **33**: 106-113 [PMID: 11137930 DOI: 10.1067/mva.2001.110356]

15 **Yu SY**, Hsieh HC, Ko PJ, Huang YK, Chu JJ, Lee CH. Surgical outcome for mycotic aortic and iliac anuerysm. *World J Surg* 2011; **35**: 1671-1678 [PMID: 21541801 DOI: 10.1007/s00268-011-1104-9]

16 **Dubois M**, Daenens K, Houthoofd S, Peetermans WE, Fourneau I. Treatment of mycotic aneurysms with involvement of the abdominal aorta: single-centre experience in 44 consecutive cases. *Eur J Vasc Endovasc Surg* 2010; **40**: 450-456 [PMID: 20719550 DOI: 10.1016/j.ejvs.2010.07.017]

17 **Sörelius K**, Mani K, Björck M, Sedivy P, Wahlgren CM, Taylor P, Clough RE, Lyons O, Thompson M, Brownrigg J, Ivancev K, Davis M, Jenkins MP, Jaffer U, Bown M, Rancic Z, Mayer D, Brunkwall J, Gawenda M, Kölbel T, Jean-Baptiste E, Moll F, Berger P, Liapis CD, Moulakakis KG, Langenskiöld M, Roos H, Larzon T, Pirouzram A, Wanhainen A; European MAA collaborators. Endovascular treatment of mycotic aortic aneurysms: a European multicenter study. *Circulation* 2014; **130**: 2136-2142 [PMID: 25378548 DOI: 10.1161/CIRCULATIONAHA.114.009481]

18 **Luo CM**, Chan CY, Chen YS, Wang SS, Chi NH, Wu IH. Long-term Outcome of Endovascular Treatment for Mycotic Aortic Aneurysm. *Eur J Vasc Endovasc Surg* 2017; **54**: 464-471 [PMID: 28826996 DOI: 10.1016/j.ejvs.2017.07.004]

World Journal of Clinical Infectious Diseases

Submit a Manuscript: https://www.f6publishing.com

World J Clin Infect Dis 2022 April 26; 12(1): 47-49

DOI: 10.5495/wjcid.v12.i1.47

ISSN 2220-3176 (online)

LETTER TO THE EDITOR

COVID-19, stigma, and people with disabilities: A mental health perspective

Raktim Swarnakar, Shreya Santra

Specialty type: Infectious diseases

Provenance and peer review: Unsolicited article; Externally peer reviewed.

Peer-review model: Single blind

Peer-review report's scientific quality classification

Grade A (Excellent): 0
Grade B (Very good): B, B
Grade C (Good): C, C
Grade D (Fair): 0
Grade E (Poor): 0

P-Reviewer: Lin CY, Luo W, Wang MK

Received: October 2, 2021
Peer-review started: October 2, 2021
First decision: December 9, 2021
Revised: December 22, 2021
Accepted: February 15, 2022
Article in press: February 15, 2022
Published online: April 26, 2022

Raktim Swarnakar, Department ofPhysical Medicine and Rehabilitation, All India Institute of Medical Sciences, New Delhi 110029, Delhi, India

Shreya Santra, R. G. Kar Medical College and Hospital, Kolkata 700004, India

Corresponding author: Raktim Swarnakar, MBBS, MD, Senior Resident Doctor, Department of Physical Medicine and Rehabilitation, All India Institute of Medical Sciences, Ansari Nagar, New Delhi 110029, Delhi, India. raktimswarnakar@hotmail.com

Abstract

Discrimination is an age-old 'illness' irrespective of its context. Stigma is a common factor that has been associated with disability and coronavirus disease 2019. The public health impact of stigma on differently-abled people during this pandemic is not known and it is a poorly investigated and neglected area. It is important to address the current research need in the concerned area and its implications for public health policymaking and changes in practices that it requires. Together we can win the war against pandemics if we reduce the mental distancing in all perspectives.

Key Words: COVID-19; Stigma; Disability; Mental health; Public health

Core Tip: Currently, coronavirus disease 2019 (COVID-19) is known to be associated with stigma. Previously, it was known that disability is also associated with stigma. The public health impact of stigma on differently-abled people during the COVID-19 pandemic is not known and is a poorly investigated area currently. This letter would like to address the current research need in the concerned area and this would have implications for public health policymaking and changes in practices that it needs.

Citation: Swarnakar R, Santra S. COVID-19, stigma, and people with disabilities: A mental health perspective. *World J Clin Infect Dis* 2022; 12(1): 47-49
URL: https://www.wjgnet.com/2220-3176/full/v12/i1/47.htm
DOI: https://dx.doi.org/10.5495/wjcid.v12.i1.47

TO THE EDITOR

"Viruses do not discriminate and neither should we"[1].

Globally, coronavirus disease 2019 (COVID-19) has become a public health emergency. In such crisis, rumors, misinformation, fear, and lack of proper public health awareness make fertile soil for the stigma to grow incessantly[2]. Unfortunately, from historical ages to the modern era, infectious diseases and disabilities are independently associated with the social stigma. COVID-19 has already made a negative impact on mental health and stigma has just aggravated it. It is well known that people with disabilities face discrimination and stigma in different spheres of life and such a pandemic situation resulted in greater difficulty in individuals with disabilities than the able-bodied population.

Stigma invariably leads to concealment of COVID-19 symptoms and delayed treatment, which leads to greater dissemination of severe acute respiratory syndrome coronavirus-2 (SARS-CoV-2) infection among the public. Many disabling conditions like people with spinal cord injury are particularly vulnerable to SARS-CoV-2 infection. People with disabilities already had physical barriers[3], but the pandemic has added mental and attitudinal barriers due to social stigma. In the context of pandemic crisis, such social stigma severely affects the mental health of people with disabilities. COVID-19 already has hampered social participation due to social distancing and has limited functional involvement due to home confinement and lockdown[4]. Moreover, vaccine inequity may also create further issues which need attention beforehand[5]. Furthermore, social stigma becomes an extra hindrance for better functionality and participation of these populations.

Social stigma in the context of mental health not only damages its victim but becomes also detrimental to the whole public health domain. Social stigma among individuals with disabilities during a pandemic can be prevented by: (1) Public health awareness program through proper information, education, and communication; (2) breaking the misconceptions about COVID-19; (3) considering people with disabilities as differently-abled; (4) improving provision of telerehabilitation emphasizing psychiatric telerehabilitation during the pandemic; (5) identifying barriers and planning to overcome them; and (6) online social-engagement, peer-group formation, and motivational sessions to boost morale and improve the mental well-being of individuals with special needs and disabilities.

Worldwide COVID-19 cases crossed 336 million, and the population with disability crossed one billion[6,7]. Putting this situation in the public and mental health perspective, COVID-19 has set a new-normal life whereas people with disabilities lead a new-normal life with different ability, and eradicating social stigma from this 'new-normal life' is each and everyone's responsibility.

We, healthcare professionals from every domain, should keep closer surveillance so that the physical distancing does not become a mental distancing.

What is the current understanding of this topic?

Currently, COVID-19 is known to be associated with stigma. Previously, it was known that disability is also associated with stigma.

What does this Letter-to-Editor add to the literature?

The public health impact of stigma on differently-abled people during the COVID-19 pandemic is not known and is a poorly investigated area currently.

What are the implications for mental health practice?

This letter would address the current research need in the concerned area and this would have implications for public health policymaking and changes in practices that it needs.

FOOTNOTES

Author contributions: Swarnakar R contributed to conception and design; Swarnakar R and Santra S contributed to literature search and writing.

Conflict-of-interest statement: Raktim Swarnakar and Shreya Santra declare no conflicts of interest for this letter.

Country/Territory of origin: India

ORCID number: Raktim Swarnakar 0000-0002-7221-2825; Shreya Santra 0000-0002-6754-2694.

S-Editor: Wang LL
L-Editor: Wang TQ
P-Editor: Wang LL

REFERENCES

1 **World Health Organization**. Stigma discrimination. 2021. [cited 21 January 2022]. Available from: https://www.who.int/docs/default-source/wpro---documents/countries/malaysia/infographics/covid-19/english-stigma-discrimination.pdf?sfvrsn=2aa46d10_2
2 **The United Nations International Children's Fund**. Social stigma associated with the coronavirus disease (COVID-19). 2021. [cited 21 January 2022]. Available from: https://www.unicef.org/documents/social-stigma-associated-coronavirus-disease-covid-19
3 **Armitage R**, Nellums LB. The COVID-19 response must be disability inclusive. *Lancet Public Health* 2020; **5**: e257 [PMID: 32224295 DOI: 10.1016/S2468-2667(20)30076-1]
4 **Asundi A**, O'Leary C, Bhadelia N. Global COVID-19 vaccine inequity: The scope, the impact, and the challenges. *Cell Host Microbe* 2021; **29**: 1036-1039 [PMID: 34265241 DOI: 10.1016/j.chom.2021.06.007]
5 **Tomczyk S**, Rahn M, Schmidt S. Social Distancing and Stigma: Association Between Compliance With Behavioral Recommendations, Risk Perception, and Stigmatizing Attitudes During the COVID-19 Outbreak. *Front Psychol* 2020; **11**: 1821 [PMID: 32849073 DOI: 10.3389/fpsyg.2020.01821]
6 **World Health Organization**. WHO Coronavirus (COVID-19) Dashboard. 2021. [cited 21 January 2022]. Available from: https://covid19.who.int/
7 **World Health Organization**. Disability. 2021. [cited 21 January 2022]. Available from: https://www.who.int/health-topics/disability#tab=tab_1

Published by **Baishideng Publishing Group Inc**
7041 Koll Center Parkway, Suite 160, Pleasanton, CA 94566, USA
Telephone: +1-925-3991568
E-mail: bpgoffice@wjgnet.com
Help Desk: https://www.f6publishing.com/helpdesk
https://www.wjgnet.com